IN THE UNITED STATES PATENT AND TRADEMARK OFFICE

In re Application of: Michael SCHUTZ *et al.*	Group Art Unit: 1656
Serial No.: 10/519,259	Examiner: Marsha M. Tsay
Filed: February 14, 2006	Atty. Dkt. No.: DEBE:046US
For: METHOD FOR DETECTING AND FOR REMOVING ENDOTOXIN	Confirmation No.: 3637

CERTIFICATE OF ELECTRONIC TRANSMISSION
37 C.F.R. § 1.8

I hereby certify that this amendment is being electronically filed with the United States Patent and Trademark Office via EFS-Web on the date below:

December 4, 2007 — Steven L. Highlander
Date

DECLARATION OF STEFAN MILLER UNDER 37 C.F.R. §1.132

Commissioner for Patents
PO Box 1450
Alexandria, VA 22313-1450

I, Dr. Stefan Miller, do declare that:

1. I am a citizen of Germany residing at Roggenweg 11, 93055 Regensburg. I currently hold the position of CSO at the PROFOS AG, Josef-Engert-Str. 11, 93053 Regensburg, Germany. My research experience includes bacteriophage biology, protein folding, assembly, isolation and expression. A copy of my *curriculum vitae* is attached.

2. The susceptibility of a bacterium to bacteriophage infection is primarily dependent on whether the bacteriophage is able to attach to specific bacteriophage receptors on the bacterial cell surface or not. This requires interaction of the bacteriophage tail fibers or tail spikes with specific attachment sites on the bacterial cell surface. Bacteriophage tail fibers or tail spikes are phage proteins attached to the phage tail, either through baseplate in tailed bacteriophages with contractile tails, or directly to the vertices in the phage head in bacteriophages without tail. Bacteriophage tail proteins recognize specific receptors on the bacterial surface, thereby conferring specificity of bacterial host cell recognition. Bacteriophage receptors are found within practically all structural components found on the host cell surface, *e.g.*, surface proteins, lipopolysaccharide, peptidoglycan, teichoic acids, components of the cytoplasmic membrane, distinct structures like flagella or pili, and additional layers like capsules or slime layers. A review summarizing the knowledge about phage receptors on the bacterial surface, including also knowledge about the tail fibers and tail spikes on the bacteriophage side, was published in 1973 (Lindberg, Bacteriophage receptors, Ann. Rev. Microbiol. 27, 205-241). The skilled artisan being a microbiologist is well aware of the fact that endotoxin is a component of the bacterial surface, particularly lipopolysaccharide. Hence, for the above-captioned invention, only bacteriophage tail proteins that bind to bacterial lipopolysaccharide are of interest because bacterial lipopolysaccharide equates with endotoxin, which is of medical significance. Furthermore, said skilled artisan knows from the Lindberg review, that the specific bacteriophage tail protein he has to use depends on the nature of the endotoxin he wants to remove or detect. He also knows, inter alia from the Lindberg Review, that bacteriophage tail proteins that bind to the lipopolysaccharide core region are likely to

have a somewhat broader specificity than others binding to the O-antigen, as the core structure is more conserved between related bacterial species. The above mentioned review, for example, provides a wealth of information for several bacteriophage tail proteins binding to different lipopolysaccharide substructures from different bacteria.

3. At the time of the invention, several examples of lipopolysaccharide binding bacteriophage tail proteins were known, which were studied in more detail. For example, an extensively studied role model in bacteriophage infection which is known to the skilled artisan as mentioned above is *E. coli* infection by bacteriophage T4. It is known that T4 has 6 long, as well as 6 short, tail fibers involved in bacterial recognition. Whereas the long tail fibers are composed of the three proteins p34, p35, and p37, and recognize OmpC or lipopolysaccharide as bacterial receptor, the short tail fibers are only composed from protein p12. The short tail fiber, namely the p12 protein of T4, was described in a paper by Mason & Haselkorn in 1972 (J. Mol. Biol. 66, 445-469), and further characterized in the work of Makhov *et al.* in 1993 (Virology 194, 117-127). Makhov *et al.* also mention that the N-terminal part of p12 binds to the bacteriophage baseplate, whereas the C-terminal part binds to the LPS core. Having knowledge about the p12 protein of bacteriophage T4, said person skilled was able to find other p12-like bacteriophage tail proteins which were likely to have similar function, i. e. endotoxin binding, but somewhat other specificities, i.e. binding to different endotoxins from other bacterial species. From the knowledge about T4p12, the person skilled in the art was able to find additional examples for p12-similar proteins. The respective literature is summarized in the next paragraph.

From the work of Riede (Mol. Gen. Genet. 206, 110-115, 1987) it is known that short tail fibers do not contribute much to host specificity, can be exchanged between several T-even bacteriophages, and bind to the LPS core. This work also reported cloning of the short tail fibers, namely, the gene 12 products (this is used as a synonym as shown in the title) of the bacteriophages T2, K3 and K3hx, providing further examples of p12 proteins similar in function and structure to T4p12. Tetart *et al.* described a number of phylogenetically-related T4-like phages before the priority date (J. Bact. 183, 358-366, 2001), and asserted that the homology especially arises in structural proteins like the phage tail proteins. Examples mentioned are the T-even phages (T4, T6, KC69 Tu1a, and RB69), the pseudoT-even phages (AR1, SV14, RB49, RB42, RB43, 42, 44RR) and the schizoT-even phages (nt-1, KVP20, KVP40, 65, and Aeh1). Additional examples of phage tail proteins from the phages Felix O-1 (FO), 6SR, and Br2 binding to structures of the LPS core were provided by Lindberg *et al.* in 1970 (Bacteriophage attachment to the somatic antigen of *Salmonella*: Effect of O-specific structures in leaky R mutants and S, T1 hybrids, Infect. & Imm. 1, 88-97]). The aforementioned Lindberg review of 1973 discusses the tailed bacteriophages T3, T4, T7, Felix O-1, C21, and the tail-less phages 6SR, Br2 from the ΦX174 group as binding in the lipopolysaccharide core structure.

4. Meanwhile, around twenty T4-like bacteriophages are sequenced completely (see http://phage.bioc.tulane.edu/), and provide another set of examples for suitable T4p12-similar short tail fibers. The respective tail proteins are called gp12, short tail fiber or tailpin.

5. The skilled artisan working with bacteriophages knows that the nomenclature of the bacteriophage tail proteins as well as the complete classification of the bacteriophages themselves is somewhat non-uniform, and that he might potentially find different technical terms for the same thing. There is a distinction between long tail fibers and short tail fibers, but on the other hand, there exists a division into tail fibers and tail spikes. The short tail fibers are sometimes also called tailspikes or tailpins. Lindberg, in his review, mentions on page 220 (last sentence of the first paragraph) short tail fibers, which he also calls tailpins. In the second and third paragraph on the same page, he connects the short tail fibers with the gene product of gene 12, which is conventionally abbreviated as gp12 or simply p12, when speaking of a protein. Riede (1987) uses the terms short tail fibers and protein 12 as synonyms. Makhov *et al.* (1993) connect the short tail-fiber of T4 also with gp12 (gene product 12). Mason & Haselkorn (1972) also describe the function of the product of T4 gene 12 as a short tail fiber. Considering all of the above mentioned literature, the person skilled in the art has a wealth of information, which bacteriophage tail proteins are subsummarized under the expression "p12 and p12-similar bacteriophage tail proteins".

6. Even taking into account the inconsistency of nomenclature which exists in the field anyway, and the several connections in the literature between short tail proteins as a gene product of gene 12, even in older reviews like the Lindberg work of 1973 (which is a milestone in the field of bacteriophage receptors) a person skilled in the art (in this case a scientist working with bacteriophages) would nonetheless be able to know which phage

tail proteins he or she could use in practicing the presently claimed invention besides p12 protein of phage T4.

7. I declare that all statements made herein of my own knowledge are true, and that all statements of my own belief are believed to be true, and further that these statements were made with the knowledge that willful false statements are punishable by fine or imprisonment, or both, under § 1001 of title 18 of the United States Code.

November 29, 2007
Date

Dr. Stefan Miller

CURRICULUM VITAE DR. STEFAN MILLER

Personal

Name	Dr. rer. nat. Stefan Miller
Born	11.11.1964 in Regensburg
Address	Roggenweg 11, 93055 Regensburg

Education

1986-1992	University of Regensburg; biology diploma
1991-1992	University of Regensburg; diploma thesis in the group of Prof. E. Heller (Institute of Biophysics and physical Biochemistry). Topic: Untersuchungen zu Vorkommen, Stabilität und Funktion von ß-poly-L-Malat im Lebenszyklus von *Physarum polycephalum*

Professional Experience

1992-1995	Doctoral thesis in the group of Prof. R. Seckler (University of Regensburg, Institute of Biophysics and physical Biochemistry). Topic: Deletions- und Punktmutanten des P22-Tailspike-Proteins: Klonierung, Reinigung und physikalisch-biochemische Analyse.
1995-1996	Postdoc in the group of Prof. R. Seckler
1996-1997	Postdoc position in the group of Prof. U. Henning (Department of Microbiology, Max-Planck-Institute for Biology, Tübingen). Topic: Function of bacteriophage-encoded chaperones in the morphogenesis of bacteriophage T4.
	Own research group.
1997-1998	Postdoc position in the group Prof. R. Seckler (University of Regensburg, Institute of Biophysics and physical Biochemistry). Topic: Function of bacteriophage-encoded chaperones in the morphogenesis of bacteriophage T4.
	Own research group.
1999	Visiting Scientist at the University of Regensburg, Institute of Biophysics and physical Biochemistry
	Preparation of founding of PROFOS GmbH.
2000	Founding of PROFOS GmbH, managing partner & CSO
2000-	CSO, chief scientific officer of Profos AG, responsible for the research and development projects. Managing of the patent and trade mark portfolio

Scientific background:

Structure, folding, assembly, stability and activity of phage proteins. In general cloning, protein-expression, protein-purification, crystallisation, re-folding of proteins, spectroscopic techniques, stability of proteins.

Languages:

German, Englisch

Scientific publications

1. Holler E., Angerer B., Achhammer G., Miller S., Windisch C.; FEMS Microbiol. Rev. 1992; 103: 109-118. Biological and biosynthetic properties of poly-L-malate.
2. Windisch C., Miller S., Reisner H., Angerer B., Achhammer G., Holler E; Cell Biol. Internat. Reports 1992; 16(11): 1211-1215. Production and degradation of ß-poly-L-malate in cultures of *Physarum Polycephalum*.
3. Danner-M; Fuchs-A; Miller-S; Seckler-R; Eur. J. Biochem. 1993; 215(3): 653-661. Folding and assembly of phage P22 tailspike endorhamnosidase lacking the N-terminal, head-binding domain.
4. Steinbacher-S; Seckler-R; Miller-S; Steipe-B; Huber-R; Reinemer-P; Science 1994; 265(5170): 383-386. Crystal structure of P22 tailspike protein: interdigitated subunits in a thermostable trimer.
5. Steinbacher-S; Baxa-U; Miller-S; Weintraub-A; Seckler-R; Huber-R; Proc. Natl. Acad. Sci. USA. 1996; 93(20): 10584-10588. Crystal structure of phage P22 tailspike protein complexed with *Salmonella sp.* O-antigen receptors.
6. Baxa-U; Steinbacher-S; Miller-S; Weintraub-A; Huber-R; Seckler-R; Biophys. J. 1996; 71(4): 2040-2048. Interactions of phage P22 tails with their cellular receptor, *Salmonella* O-antigen polysaccharide.
7. Steinbacher-S, Miller-S, Baxa-U, Weintraub-A, Seckler-R; Biol. Chem. 1997; 378: 337-343. Interaction of *Salmonella* Phage P22 with Its O-Antigen Receptor Studied by X-Ray Crystallography.
8. Steinbacher-S, Miller-S, Baxa-U, Budisa-N, Weintraub-A, Seckler-R, Huber-R; J. Mol. Biol. 1997; 267: 865-880. Phage P22 Tailspike Protein: Crystal Structure of the head-binding Domain at 2.3 Å, Fully Refined Structure of the Endorhamnosidase at 1.56 Å Resolution, and the Molecular Basis of O-Antigen Recognition and Cleavage.
9. Miller-S, Schuler-B, Seckler-R; Prot. Sci. 1998; 7: 2223-2232. Phage P22 tailspike protein: Removal of head-binding domain unmasks effects of folding mutations on native-state thermal stability.
10. Miller-S, Schuler-B, Seckler-R; Biochemistry 1998; 37: 9160-9168. A reversibly unfolding fragment of P22 tailspike protein with native structure: The isolated ß-helix domain.
11. Burda-MR, Miller-S; Europ. J. Biochem. 1999; 265: 771-778. Folding of coliphage T4 short tail fiber *in vitro*: Analysing the role of a bacteriophage-encoded chaperone.
12. Burda-MR, Hindennach-I, Miller-S, Biol. Chem. 2000; 381: 255-258. Stability of phage T4 short tail fiber protein.
13. Van Raaij-MJ, Schoehn-G, Jaquinod-M, Ashman-K, Burda-MR und Miller-S, Biol. Chem.;382: 1049–1055, 2001; Identification and crystallisation of a heat- and protease-stable domain of the bacteriophage T4 short tail fibre.
14. Van Raaij-MJ, Schoehn-G, Burda-MR und Miller-S, J. Mol. Biol.; 314: 1137-1146, 2001, Crystal structure of a heat- and protease-stable part of the bacteriophage T4 short fibre.
15. Mitraki-A , Miller-S und van Raaij-MJ, J Struct. Biol.; 137, 236–247, 2002; Conformation and folding of novel beta-structural elements in viral fiber proteins: the triple beta-spiral and triple beta-helix
16. Thomassen, E., Gielen, G., Schütz, M., Schoehn, G., Abrahams, J. P., Miller, S: and van Raaij, M. J. J. Mol. Biol.; 331: 361-373, 2003; The structure of the receptor-binding domain of the bacteriophage T4 short tail fibre reveals a knitted trimeric metal-binding fold
17. Krylov V. N., Bourkaltseva M. V., Sykilinda N. N., Pleteneva E. A., Shaburova O. V., Kadykov V. A., Miller S., and Biebl M. Russ. J. Genetics; 40: 363-368, 2004 Comparisons of the Genomes of New Giant Phages Isolated from Environmental Pseudomonas aeruginosa Strains of Different Regions.
18. Krylov, V. N., Miller, S., Rachel, R., Biebl, M., Pletneva, E. A., Schütz, M., Krylov, S. V., Shaburova, O. V. Genetika; 42: 159-168, 2006; Ambivalent bacteriophages of different species active on Escherichia coli K12 and Salmonella sps. strains

19. Walter M., Fiedler C., Grassl R., Biebl M., Rachel R., Hermo-Parrado L. X., Llamas-Saiz A. L., Seckler R., Miller S., and van Raaij M.J. submitted 2007; Structure of the receptor-binding protein of bacteriophage Det7: A podoviral tailspike in a myovirus.

20. Miller-S, Haase-Pettingell-C, Kremer-W, Kalbitzer-HR, King-J, Seckler-R, manuscript in preparation; Folding and capsid binding of an amino-terminal domain from bacteriophage P22 tailspike protein.

Books & reviews

1. Kretzer J. W., Biebl M. and Miller S. submitted 2007; Sample preparation - an essential prerequisite for high-quality bacteria detection; Handbook of bacteria detection: Biosensors, Recognition receptors and Microsystems

Mol Gen Genet (1987) 206:110–115

T4II, 57

MGG

Receptor specificity of the short tail fibres (gp12) of T-even type *Escherichia coli* phages

Isolde Riede*

Max-Planck-Institut für Biologie, Corrensstraße 38, D-7400 Tübingen, Federal Republic of Germany

Summary. Short tail fibres of T-even like phages are involved in host recognition. To determine the specificity of the fibres, the region containing gene 12 of phages T2, K3, and K3hx was cloned. The genes 11, 12, *wac*, and 13, coding for the baseplate outer wedge, short tail fibres, collar whiskers, and a head completion component, respectively, were localized on the cloned fragments. Plasmid-encoded gene 12 could be expressed without helper phage. Efficient expression of gene 12 from T2 and K3hx made an extraction of protein 12 possible. Hybrid phages obtained by in vitro complementation, recombination analysis and protein 12 binding to host range mutant bacteria excluded a role of the short tail fibres from T2, K3 or K3hx in the recognition of outer membrane proteins. Binding patterns of protein 12 to different *Escherichia coli* lipopolysaccharide mutants and inhibition of binding of protein 12 by a monoclonal antibody against the core region of *E. coli* K12 lipopolysaccharide suggested that heptose residues are necessary for efficient binding. The binding site of the same monoclonal antibody is different from the short tail fibre binding site in an *E. coli* B strain suggesting different binding specificities of protein 12. Thus, the ability of different bacterial strains to inactivate phage could be related to differences in the binding specificity of the short tail fibres for the lipopolysaccharides of these bacteria.

Key words: T-even type phages – Short tail fibres – Lipopolysaccharide – Receptor recognition

Introduction

The attachment of bacteriophage T4 to *Escherichia coli* is mediated by two phage structures: the long tail fibres coded by genes (g) 34 to 37 and the short tail fibres coded by g12. The free ends of the six long tail fibres, consisting of the C-terminal regions of gene product (gp) 37 interact directly with the bacterial surface (Beckendorf 1973; Simon and Anderson 1967). The final permanent attachment of T4 seems to be determined by the interaction between the short tail fibres and the host cell wall (Simon et al. 1970).

Although the lipopolysaccharide (LPS) of *E. coli* B is sufficient as a receptor for phage T4 the situation in *E. coli* K12 is somewhat different. It appears that there are two types of receptors for T4: LPS and the cell surface protein OmpC (Goldberg 1983; Henning and Jann 1979; Yu and Mizushima 1982). The short tail fibres of T4 bind to the LPS of the outer membrane (Zorzopulos et al. 1982) but the exact binding site has not yet been identified. T4 short tail fibres are composed of a trimeric gp12 (Kells et al. 1975; Mason and Haselkorn 1972). For gp12 assembly gp57 is required (Kells and Haselkorn 1974). To investigate how gp12 determines the specificity of recognition, gene 12 of two other phages was cloned, expressed and the gene products identified.

Phage T2 most likely uses the outer membrane protein OmpF as a receptor (Hantke 1978). T-even type phage K3 uses the OmpA protein as a receptor and a host range mutant of K3, K3hx, also recognizes OmpA but a different part of it (Hancock and Reeves 1975; Riede et al. 1985b). The results presented here show that gp12 is not involved in the recognition of outer membrane proteins but, probably in the case of all T-even type phages, recognizes LPS. In addition, the site on *E. coli* K12 LPS, involved in binding gp12 of K3hx, was determined.

Materials and methods

Bacteriophages and bacteria. T4 amber mutants N69 (g17), N128 (g12) and NG329 (g13) were obtained from N. Murray (Wilson et al. 1977); T4 am E198 (g57) was obtained from W.B. Wood. Phages T2, K3 and K3hx were from the laboratory collection (Riede et al. 1985b, 1984).

All phages were propagated on strain P400 or JC6650 (Table 1). For defective lysates amber phages were grown on JC6256 or $F^-Z^-\Delta$ M15 (Table 1).

Cloning of short tail fibre genes and DNA sequencing. Phage DNA was isolated and cloned as described (Riede et al. 1984). For detecting clones with g12 either a T4 *Eco*RI fragment containing part of g11 and g12 (Wilson et al. 1977) was labelled with ^{32}P-dATP by nick translation (Maniatis et al. 1975) and used for colony hybridization (Hanahan and Meselson 1980) or amber mutant N69 (T4 g12) was used directly for marker rescue tests on individual clones. All DNA manipulations were performed essentially as described by Maniatis et al. (1982). The enzymes were obtained from Boehringer, Mannheim. The partial sequences were obtained according to the dideoxy chain termination method (Sanger et al. 1977) directly from the plasmid pUC8 (Vieira and Messing 1982).

Subcloning of g57 of T4. pCG57-7 (Herrmann 1982; Herrmann and Wood 1981) was obtained from H. Schaller. The 700 bp *Hin*dIII-*Eco*RI fragment containing g57 was sub-

* *Present address:* European Microbiological Laboratory, Meyerhofstraße 1, D-6900 Heidelberg, Federal Republic of Germany

Table 1. Strains of *Escherichia coli*

Strain	Genotype/phenotype	Reference
P400	F⁻, *thi 1, argE-3, proA-2, thr, leu, mtl, xyl, ara, galK, lacY, rpsL, non, supE*	Skurray et al. (1974)
P2811	(P400) Bar 3, *pyrD-34*, zeb:: Tn *10-43*	Puspurs et al. (1983)
P2812	(P400) Wrm1, *pyrD-34*, zeb:: Tn *10-43*	Puspurs et al. (1983)
P2813	(P400) Bar8, *pyrD-34*, zeb:: Tn *10-43*	Puspurs et al. (1983)
JC6256	*supO*	Achtman et al. (1971)
JC6650	*lac, supF*, F⁻	Achtman et al. (1971)
JC6650 ompA	(JC6650) *ompA*	
70-6	*malT, thi, glpT, glpA, rel 1, phoA, supO, ompF*	Hantke (1978)
F⁻Z⁻*d* M15	*(lac, pro)d, thi, ara, rpsL, recA, ϕ80 lacZd M15*	Rüther et al. (1981)
B/r		Henning et al. (1977)

cloned into the *Eco*RI site of pACYC184 (Chang and Cohen 1978). Chloramphenicol-sensitive, tetracycline-resistant clones were tested for in vivo complementation of E198 (g57). One plasmid complementing gp57 was designated pTU T4-57 and used for further studies.

In vivo complementation assay. Phage genes present in recombinant plasmids were identified by spot tests: 10 µl drops of the different T4 amber mutants were applied to a lawn of cells containing plasmid DNA and the plates incubated at 37° C. In cases of complementation the efficiency of plating (e.o.p.) of the phage was the same as that on the *supF* host JC6650 (Table 1).

In vitro complementation assay. Plasmid-containing bacteria were grown on M9 minimal medium (Miller 1972) supplemented with 0.1% casamino acids to 3×10^8 cells/ml and concentrated ten fold in phage buffer (10 mM Tris-HCl, pH 7.9, 10 mM NaCl, 10 mM $MgCl_2$) containing chloramphenicol (200 µg/ml) to block phage propagation. A 0.5 ml aliquot of the bacteria was sonicated at 0° C and pelleted for 10 min at 4,000 *g* at 4° C. Then, 20 µl of the supernatant was incubated with 20 µl of defective phage (10^{10}/ml) for 30 min at 37° C. Complemented hybrid phages were titrated on strain JC6650 by spot tests.

Defective phages, lacking gp12, were prepared by propagating N69 (g12) on strain F⁻Z⁻*d* M15 or JC6256 on minimal medium as described (Mason and Haselkorn 1972). Always about 1 wild-type phage per 10^6 defective, non-infectious particles, was present. Gp12 and defective phages were stable at 4° C for several months.

Extraction of gp12 of K3hx. pTU hx-3AH (Fig. 2) was grown in M9 minimal medium with 0.1% casamino acids to 0.5×10^8 cells/ml, induced with 0.1 mM isopropyl-1-thio-*β*-D-galactopyranoside (IPTG) and grown for three generations. After centrifugation the cells were resuspended in 60 mM Na_2HPO_4/NaH_2PO_4, pH 6.5, 10 mM Na_2 EDTA, pH 8.0 and sonicated at 4° C. After centrifugation at 60,000 *g* for 1 h the supernatant was dialysed against 60 mM Na_2HPO_4/NaH_2PO_4, pH 6.5 and used for in vitro complementation assays.

Antisera. To detect phage proteins on Western blots (Towbin et al. 1979), anti-K3 or -T4 serum (Schwarz et al. 1983) or serum against SDS-denatured phage K3 raised in rabbits (Henning et al. 1979) was used. Monoclonal anti-LPS antibody mAb 786-D10 (IgG3) recognizing *E. coli* K12 LPS and *E. coli* B LPS (D. Bitter-Suermann, personal communication) was the gift of D. Bitter-Suermann (antigenic determinant, Hex-Glc-Glc-Hep in *E. coli* K12; Peters et al. 1985).

Immunoprecipitation. Cells harbouring pTU hx-3AH (Fig. 2, complete g12) and pTU hx-3AR (Fig. 2, incomplete g12) were grown in M9 medium supplemented with the required amino acids to 3×10^8 cells/ml. Cells (10 ml) were harvested and resuspended in 1 ml minimal medium. Then, 5 µCi ^{14}C-amino acids (Amersham 57 mCi/matom C) were added and the cells incubated for 15 min at 37° C. After precipitation the cells were resuspended in 200 µl A-buffer (10 mM Tris, pH 8.0, 100 mM NaCl, 1.5 mM $MgCl_2$). After sonication and repelleting the supernatant was incubated for 1 h at 37° C with anti-K3 (native) serum. The precipitate was redissolved in 100 µl 4 M $MgCl_2$ for 4 h at 4° C. After repelleting the supernatant was diluted with 900 µl A-buffer. Anti-K3 (native) antibody was added and after 1 h incubation at 37° C and centrifugation, the pellet was dissolved in sample buffer and subjected to SDS-polyacrylamide gel electrophoresis.

Gel electrophoresis and stains. Proteins were separated on 10% SDS-polyacrylamide gels (SDS-PAGE) according to Laemmli (1970). LPS was separated on 14% polyacrylamide gels containing 4 M urea and stained with silver (Tsai and Frasch 1982) or periodic acid-Schiff (PAS) (Segrest and Jackson 1972).

Lipopolysaccharide. P400 and B/r LPS were a gift from U. Henning. P2812 LPS was purified according to Galanos et al. (1969). No protein contamination could be detected (silver stain, Coomassie stain and PAS). The isolated LPS exhibited the characteristic inactivation kinetics of T4 (Henning and Jann 1979).

Results

Localization of the genes on the cloned DNA and expression of gp12

Clones containing g12 DNA of the bacteriophages T2 and K3hx are shown, in Fig. 1, aligned to the restriction and genetic maps of phage T4. T2 and K3hx have the same location as that previously published for g12 of T4 (Wood and Revel 1976). Obviously, the restriction map of T2 and K3hx DNA is very similar indicating that the DNA including and surrounding g12 is highly conserved. The relevant clones and subclones containing g12 DNA are shown in Fig. 2. With these clones and subclones the precise localization of the genes was possible (Table 2).

In vivo complementation indicated that gp11, gp12, and gp13 of K3hx and T2 complement amber mutants of T4.

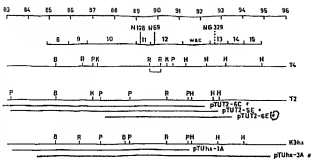

Fig. 1. Alignment of the restriction maps of the g12 region of bacteriophages T4, T2, and K3hx. The numbers in the upper line indicate the position numbers (in kb) of the map of T4 (Kutter and Rüger 1984). The second line shows the genes aligned to the T4 map. This line is a composite of the data of Kutter and Rüger (1984) and Wood and Revel (1976) and takes into account the molecular weights of the gene products. Positions of the amber mutants used in this communication are indicated. The next line indicates the restriction sites of T4 DNA (B, *Bam*HI; R, *Eco*RI; P, *Pst*I; K, *Kpn*I; H, *Hin*dIII; Kutter and Rüger 1984). The *bar* represents the *Eco*RI fragment used to identify the T2, K3 and K3hx clones. The map of T2 DNA is a composite of the maps of the inserts from plasmids pTU T2-6C, −5E, and -6E. pTU T2-6C extends further to the left of the map (indicated by the *dotted line*). K3 DNA has exactly the same restriction sites as K3hx DNA (last lines) and is therefore omitted

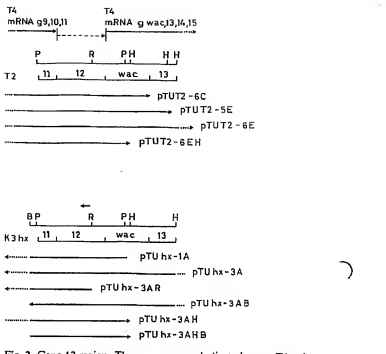

Fig. 2. Gene 12 region. The *upper arrows* indicate known T4 polycistronic transcripts of g 9, 10, 11 and *gwac*, 13, 14 and 15 (Wood and Revel 1976). The *broken line* shows the direction of transcription of g12 as proposed here. The relevant part of the restriction map of T2 and the localization of g 11, 12, *wac* and 13 (see text) are aligned. The *arrows* show the inducibility of the insert DNA of the clones and subclones via the *lac* promoter of the pUC-plasmids. Above the map of K3hx DNA the *arrow* indicates the DNA sequenced. Restriction sites as in Fig. 1. pTU T2-6EH, subclone of pTU T2-6E, deletion of the fragments to the right of the *Hin*dIII site. pTU hx-3AR, subclone of pTU hx-3A, deletion of the fragments to the right of the *Eco*RI site. pTU hx-3AB, subclone of pTU hx-3A, deletion of the fragments to the left of the *Bam*HI site. pTU hx-3AH, subclone of pTU hx-3A, deletion of the fragments to the right of the *Hin*dIII site. pTU hx-3AHB, subclone of pTU hx3AH, deletion of the fragments to the left of the *Bam*HI site

Thus the gene products are interchangeable between these phages.

To maximize the yield of gp12 for further experiments, the amount of active gp12 produced in uninfected cells was assessed by in vitro complementation with defective phage N69 (Table 2). Complementation increased with increasing proximity of the *lac* promoter to the left-hand side of g12 (Fig. 2, Table 2). This finding suggests that g12 is transcribed in the same orientation as g11 and *gwac*.

To test this possibility, a short DNA sequence from the *Eco*RI site in g12 (arrow in Fig. 2) was determined. The sequence in the direction of the arrow has stop codons in all three reading frames. Thus this region must be translated in the same orientation as the surrounding genes.

Gp57 is needed as helper protein for gp12 assembly (Kells and Haselkorn 1974). To test whether this influence can be reproduced with plasmid-coded proteins, T4 g57 was cloned into pACYC184 (pTU T4-57, see Materials and methods). pTUhx-3AH and pTUT4-57 were cotransformed and the resulting Amp^r Tet^r colonies contained both plasmids. Gp12 in vitro complementation activity was increased tenfold. Apparently, in addition to g12 expression, gp57 is also produced in the cells and exhibits its helper function for gp12.

Gp12 could not be detected by the Western blotting technique and, therefore, the protein was identified by immunoprecipitation. The precipitated gp12 of K3hx had an apparent molecular weight (55 kDa, Fig. 3) similar to that of gp12 of T4 (57 kDa, Vandersliee and Yegian 1974).

Short tail fibres do not recognize proteins involved in host specificity

Phage K3hx uses the OmpA protein as a receptor. To determine if the short tail fibres are involved in OmpA recognition, hybrid phages were constructed. *E .coli* mutants lacking the OmpA protein cannot be infected by phage K3hx but are lysed by phage T4. Hybrid phages obtained by in vitro complementation of a defective lysate of N69 (T4 lacking gp12) with short tail fibres of K3hx (gp12 expressed from pTU hx-3AH), recognize all OmpA-deficient mutants tested. In addition, hybrid phages of N69 with short tail fibres of T2 (expressed from pTU T2-6EH) also infected the T2-resistant but T4-sensitive strain 70-6 (lacking the OmpF protein). Thus gp12 of K3hx, or of T2, does not contribute any receptorprotein binding specificity to T4.

To support this finding, an in vitro binding test of gp12 to whole bacteria was developed (Table 3). Binding of extracted gp12 expressed from pTU hx-3AH to cells of JC6650 and JC6650 ompA (Table 1) treated with chloramphenicol was examined. After centrifugation of the cells unbound gp12 in the supernatant was assayed by quantitative in vitro complementation. Both strains bound exactly the same amount of gp12, also suggesting that gp12 binding is independent of OmpA (Table 3a).

Table 2. Behaviour of the plasmids

Plasmid	In vivo complementation[a]			In vitro complementation[b]	Expression of
	N128 (gI1)	N69 (g12)	NG329 (g13)	N69 defective (gp12)	gpwac[c]
pTU T2-6C	++	++	−	+/+	+/+
pTU T2-5E	++	++	+	++/++	++/++
pTU T2-6E	++	++	++	+++/+++	++/++
pTU T2-6EH	++	++	−	+++/+++	−/−
pTU hx-1A	++	++	−	+++/+	−/−
pTU hx-3A	++	++	++	+/+	++/++
pTU hx-3AR	++	+	−	−/−	−/−
pTU hx-3AB	++	++	++	+/+	++/++
pTU hx-3AH	++	++	−	+++/+++	−/−
pTU hx-3AHB	++	++	−	++/+++	−/−

[a] In vivo complementation: (−), no marker rescue could be determined; (+), marker rescue by recombination; (++), complementation of the gene product

[b] In vitro complementation: (+) (++) (+++), complementation of defective phages by a factor of about (10^2) (10^4) (10^6), respectively, over background. Cells were grown + glucose − IPTG or − glucose + IPTG

[c] Expression of gpwac: a 50 kDa protein band can be detected with antibodies against T4 or K3 on Western blots. Cells were grown + glucose − IPTG or − glucose + IPTG

Since pTU T2-6C has a complete *gwac* but does not contain the allele of NG329 (g13), the insert ends at the beginning of g13. *Hin*dIII cuts within *gwac* (pTU hx-3AH lacks gpwac expression) and *Eco*RI within g12 (pTU hx-3AR still rescues N69 (g12) but complementation is absent). pTU hx-3AHB still complements N128 (gI1) showing that the whole gene is to the right of the *Bam*HI site

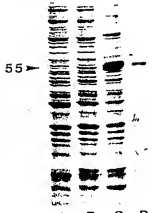

Fig. 3. Identification of gp12. Polyacrylamide gel electrophoresis of F⁻Z⁻*d* M15 containing: A, pTU hx-3AR (incomplete g12); B, pTU hx-3A (low in vitro complementation activity); C, pTU hx-3AH (high in vitro complementation activity). Autoradiogram of immunoprecipitate of: D, pTU hx-3AH; E, pTU hx-3AR. The *arrow* indicates gp12 (55 kDa)

Table 3. Binding of gp12 of K3hx (in vitro)

Escherichia coli strain	% gp12 bound			
	to cells[a]	to LPS[b]	to LPS + antibody[c]	to LPS + excess antibody[d]
JC6650	95	nd	nd	nd
JC6650 ompA	95	nd	nd	nd
B/r	93	95	95	94
P400	92	90	84	23
P2811	85	nd	nd	nd
P2813	89	nd	nd	nd
P2812	25	54	54	47

nd, not determined

[a] *E. coli* was grown to 1×10^9 cells/ml in LB and treated with chloramphenicol for 10 min at 20° C. After incubation with partially purified gp12 for 30 min at 37° C the cells were centrifuged for 5 min at 12,000 *g*. Bound gp12 was then determined by comparing the in vitro complementation activity of the supernatant with that of a control without bacteria (0% binding). The numbers given are averaged from 3 experiments

[b] Lipopolysaccharides from the different strains (250 µg/ml) were incubated with partially purified gp12 for 1 h at 37° C. After 15 min centrifugation at 12,000 *g* the in vitro complementation activity of the supernatant was determined (control without LPS 0% binding). The numbers are averages from 3 experiments

[c] LPS was preincubated with a 1:100 dilution of mAB-786-D10 for 10 min at 37° C before adding gp12

[d] LPS was preincubated with undiluted mAB-786-D10

Table 4. Plating efficiency of K3 and K3hx

E. coli strain	K3 e.o.p.[a]	K3hx e.o.p.[a]	Lipopolysaccharide[e]
B/r	6[b]	2[b]	Gal Hep —Glc—Glc—Hep—Hep—KDO—
P400	1	1	Hep Glc—Hep—Hep—KDO—
P2811	0.1	0.1	Hep—Hep—KDO—
P2813	0.1	0.1	Hep—Hep—KDO—
P2812	0.1[c]	0[d]	KDO—

[a] Plating efficiency (e.o.p.) of phage on P400 is set at 1

[b] Plaques extremely large

[c] Plaques turbid and small

[d] No plaques

[e] Tentative structure of the oligosaccharide region of LPS

Influence of different LPS on phage binding is due to gp12

Plating efficiencies and plaque morphology of K3 and K3hx appeared to be related to the type of LPS of the host bacteria (examples are given in Table 4). To quantitate this effect, inactivation of K3 or of K3hx by three different strains was measured (Fig. 4). Both phages were most efficiently inactivated by *E. coli* B/r (Fig. 4); the efficiencies of plating were highest and the plaques large (Table 4). Inactivation

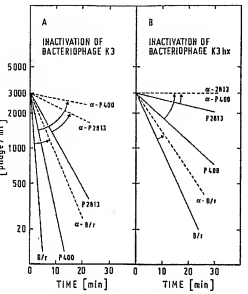

Fig. 4A, B. Inactivation of bacteriophages K3 (A) and K3hx (B) by different *Escherichia coli* strains. P2813, P400, or B/r were grown in LB to 5×10^8 cells/ml and incubated for 5 min at 20° C with chloramphenicol (150 μg/ml). At time zero one volume of bacteriophage was added (appropriate dilution in LB) and the mixture incubated at 37° C. At various times 0.5 ml aliquots were removed and diluted tenfold in ice-cold phage buffer containing chloramphenicol (20 μg/ml). The number of unbound phage was then determined from the e.o.p. on P400 (———). To determine the effect of the monoclonal antibody (anti-LPS) bacteria were incubated with mAB 786-D10 for 10 min at 37° C before adding the phage (----)

by P2813, a rough mutant of *E. coli* K12 (Table 4), was slow (Fig. 4); the efficiency of plating on this strain was reduced and the plaques were small. When chloramphenicol-treated bacteria were incubated with a monoclonal antibody directed against the inner core region of LPS, and tested for phage inactivation (Fig. 4), the rate of inactivation was reduced in all cases. The effect on strains B/r and P2813 was less significant than the effect on P400. Because the monoclonal antibody does not interact with P2813 LPS (Bitter-Suermann, personal communication), the minor difference in inactivation rates with or without the antibody was due to nonspecific steric hindrance (Fig. 4).

To determine whether the effects described are caused by gp12, similar experiments were carried out using partially purified gp12 instead of bacteriophage (Table 3a). Binding of partially purified gp12 to whole cells also appeared to be related to the type of cellular LPS. The behaviour of the phage (K3hx, Fig. 4B) is the same as the behaviour of its gp12 (Table 3a). Data obtained with other *E. coli* K12 strains containing additional LPS mutations (data not shown) indicated that gp12 binding and K3hx inactivation is drastically reduced whenever the heptose is missing.

To prove that LPS rather than some other surface component was responsible for differences in gp12 binding, binding of extracted gp12 to LPS isolated from three different strains of *E. coli* was determined (Table 3b–d). Binding of gp12 to isolated LPS exhibited the same pattern as gp12 binding to whole bacteria. In addition, preincubation of LPS with mAB 786-D10 abolished binding of gp12 to P400 LPS but had no effect on binding of gp12 to B/r LPS (Table 3c, d, compare with Fig. 4).

The binding site of mAB 786-D10 is proposed to be the Hex-Glc-Glc-Hep region within the core of *E. coli* K12 LPS (Peters et al. 1985). Because this antibody reduces gp12 binding to K12 LPS and because gp12 binds poorly to species of LPS lacking the heptose residue, (P2812 and other strains tested; Yu and Mizushima 1982; unpublished results) the inner core region, especially the heptose, appears to be involved in gp12 binding (Table 4).

B/r LPS recognized by mAB 786-D10 in immunoblots and in ELISA (Bitter-Suermann, personal communication). The antibody does not specifically reduce K3 or K3hx inactivation by B/r cells (Fig. 4) and cannot abolish gp12 binding to B/r LPS (Table 3c, d). Thus the binding site of gp12 is different from the mAB 786-D10 binding site in B/r LPS.

Discussion

Efficient expression of cloned phage genes combined with in vitro complementation assays have the following advantages: only a partial purification is required to test the reactions of the gp. No other unknown phage components are present which could interfere with the reaction. In the case of host recognition by T-even proteins the complicated multi-step reaction of infection by phage can be dissected into the single steps which can be tested individually. Here, the ability of different *E. coli* strains to inactivate bacteriophage K3 and its host range mutant K3hx could be associated with the different abilities of LPS in the strains to bind gp12. Gp12 binding to OmpA and OmpF is excluded. Because K3 and K3hx cannot infect *E. coli* lacking the OmpA protein, the first step of recognition, long tail fibre binding to the outer membrane, seems to be the stringent step in host recognition. Gp12 binding to the LPS in the outer membrane, the second step in phage infection, is less specific and influences the efficiency of phage infection.

Most likely gp12 specificity is the same in all T-even type phages: T4N69 defective phage complemented with gp12 of T2 or K3hx behaves as a normal T4 phage with the host specificity of T4. Furthermore, the DNA including g12 is highly conserved. Even the restriction maps are similar. In contrast, the genes coding for the long tail fibres are very heterologous with respect to the restriction sites and DNA sequences (Riede et al. 1984, 1985).

The heptose of *E. coli* K12 LPS is necessary for efficient binding of gp12: whenever the heptose was missing in the LPS of bacteria (P2812 and other strains tested, unpublished results), the binding of gp12 to the bacterial surface decreased drastically. The binding of gp12 to the LPS of K12 could be suppressed with a monoclonal antibody directed against the inner core region. We do not yet know which structure in *E. coli* B LPS is recognized. The observation that the same monoclonal antibody has a binding specificity to B/r LPS different from that of gp12 suggests that short tail fibres have several different binding specificities.

Acknowledgements. I am very grateful to U. Henning and S. MacIntyre for critical aid in the preparation of the manuscript, to M.L. Eschbach for excellent technical assistance, to D. Bitter-Suermann, H. Peters and H. Schwarz for providing antibodies, to N. Murray, W.B. Wood and H. Schaller for donating phage amber mutants and g57 DNA and to U. Henning for the gift of LPS.

References

Achtman M, Willetts N, Clark AJ (1971) Beginning a genetic analysis of conjugational transfer determined by the F-factor in *Escherichia coli* by isolation and characterization of transfer-deficient mutants. J Bacteriol 106:529–538

Beckendorf SK (1972) Structure of the distal half of the bacteriophage T4 tail fiber. J Mol Biol 73:37–53

Chang ACY, Cohen SN (1978) Construction and characterization of amplifiable multicopy DNA cloning vehicles derived from the P15A cryptic miniplasmid. J Bacteriol 134:1141–1156

Galanos C, Lüderitz O, Westphal O (1969) A new method for the extraction of R-lipopolysaccharides. Eur J Biochem 9:245–249

Goldberg E (1983) Recognition, attachment and injection. In: Mathews CK, Kutter EM, Mosig G, Berget P (eds) Bacteriophage T4. American Society for Microbiology, Washington, DC, pp 32–39

Hanahan D, Meselson M (1980) Plasmid screening at high colony density. Gene 10:63–67

Hancock REW, Reeves P (1975) Bactriophage resistance in *Escherichia coli* K12: general pattern of resistance. J Bacteriol 121:983–993

Hantke K (1978) Major outer membrane proteins of *Escherichia coli* K12 serve as receptors for the phages T2 (protein Ia) and 434 (protein Ib). Mol Gen Genet 164:131–135

Henning U, Jann K (1979) Two component nature of bacteriophage T4 receptor activity in *Escherichia coli* K-12. J Bacteriol 137:664–666

Henning U, Schmidmayr W, Hindennach I (1977) Major proteins of the outer cell envelope membrane of *Escherichia coli* K12: multiple species of protein I. Mol Gen Genet 154:293–298

Henning U, Schwarz H, Chen R (1979) Radioimmunological screening method for specific membrane proteins. Anal Biochem 97:153–157

Herrmann R (1982) Nucleotide sequence of the bacteriophage T4 gene 57 and a deduced amino acid sequence. Nucleic Acids Res 10:1105–1112

Hermann R, Wood WB (1981) Assembly of bacteriophage T4 tail fibers: Identificaton and characterization of the nonstructural protein gp57. Mol Gen Genet 184:125–132

Kells SS, Haselkorn R (1974) Bacteriophage T4 short tail fibers are the product of gene 12. J Mol Biol 83:473–485

Kells SS, Ohtsuki M, Haselkorn R (1975) The structure of bacteriophage T4 gene 12 protein. J Mol Biol 99:349–351

Kutter E, Rüger W (1984) Map of the T4 genome and its transcriptional control sites. In: Mathews CK, Kutter EM, Mosig G, Berget P (eds) Bacteriophage T4. American Society for Microbiology, Washington, DC, pp 277–290

Lämmli UK (1970) Cleavage of structural proteins during the assembly of the head of bacteriophage T4. Nature 227:680–685

Maniatis T, Fritsch EF, Sambrook J (1982) Molecular cloning, a laboratory manual. Cold Spring Harbor Laboratory Press, NY

Maniatis T, Jeffrey A, Kleid DG (1975) Nucleotide sequence of the rightward operator of phage λ. Proc Natl Acad Sci USA 72:1184–1188

Mason WS, Haselkorn R (1972) Product of T4 gene 12. J Mol Biol 66:445–469

Miller JH (1972) Experiments in molecular genetics. Cold Spring Harbor Laboratory Press, NY

Peters H, Jürs M, Jann B, Jann K, Timmis KN, Bitter-Suermann D (1985) Monoclonal antibodies to enterobacterial common antigen and to *E. coli* lipopolysaccharide outer core: demonstration of an antigenic determinant shared by enterobacterial common antigen and *E. coli* K-5 capsular polysaccharide. Infect Immun 50:459–466

Pugsurs A, Medon P, Corless C, Hackett J, Reeves P (1983) A class of *ompA* mutants of *Escherichia coli* K12 affected in the interaction of OmpA protein and the core region of lipopolysaccharide. Mol Gen Genet 189:162–165

Riede I, Eschbach ML, Henning U (1984) DNA sequence heterogencity in the genes of T-even type *Escherichia coli* phages encoding the receptor recognizing protein of the long tail fibers. Mol Gen Genet 195:144–152

Riede I, Drexler K, Eschbach ML (1985a) The nucleotide sequences of the tail fiber gene 36 of bacteriophage T2 and of genes 36 of the T-even type *Escherichia coli* phages K3 and Ox2. Nucleic Acids Res 12:605–616

Riede I, Eschbach ML, Henning U (1985b) Presence of DNA encoding parts of bacteriophage tail fiber genes in the chromosome of *Escherichia cali* K12. J Bacteriol 163:832–836

Rüther U, Koenen M, Otto K, Müller-Hill B (1981) pUR222, a vector for cloning and rapid chemical sequencing of DNA. Nucleic Acids Res 9:4087–4098

Sanger F, Nicklen S, Coulson AR (1977) DNA sequencing with chain terminating inhibitors. Proc Natl Acad Sci USA 74:5463–5467

Schwarz H, Riede I, Sonntag I, Henning U (1983) Degrees of relatedness of T-even type *Escherichia coli* phage using different or the same receptors and topology of serologically cross-reacting sites. EMBO J 2:375–380

Segrest JP, Jackson RL (1972) Molecular weight determination of glycoproteins by polyacrylamide gel electrophoresis in sodium dodecyl sulfate. Methods Enzymol 28:54–63

Simon LD, Anderson TD (1967) The infection of *Escherichia coli* by T2 and T4 bacteriophages as seen in the electron microseope. Virology 32:279–297

Simon LD, Swan JG, Flatgaard JE (1970) Functional defects in T4 bacteriophages lacking the gene 11 and gene 12 products. Virology 41:77–90

Skurray RA, Hancock REW, Reeves P (1974) Con mutants: class of mutants in *Escherichia coli* K12 lacking a major cell wall protein and defective in conjugation and adsorption of a bacteriophage. J Bacteriol 119:726–735

Towbin H, Staehelin T, Gordon J (1979) Electrophoretic transfer of proteins from polyacrylamide gels to nitrocellulose sheets: Procedure and some applications. Proc Natl Acad Sci USA 76:4350–4354

Tsai CM, Frasch CE (1982) A sensitive silver stain for detecting lipopolysaccharides in polyacrylamide gels. Anal Biochem 119:115–119

Vanderslice RW, Yegian CD (1974) The identification of late bacteriophage T4 proteins on sodium dodecyl sulfate polyacrylamide gels. Virology 60:265–275

Vieira J, Messing J (1982) The pUC plasmids, an M13mp7-derived system for insertion mutagencsis and sequencing with synthetic universal primers. Gene 19:259–260

Wilson GG, Tanyashin VI, Murray NE (1977) Molecular cloning of fragments of bacteriophage T4 DNA. Mol Gen Genet 156:203–214

Wood WB, Revel HR (1976) The genome of bacteriophage T4. Bacteriol Rev 40:847–868

Yu F, Mizushima S (1982) Roles of lipopolysaccharide and outer membrane protein OmpC of *Escherichia coli* K-12 in the receptor function for bacteriophage T4. J Bacteriol 151:718–722

Zorzopulos J, Delong S, Chapman V, Kozloff LM (1982) Host receptor site for the short tail fibers of bacteriophage T4D. Virology 120:33–41

Communicated by G. Melchers

Received August 18, 1986

129. Teplitz, R. L., Gustafson, P. E., Pellett, O. L. 1968. *Exp. Cell Res.* 52:379
130. Travers, A. A., Kamen, R. I., Schlief, R. F. 1970. *Nature* 228:748
131. van Heyningen, V., Craig, I., Bodmer, W. 1973. *Nature.* In press
132. Wallace, H., Birnstiel, M. L. 1966. *Biochim. Biophys. Acta* 114:296
133. Watkins, J. F., Chen, L. 1969. *Nature* 223:1018
134. de Weerd-Kastelein, E. A., Keijzer, W., Bootsma, D. 1972. *Nature New Biol.* 238:80
135. Weiss, M. C. 1970. *Proc. Nat. Acad. Sci. USA.* 66:79
136. Weiss, M. C., Chaplain, M. 1971. *Proc. Nat. Acad. Sci. USA* 68:3026
137. Weiss, M. C., Ephrussi, B. 1966. *Genetics* 54:1095
138. Weiss, M. C., Green, H. 1967. *Proc. Nat. Acad. Sci. USA* 58:1104
139. Weiss, M. C., Todaro, G. J., Green, H. 1968. *J. Cell Comp. Physiol.* 71: 105
140. Westerveld, A., Visser, R. P. L. S., Meera Khan, P., Bootsma, D. 1971. *Nature New Biol.* 234:20
141. Wiener, F., Klein, G., Harris, H. 1971. *J. Cell Sci.* 8:681
142. Yerganian, G., Nell, M. B. 1966. *Proc. Nat. Acad. Sci. USA* 55:1066
143. Yoshida, M. C., Ephrussi, B. 1967. *J. Cell Physiol.* 69:33
144. Zepp, H. D., Conover, J. H., Hirschhorn, K., Hodes, H. L. 1971. *Nature New Biol.* 229:119
145. Zinder, N. D., Lederberg, J. 1952. *J. Bacteriol.* 64:679

BACTERIOPHAGE RECEPTORS

❖ 1616

Alf A. Lindberg[1]

Department of Bacteriology, National Bacteriological Laboratory, Stockholm, Sweden

CONTENTS

INTRODUCTION

The susceptibility of a bacterium to bacteriophage infection is primarily dependent on whether or not the bacteriophage can attach to specific attachment sites, receptors, on the cell. A successful attachment may then be followed by the penetration of the phage nucleic acid into the cell. Intracellularly the replication of phage nucleic acid may follow, ultimately ending in the release of new phage progeny. The events

[1]Present address: Department of Medical Microbiology, Stanford University School of Medicine, Stanford, California 94305.

involved in the replication and synthesis of phage have been of primary interest to microbiologists and biochemists during the last two decades, whereas the attachment-penetration step has received little attention. In fact the last reviews dealing with bacteriophage receptors (44, 162, 172), which are about 15 years old, dealt almost exclusively with the *coli* T phages and the receptors in the *Escherichia coli* B cell wall. Although a vast amount of information has been accumulated about the replication of the T phages, today we know little more about their receptors. The recognition of the receptor is a highly specific process and is part of the natural mechanism of host recognition. The T4 phage which ordinarily lyses only strains of *Escherichia* and *Shigella* can, when the attachment step is bypassed, infect and grow in spheroplasts of strains of *Salmonella*, *Aerobacter*, *Proteus*, and *Serratia* (168). In the same way the inability of male-specific bacteriophages to infect female bacteria is due to the lack of receptors for the phages. Spheroplasts of female bacteria are as susceptible to infection by isolated phage nucleic acid as are spheroplasts of male cells (176). In spite of our ignorance about the receptors for the T phages, some information about the receptors for other bacteriophages has emerged. It is the intent of this review to summarize this information. No attempt will be made to analyze the mechanisms of the triggering of the nucleic acid or its penetration into the cell.

During the last decade the cell envelopes of both Gram-negative (41, 98, 118, 158) and Gram-positive (41, 46, 118) bacteria have been studied intensively from structural, biosynthetic, genetic, and functional viewpoints. As a result of these studies information of considerable value for investigations of phage receptor sites has emerged. Furthermore information concerning the assembly, structure, and function of flagella (58) and pili (14, 15) has been obtained. When phage receptors were studied during the 1950s, the phages of choice were the coli T phages (44, 162, 172). During the last decade new classes of phages have been isolated and identified such as the single-stranded DNA phages and RNA phages (14, 15, 53). Furthermore the principles of the structure, from a morphological viewpoint, and assembly of phages have been established (53). No generally accepted classification system exists, however, for bacteriophages. Of the ones at hand the classification proposed by Bradley (10), which defines six groups of bacteriophages based on their morphology and type of nucleic acid, is perhaps the most simple. It was tempting to base this review on the six groups and try to analyze the receptors for each group. Undoubtedly the receptor for a phage provided with a 40 nm wide base plate with both tail fibers and tailpins like T4 (148, 149) may differ from that of a phage which lacks tail and attaches with the aid of one or more of 3 nm long apical capsomeres like ϕX174 (7). But some phages belonging to different morphological groups have their receptors in the same structural components of the cell wall, e.g. the outer membrane of Gram-negative bacteria, which would make repetition unavoidable. The receptors are therefore discussed on the basis of the structural component of the bacterial cell where they are found and in the following order; receptors in 1. the outer membrane of Gram-negative bacteria, 2. the cell wall of Gram-positive bacteria, 3. the capsular layer of Gram-negative bacteria, 4. the flagella, and 5. the pili.

METHODOLOGICAL ASPECTS

The most commonly used methods for studies of the attachment of bacteriophage to bacteria for a demonstration of bacteriophage receptors are outlined in the now classic book by Adams (1). Briefly they consist of mixing phage and bacteria, and at time intervals taking samples from the mixture and assaying either for phage that has adsorbed and infected or for free phage. This can be done in several ways such as centrifuging the complex of phage and bacteria, shaking the sample with chloroform to kill the cells, filtering the sample through a filter permeable to phage but not to bacteria, or adding antiphage antiserum to neutralize nonattached as well as reversibly attached phage.

The kinetics of attachment is a first-order process, with respect to bacterial concentration (1, 44, 154, 162, 172). There are, however, several observations which show that the attachment deviates from strict first order kinetics: 1. attachment seems to take place in two steps—a temperature-independent reversible step followed by a temperature-dependent irreversible step (for a discussion see Stent, 154); 2. above certain bacterial concentrations the increase in bacterial density does not lead to a corresponding increase in attachment rate (1, 154); and 3. the attachment rate is more dependent on temperature than would be expected if the collision frequency were the only rate-determining factor (1, 154). The reasons for these deviations from simple first-order kinetics are not understood, but with these limitations in mind the numerical values of the observed attachment rates can be used for comparing availability of the receptors on bacteria; however, they permit no conclusions about the number of receptor sites or the mechanism of attachment. It must also be emphasized that in some bacteriophage-bacteria systems, such as those in which male-specific phages attach to pili, an attachment rate constant may be misleading since up to 85% of the pili can be found in the culture fluid (16).

The attachment rate depends not only on the concentration of the reactants but also on the ionic environment, temperature, pH, and organic cofactors. The importance of these factors upon the efficiency of the attachment process is thoroughly discussed by Adams (1) and Stent (154).

To characterize the receptor it is desirable to isolate it from the bacteria. This can be done in either of two ways: 1. isolating material from the cell by commonly used extraction and fractionation procedures, and testing whether the fractions inactivate the phage, reversibly or irreversibly, or 2. isolating from phage-infected bacteria the structural entity to which the phage is irreversibly attached. The former technique is the most commonly used. Several authors have used as a criterion of adsorbing capacity the ability of an isolated receptor to irreversibly inactivate the phage. For the larger tadpole-shaped DNA bacteriophages like T2, T4, and T6 this requirement is met only by isolated outer-membrane components. For a triggering of the irreversible attachment in these phages tail fibers as well as tail spikes must interact with the receptor (150); this explains the necessity for a large macromolecular complex. In some situations, however, only a reversible attachment can be demonstrated. The specificity of such an attachment can be tested by appropriate controls. An experi-

mental system with a specific reversible attachment is in fact better suited for a study of the phage-receptor interaction than is a system with the irreversible reaction.

RECEPTORS IN THE OUTER MEMBRANE OF GRAM-NEGATIVE BACTERIA

The outer membrane constitutes the surface layer of Gram-negative bacteria and may represent as much as 90% of the weight of the cell wall (46). It is composed of a complex of lipopolysaccharide (LPS), protein, and phospholipid. Only the LPS has been shown with certainty to be exposed at the cell surface (145) and thus accessible to phages, but the finding of the receptors for the T2 and T6 phages in a protein fraction isolated from the outer membrane (108, 172) indicates that the protein(s) is exposed as well. The structural integrity of the outer membrane and its association with the cell wall is incompletely known. Present information suggests that the outer membrane is not covalently bound to the peptidoglycan network but bound primarily by physical forces, i.e. ionic and/or hydrophobic, since mild treatments such as washing with distilled water or buffers (80) or treatment with a chelating agent like EDTA causes release of a complex of LPS, protein, and phospholipid into the surrounding medium (143, 145). The outer membrane is probably bound to a lipoprotein, which is covalently linked through its protein part to the peptidoglycan network and whose lipid part may extend out into the outer membrane to interact with the lipid A of LPS or other hydrophobic regions of the outer membrane (12).

The LPS is the only component of the outer membrane which has been fully characterized, and thus can give us information about the structure of phage receptors. Lipopolysaccharides are long-chain phosphate-containing heteropolymers composed of hydrophilic polysaccharide side chains linked to a hydrophobic lipid (lipid A) (98, 145). In members of the *Salmonella, Escherichia,* and *Shigella* genera the polysaccharide side chains consist of polymerized oligosaccharide repeating units, which carry the O-antigenic specificity, covalently linked to a core oligosaccharide (98). The core is identical or very similar in all *Salmonella* LPS (Figure 1) whereas at least four different cores have been identified in the LPS of different *Escherichia* strains (141; and B. Jann, personal communication). In *Shigella* only the *Shigella flexneri* core has been studied (65). Bacteriophage receptors have been found in the outer membrane of Gram-negative bacteria other than *Salmonella, E. coli,* and *Shigella* but since almost nothing is known about the structure of the LPS and proteins in these genera a discussion of their phage receptor systems will be omitted. The emphasis will instead be focused on the receptors found in *Salmonella,* in particular, and in *Escherichia* and *Shigella.* The topic of receptors in the LPS of Gram-negative bacteria was recently exhaustively covered (132) and the reader will find additional information in that review.

Bacteriophages representative of four of the six morphological groups of Bradley (10) have their receptors in the outer membrane. Phages of Bradley's group A phages, such as the coli phages T2, T4, T6, P1, and P2 and the *Salmonella* phages FO and C21, are double-stranded DNA-coutaining phages with a tail with a contractile sheath attached to it. The tail has an appendage, a base plate, which in T2 and T4 has the shape of a flat hexagon with a vertex-to-vertex diameter of 40 nm (149). The base plate has six long tail fibers, one extending from each vertex, and at least four short tailpins (148). Group B phages, such as the coli phage T5, differ from the group A phages in having a long tail without a contractile sheath. T5 has a small thickened disc, with a diameter of about 18 nm, near the end of the tail (10). There are also several thin fibers at the tip. Among the group C phages, which have a short noncontractile tail, are the *Salmonella* phages P22, ϵ^{15}, and ϵ^{34} and the coli phages T3, T7, and Ω8. The tail of P22 has a hexagonal base plate, about 20 nm wide, composed of six identical spikes arranged around a neck (61). The group D phages, such as the coli phage ϕX174 and the *Salmonella* phages 6SR and Br2, have no tail but attach with the aid of apical capsomeres, about 3 nm in size, which protrude from each of the 12 vertices of the icosahedron capsid (7, 10). Thus the part of the phage that attaches to the receptor varies widely in both size and structure.

Receptor Sites in the O Side Chain

The relationship between antigenic structure and phage susceptibility was first studied by Burnet who found in *Salmonella* a striking correlation between the presence of heat-stable antigens, what we now know as the O antigens, and phage susceptibility (19). Attempts to isolate receptor-active material failed, however. An extract, which retained its antigenic specificity, did not inactivate phage. Levine & Frisch (77) were the first to demonstrate that a saline extract of *Salmonella* with O-antigenic specificity, a fraction which presumably contained outer membrane, inactivated phages. Subsequently Burnet succeeded in isolating a phage-inactivating agent (PIA) from autolysates of *Salmonella;* here also the receptor-active material was presumably an outer membrane fraction (20). It can be assumed that the receptor specificity for several of the smooth specific phages concerned resided in the O side chain.

Four phages of Bradley's group C, ϵ^{15}, ϵ^{34}, g_{341}, and P22, attach to (or have as critical sites in the receptor) the O side chains of *Salmonella* bacteria (49, 91, 182, 188), whereas Ω8 attaches to the O polysaccharide chain of *E. coli* (62a, 132a). Common to all four phages is the ability to cause lysogenic conversion, i.e. the appearance of new O-antigenic specificities (164). The O side chains of *Salmonella anatum* (serogroup E1, O antigens, 3,10) is built by polymerized repeating units attached to LPS core:

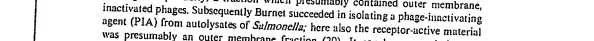

The linkage between the repeating units is Gal 1 $\xrightarrow{\alpha}$ 6 Man. Phages ϵ^{15} and g_{341} attach to whole bacteria of *S. anatum* and are inactivated by phenol-water extracted LPS of *S. anatum* (49, 91). Rough mutants of *S. anatum* (making LPS

core without O chains) are resistant to ϵ^{15} and g_{341}, as are also semirough mutants (i.e. those with one repeating unit only in the O chain). Lysogenization with ϵ^{15} (133) causes 1. a block in transacetylase synthesis so that O-acetyl groups are not transferred to C-6 of the D-galactose residue of the O repeating unit, 2. production of a new repeating unit polymerase and of an inhibitor of the α-polymerase so that the anomeric configuration of the linkage between the repeating units is changed from α to β. The nonlysogenic *S. anatum* strain adsorbs phages ϵ^{15} and g_{341} able to effect the conversion; the converted strains (to O antigens 3,15) by lysogeny for either of these phages fail to adsorb either of them (49, 133). Phage ϵ^{15} could attach to a *S. anatum* mutant which retained the α linkage between the repeating units but lacked the O-acetyl group on D-galactose, but did not attach to a lysogenized strain which had the linkage between the repeating units in β configuration but retained the O-acetyl groups (91). This shows that the Gal 1-α? 6 Man linkage is a critical site in the receptor for this phage (91). The use of similar mutants for phage g_{341} revealed that, by contrast, the O-acetyl group is a critical site in the receptor (49). Another converting phage ϵ^{34} does not attach to and lyse *S. anatum* (O antigen 3,10) until it has been lysogenized and converted to O antigen 3,15 by ϵ^{15} (182). This indicates that the anomeric nature of the linkage between the repeating units is a critical site in the receptor for ϵ^{34}, but in contrast to ϵ^{15}, phage ϵ^{34} prefers the β linkage. Lysogenization with ϵ^{34} leads to the appearance of a new O-antigen specificity, O-34, due to glucosylation of C-4 of at least 80% of the D-galactose residues of the repeating unit (183). The attachment rate for ϵ^{34} to the converted (O antigens 3,34) bacteria is only 10% of the rate to non-ϵ^{34} converted (O antigens 3,15) bacteria (183). Thus access of ϵ^{34} to its receptor site is prevented by glucosyl residues on C-4 of D-galactose whereas ϵ^{15} is not prevented from attaching to strains with O-acetyl residues on C-6 of D-galactose. Both phages are morphologically indistinguishable; the difference may be because the O acetyl is smaller than the D-glucose residue and does not constitute the same hindrance, or because the glycosylation of D-galactose is more complete than the substitution with O acetyls, or because an unsubstituted C-4 of D-galactose is more essential in the receptor site for ϵ^{34} than an unsubstituted C-6 carbon is in the receptor site for ϵ^{15}.

Phage P22 attacks only strains of *Salmonella* with O-antigen 12 specificity; i.e. serogroups A, B, and D1 (188). Rough mutants and semirough strains with an O side chain containing only one repeating unit are resistant (Figure 1) (112). This implies that as for ϵ^{15} and g_{341} one repeating unit only is insufficient as a receptor for P22. The repeating unit of the O side chains of serogroups A, B, and D1 are all built of units Man 1 -α? 3 Rha 1 -α? 4 Gal substituted at C-3 of D-mannose by a dideoxyhexose (96–98). The linkage between the repeating units is Gal 1 -α? 2 Man in all serogroups (71, 98). The serogroups differ only in the nature of the dideoxy sugar linked to D-mannose (71, 98). The linkage between successive repeating units is again thought to be a critical site in the receptor since lysogenization with phage P27, which alters the linkage between the repeating units from Gal 1 -α? 2 Man to Gal 1 -α? 6 Man, reduced the P22 attachment rate from 410×10^{-11} ml min^{-1} to $<5 \times 10^{-11}$ ml min^{-1} (82). Any part of the repeating unit

or even several repeating units may constitute a critical site since the alteration of the linkage between repeating units is supposed to have an influence on the conformation of the entire O side chain. Substitution of the D-galactose residue of the repeating unit with a D-glucose residue in α-1,6 linkage (Figure 1), the lysogenic conversion caused by P22, reduces the attachment rate from two- to tenfold (82, 188). The varying degrees of reduction in attachment rate is expected since the P22-mediated 1,6 glucosylation is subject to form variation (159); i.e. only a fraction of the bacteria express the information and thus acquire the α-1,6-linked D-glucose residues.

Receptor Sites in the Basal Core

Among the phages isolated by Burnet (19) were some that were active on both smooth and rough strains and others active on rough strains only. In both of these classes the receptors were found in extracts which presumably contained the outer-membrane fraction (20). Phages active on both smooth and rough strains presumably adsorb to rough-specific structures, i.e. sites in the basal core accessible to the phage even in smooth strains, or both the O side chains and the core may contain identical or similar structures able to act as receptors. Among phages with a smooth-rough specificity the *Salmonella* phage Felix O (FO) and the coli phages P1 and P2 will be discussed. Resistance of a smooth strain to a bacteriophage active only on the rough mutant, if due to failure of attachment, might result either from the absence of the relevant chemical structure which creates the attachment site or from masking the attachment site by more superficial components. Rough-specific phages to be discussed are the *Salmonella* phages 6SR, Br2, and C21 and the coli phages T3, T4, and T7.

The FO phage lyses most smooth *Salmonella* strains and all rough strains with a complete basal core, i.e. with a terminal nonreducing N-acetyl-D-glucosamine residue (Figure 1). The phage attaches irreversibly to extracted LPS; the tail sheath contracts and the nucleic acid is ejected (78). The amino sugar is a critical site in the receptor; isogenic rough mutants lacking only the amino sugar are resistant to the phage and neither attachment to whole cells nor inactivation by their LPS can be demonstrated (78, 81). The fact that smooth strains are susceptible to FO is not due to the presence of receptor-active material in the O side chain, revealed by the structural analyses of the latter (98), but merely that the core is accessible to the phage. This may be because some core stubs do not carry an O side chain, even if this has not been revealed in structural analyses of smooth strains; or because the amino sugar is a terminal (nonreducing) branch of the core (81, 98). Not merely the presence of the terminal N-acetyl-D-glucosamine residue but also its anomeric configuration and linkage to the preceding sugar is important. The core of *Sh. flexneri* also has α-linked N-acetyl-D-glucosamine as a terminal nonreducing sugar (65) but linked to C-4 of D-galactose as compared to C-2 of D-glucose in the *Salmonella* core (Figure 1). With the amino sugar linked to the C-4 of D-galactose no attachment of the FO phage to the bacteria could be demonstrated (79). *E. coli* strains susceptible to the FO phage have a basal core structure named *coli* R2. Structural studies

of the *coli* R2 LPS revealed that the core oligosaccharide was identical to that of *Salmonella*, except that the D-galactose I residue had been replaced by a D-glucose residue (57). This change in the next to subterminal sugar residue did not alter the FO attachment rate as compared to that of *Salmonella* rough mutants with a complete basal core (79).

Though the N-acetyl-D-glucosamine residue seems to be accessible in smooth strains the presence of O side chains reduces the attachment rate from a mean value of 265×10^{-11} ml min^{-1} in complete-core rough mutants to $<5 \times 10^{-11}$ ml min^{-1} in smooth strains (Figure 1) (84, 87). Since the attachment rate to semirough strains, with an O side chain of one repeating unit only, is almost the same as to rough mutants with no O side chain (Figure 1) (81, 84, 87), substitution of C-4 of the subterminal D-glucose II residue of the core with an O side chain cannot be the cause of the reduced attachment rate. The most likely explanation is that the O side chain causes a steric hindrance for the access of the phage to its receptor. This theory finds support in a recent study on strains of *Salmonella* serogroup E1 (182). The smooth strain *Salmonella anatum* A1 is resistant to the FO phage but rough mutants with a complete core are susceptible. Lysogenization of strain A1 with phage ϵ^{34}, which cannot express its glucosylation in strains with α-linked galactose residues (see above), results in accumulation of glucose on the antigen-carrier lipid (182). This interfered with O side chain biosynthesis, and the observed reduction of O side chain sugars by 30%, as compared to the nonlysogenized strain, was accompanied by appearance of FO susceptibility (182).

The bacteriophages P1 and P2 were both isolated from the lysogenic *E. coli* strain Lisbonne and Carrère (8) and are identical (or closely related) to the phages H^- and H^+ respectively (8), whose receptors have been studied (9). In this review the designations P1 and P2 will be used. P1 and P2 have a broad lytic spectrum and lyse the *E. coli* strains B, C, and K12 as well as *Shigella dysenteriae, Sh. flexneri,* and *Sh. sonnei* strains (8, 9). Since both smooth and rough strains are lysed P1 and P2 can be classified as smooth and rough specific. Both are irreversibly inactivated by LPS (9) and since rough strains *E. coli* B and K12 are both susceptible it can be reasonably assumed that the structures determining the receptor specificity are to be found in the basal core. Because of our ignorance of the core in these strains the identification of critical sites in the receptor can only be tentative. The core polysaccharide of *E. coli* B contains 2-keto-3-deoxyoctonate (KDO), a heptose, and D-glucose, whereas that of strain K12 in addition contains D-galactose (and L-rhamnose) (96; G. Schmidt, personal communication). The mutation *galU* in *E. coli* K12, which prevents addition of hexoses to heptose in the basal core, makes the strain resistant to phage P1c1r (a cI mutant of phage P1kc) (40); this suggests that D-glucose linked to heptose is part of the receptor. Measurable attachment of the P1 phage was observed only onto a chemotype Rc mutant (galactose deficient) (Figure 1) in an investigation of P1 transduction to a series of isogenic rough mutants of *Salmonella typhimurium* (117), as expected if a terminal D-glucose residue is a critical part of the P1 receptor. The fact that P1 attaches to parent *E. coli* K12 bacteria and to *Shigella sonnei* phase II cells (9), both making LPS which includes D-galactose residues (96), does not contradict the theory; the

D-glucose residue(s) concerned may be present in a terminal nonreducing position in the core side chain, e.g. as a branch(es). The same arguments and an analogy with the morphologically similar FO phage can be used to explain the susceptibility of smooth *Sh. flexneri* strains to P1 infection (48). No similar data are available to infer the structure of the P2 receptor except that it is found in core LPS containing heptose and D-glucose (9).

The C21 bacteriophage lyses mutants of *E. coli* B, *E. coli* K12, and *S. typhimurium* lacking either UDP-galactose-4-epimerase (galE) or D-galactose-1-transferase (*rfaH*), or UDP-glucose-pyrophosphorylase (*galU*) or D-glucose-1-transferase (*rfaG*) (158, 178). In *Salmonella* mutations *galE* and *rfaH* result in a core side chain terminating with glucose I α-2 3 heptose (Figure 1); mutations *galU* and *rfaG* result in a core terminating with only heptose (178). The attachment rates of C21 to C21-sensitive *galE* and *galU* mutants of *E. coli* K12 were approximately the same, but only the LPS extracted from the *galE* mutants inactivated the phage (132). Thus no clear data about the C21 receptor sites were obtained (132). The mean attachment rate to five *S. typhimurium* mutants either with deletions covering the galactose operon, and therefore unable to incorporate galactose in the basal core, or with point mutations of the epimerase gene (*galE* m mutants) was 77×10^{-11} ml min^{-1} (Figure 1) (83). The mean attachment rate to seven *S. typhimurium* mutants unable to add the D-glucose I residue to heptose (Figure 1), due to either a transferase (*rfaG*) or a pyrophosphorylase (*galU*) defect was $<5 \times 10^{-11}$ ml min^{-1} and the relative efficiency of plating about 5×10^{-2} (83). This suggests, in accordance with the LPS inactivation experiments (132), that a core structure with a terminal D-glucose residue linked to heptose better satisfies the complementary structure(s) on the C21 phage tail than a core structure without the D-glucose residue. It seems less likely that the terminal nonreducing heptose III residue (Figure 1) is a critical component in the C21 receptor because chemotype Rb_3 (Figure 1) mutants and all mutants with more distal defects in the core polysaccharide (Rb_2, Rb_1, Ra) (Figure 1) are C21 resistant and the phage does not adsorb to these strains (83, 178). Phage C21 is morphologically similar to FO and the addition of the D-galactose II residue to the side branch of the D-glucose I residue would not be expected to cause a steric hindrance to the access of the phage to the heptose III residue.

Phages of the ϕX174 group lyse rough mutants of several genera of *Enterobacteriaceae* such as *Escherichia, Shigella, Salmonella,* and *Citrobacter* (11, 100, 141, 170, 178). The best-studied members of this group are ϕX174, 6SR=ϕR, S13, Br2, and U3. All the phages have the same morphology; they are icosahedral with a vertex-to-vertex diameter of 25 to 30 nm (7, 10). The particles have no tails but rather small apical capsomeres (spikes) about 3 nm in size protrude from each of the 12 vertices (10). Attachment of the ϕX-type phages apparently takes place with the aid of the vertex capsomeres. Evidence for this is 1. mutants within any of the cistrons B, G, or H (previously labeled IV, III, and II) affect the attachment of the phage to its host *E. coli* (113); 2. removal of the vertex capsomeres with 4 *M* urea destroys the ability of the phage coat to attach to bacteria but leaves the capsid containing DNA (35). The fact that the phages do not agglutinate bacteria (70) or

isolated receptor-containing LPS (79) suggests that only one of the vertex capsomeres is specialized for attachment to the receptor. The first detailed study of ϕX174 attachment was to isolated cell walls of *E. coli* C (42), a strain unclassified in terms of core structure. The phage adsorbed to a phenol-insoluble cell wall fraction and to trypsin-treated cell walls but not to lysozyme-treated cell walls. This led the authors to conclude that the receptor was to be found in the mucopeptide, a hypothesis also supported in a recent paper (18). No chemical analysis of the receptor-containing fractions (i.e. criteria of homogeneity and purity) and no analyses of which cell wall components were present were done. Available data on the receptors for the 6SR and Br2 phages show that they attach irreversibly to the LPS part of the outer membrane (81, 85). Phage ϕX174 has a host range similar to that of 6SR when tested on different rough mutants of *S. typhimurium* (178), and the lytic spectrum of the ϕX-like phages in several rough mutants of *Salmonella* and *Escherichia* is influenced by the structure of the core side chain (141, 178). It is thus reasonable to assume that the ϕX-like phages have their attachment sites in the LPS.

The structure in the *Salmonella* basal core which provides optimal attachment for phage Br2 has either the N-acetyl-D-glucosamine or the D-glucose II residue as the terminal nonreducing sugar (Figure 1) (181). Both residues are α1,2 linked to the preceding monosaccharide (81). A measurable attachment rate (67×10^{-11} ml min^{-1} as compared to 444×10^{-11} ml min^{-1} to complete-core mutants) was also found for *S. typhimurium galE* mutants (83). These mutants have the α1,3 D-glucose I residue as the terminal sugar (Figure 1). The Br2 attachment rate to *S. typhimurium* mutants with terminal α1,3-linked D-galactose-I residues was 38×10^{-11} ml min^{-1} (81) whereas no attachment was demonstrable to mutants with terminal D-galactose II or heptose residues (Figure 1) (81, 83). The relative efficiency of plating for phage Br2 on these mutants was also $<10^{-2}$ (79, 80). The 6SR phage attaches with a high rate only to *S. typhimurium* rough mutants with a terminal nonreducing α1,2-N-acetyl-D-glucosamine residue (Figure 1) but the phage lyses bacteria terminating with the D-glucose II-, D-galactose I-, and D-glucose I residues (Figure 1) (81, 178). However, the attachment rate is reduced tenfold as conipared to complete-core mutants (81, 83); the relative efficiency of plating is also reduced, to $<10^{-1}$ (83). Neither Br2 nor 6SR adsorbs to or lyses semirough strains (81, 178). This might be due either to steric hindrance or to the requirement that the D-glucose II residue be unsubstituted (the site where the O chains are attached).

Among the T phages T3, T4, and T7 have their receptors in the LPS (64, 172). The evidence that phages T3, T4, and T7 are rough specific is that 1. *E. coli* B and *E. coli* K12 are rough mutants (whose smooth parent strains are unknown); 2. *Shigella sonnei* phase I bacteria are resistant, whereas the phase II bacteria, which are susceptible, possess characteristics which classify them as rough mutants, i.e. rough-colony morphology and autoagglutinability in saline and acriflavine; and 3. smooth strains of *Sh. flexneri* are resistant to T3, T4, and T7, but their spontaneous mutants are sensitive to one or more of T3, T4, and T7 (9). Thus the T3, T4, and T7 receptors are probably found in the basal core of *E. coli* and *Shigella* bacteria. Because of our lack of knowledge of the core structure in these genera, with a few

exceptions (57, 65), attempts to infer the structure of the T3, T4, and T7 receptors can only be tentative. Isolated LPS from *E. coli* B (172) and *Sh. sonnei* phase II bacteria (64) cause irreversible attachment, i.e. contraction of the tail sheath, and in the interaction with *Sh. sonnei* LPS the phage DNA becomes susceptible to DNase (64). Bacterial mutants resistant to T3, T4, and T7 were isolated in *E. coli* B (172) and *Sh. sonnei* (64) and studies on their chemical composition revealed that resistance was accompanied by a loss of hexoses and heptose. The *E. coli* B mutants, selected as T4-resistant colonies and unable to adsorb any of the T3, T4, or T7 phages (95), were found in later investigations to have very low levels of UDP-glucose-pyrophosphorylase (*galU*) (50). Hence the core side chain must terminate with heptose, only a few residues of which are expected to carry D-glucose residue(s). This would indicate that the D-glucose residue(s) linked to heptose forms an essential part of the receptor for phages T3, T4, and T7. This is contradictory to the results obtained with mutants lacking pyrophosphorylase (*galU*) of *E. coli* K12. The attachment rate for T4 to the parent strain was 260×10^{-11} ml min^{-1} and to the mutant strain 290×10^{-11} ml min^{-1} (43), and though attachment rates for the other phages were not estimated the efficiency of plating of T3 on the mutant strain was 1.0 (43). Since it is assumed that the different basal core types of *E. coli* are identical in the KDO-heptose region and differ only in the structure of the hexose region (B. Jann, personal communication) the data for *E. coli* B, *E. coli* K12, and the T3, T4, and T7 receptors are at present inconclusive.

Receptor Sites in the Protein Part of the Outer Membrane

Receptor activity for the T2 and T6 phages were found by Weidel (172) and Jesaitis & Goebel (64) in phenol-soluble extracts presumably containing the outer membrane; it was inferred but never proven that the receptor sites were protein. That this is so has been shown by independent observations (31, 108). An outer membrane fraction, rich in LPS and protein but with a low phospholipid content, was isolated by Triton X-100 treatment of the outer membranes of T2-infected *E. coli* K12 (31) obtained from spheroplasts. This fraction, purified by sucrose gradient centrifugation followed by isopycnic sedimentation in cesium chloride, retained the attached T2 particles with the base plate 30 to 35 nm from the surface and with the tail needle penetrating the surface of the membrane fragments (31). Since the LPS does not inactivate the phage (64, 172), the protein fraction, where the dominating component representing 70% of the proteins has a molecular weight of about 44,000 (143), is inferred to be the carrier of the T2 receptor (31). The protein fraction was also isolated from the outer membrane of spheroplasts of *E. coli* B dissociated from the LPS by treatment with 2 *M* urea and separated by gel electrophoresis (108). This fraction, which contained 95% protein, 3% lipid, and 2% sugar, in a concentration of 100 μg inactivated 93% of added T6 phages. This inactivation could be inhibited by *E. coli* B antiserum, previously absorbed with *E. coli* B LPS; the phage-receptor activity can therefore be assumed to be caused by the protein and not by contuminating lipids or polysaccharides (LPS?) (108). The T2 and T6 inactivating capacity could furthermore be abolished by treating the protein fraction with proteolytic

enzymes (108). However, phages T2 and T6 do not have the same receptor since mutants of *E. coli* resistant to one phage but susceptible to the other have been isolated (172). Treatment of trypsinized *E. coli* strain Cullen cell walls, which inactivated T2 and T6, with either papain, ficin, pepsin, or pronase selectively destroyed the T2 receptor, whereas the T6 receptor activity was unaltered (173).

The T5 receptor was found in a complex that could be extracted from *E. coli* B by weak alkali (172). Chemically it was inferred to consist of lipoprotein surrounding a core of LPS—thus representing an outer membrane fraction; the purified (outer membrane) fraction, a uniform complex with a molecular weight of 11.4 X 10^8, triggered the release of T5 nucleic acid (172). The receptors for T3, T4, and T7 hidden in the LPS core were unmasked by extraction of the complex with phenol-water, which concomitantly destroyed the T5 receptor (172). The conclusion was that the T5 receptor resided in the lipoprotein layer (172). No further studies on this receptor substance have been reported.

Localization of the Receptors on the Bacterial Surface

Receptor sites, forming part of the LPS that is a component of the outer membrane, are readily available to the phages concerned (79, 84). There was a direct correlation between rates of phage attachment to whole cells and the phage-inactivating capacity of LPS isolated from the same strain; a strain which adsorbed phage rapidly yielded a LPS with a high phage-inactivating capacity (i.e. the concentration of LPS that inactivates 50% of added phage) (78), whereas strains which adsorbed slowly yielded LPS with a low phage-inactivating capacity. Thus the protein and phospholipid components of the outer membrane do not seem to interfere with the attachment of phages to its LPS component, not even when the receptor is in the LPS core. The ability of the phage to attach seems to depend only on whether or not the receptor site is present (and exposed) and whether or not the exposed site is accessible to the phage. For phages with the receptor in the O side chain, like ϵ^{15} and P22, the receptor is present if the O side chain contains more than one repeating unit and is then always accessible (62, 68, 159, 188). Phages with the receptor in the LPS core face the problem of interference of the attachment caused by the presence of O side chains in both smooth and semirough (with one repeating unit) strains. The O side chains were estimated to extend up to 150 nm out from the cell surface (145). The FO phage can lyse smooth strains because a critical site in the receptor, the N-acetyl-D-glucosamine residue (Figure 1), forms a branch of the core (81) or because some of the core stubs are left uncapped by O side chains. The ϕX group of phages have their receptors in the core, and for Br2 and 6SR the complete core of *Salmonella* is the best receptor structure (Figure 1) (81). Neither smooth nor semirough strains are susceptible to these phages; this may be because the O side chain interferes with the access of the apical capsomer(es) to the receptor or because adsorption of these phages requires a D-glucose II residue unsubstituted at C-4, the site to which the O chain is attached (Figure 1). The resistance of smooth and certain classes of rough mutants to phage C21 probably results from masking of the receptor site, the D-glucose I-heptose region of the LPS core, by the distal sugars, D-galactose I and II etc (Figure 1) (83, 86, 132).

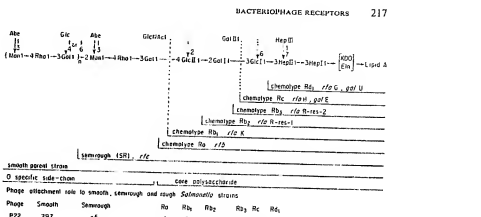

Figure 1 General structure of the polysaccharide side chain of the lipopolysaccharide of *Salmonella typhimurium* (76, 81). The designation of the chemotypes is according to Lüderitz, Staub & Westphal (97). Semirough mutants (genotype *rfc*) lack the repeating unit polymerase and consequently only one repeating unit is added to the core; chemotype Ra mutants (*rfb*) have a defect in the synthesis of the repeating unit; chemotype Rb_1 mutants (*rfaK*) lack the N-acetyl-D-glucosamine transferase; chemotype Rb_2 mutants (*rfa* R-res-1) lack the D-glucose II transferase; chemotype Rb_3 mutants (*rfa* R-res-2) terminate with the D-galactose II residue but have normal D-galactose I transferase activity, i.e. the nature of the defect is unknown; chemotype Rc mutants are the result of either the lack of D-galactose I transferase activity (*rfaH*) or the lack of UDP-D-galactose-4-epimerase activity (*galE*); chemotype Rd_1 mutants are the result of either the lack of D-glucose I transferase activity (*rfaG*) or the lack of UDP-D-glucose-pyrophosphorylase activity (*galU*). The table gives the mean attachment rate for phages P22 (smooth specific), FO (active on smooth and chemotype Ra mutants), and 6SR, Br2, and C21 (all active on rough mutants only) onto isogenic series of mutants of *S. typhimurium* strains LT2 and 395MS (79, 81, 83, 84, 87). The value for the attachment rate is x 10^{-14} ml min^{-1}. Abbreviations used: Abe, abequose; Man, D-mannose; Rha, L-rhamnose; Glc, D-glucose; Gal, D-galactose; GlcNAc, N-acetyl-D-glucosamine; Hep, L-glycero-D-mannoheptose; KDO, 2-keto-3-deoxyoctulosonic acid, Etn, ethanolamine; P, phosphate; *n* indicates the number of repeating units in the O side chain (values from 4 to 30 have been found).

The molecular architecture of the outer membrane and thus the distribution of receptor sites on the surface is not understood (41). There are no data that tell us how much of the surface is occupied by LPS nor how much by the protein and phospholipid components, nor how the LPS is distributed. The calculations by Rothfield & Romeo (135) indicate that an LPS molecule, containing three polysaccharide side chains, has a surface area of 23.2 ± 5 nm^2. The space occupied by the other structural components of the outer membrane was not determined. The poly-

saccharide side chains extending towards the surface are close to each other (97). The observation that only a few antibodies could bind to each *Salmonella* polysaccharide molecule was interpreted as indicating that the space between the O side chains was too narrow to allow antibody molecules to reach antigenic determinants situated in the proximal parts of the O chains (97). On this assumption the surface of a smooth bacterium can be visualized as tightly covered by O side chains and thus providing a mosaic of receptor sites, and so in theory the entire surface could presumably be covered by adsorbed O-specific phage. Measurements of the maximal number of phage particles attached to a single bacterium vary from 250 to 350 for the large DNA phages (30, 140, 169) to 1450 for the phages in the ϕX group (70).

The interesting question is whether any site will trigger the events leading to penetration of phage nucleic acid; i.e. are all sites equally good and lead to penetration or do some receptor sites permit only reversible attachment? Bayer (6, 7) has proposed a theory about the localization of the receptor sites on the basis of electron microscopic studies of T-phage attachment to *E. coli* B (6) and ϕX174 attachment to *E. coli* C (7). In ultrathin sections 75% or more of the phages seen attached to plasmolyzed bacteria were at points where the cell wall and membrane appeared to adhere to each other. The number of wall-membrane associations was of the same order of magnitude as the maximal number of phages found to attach to one cell. Furthermore the number of phages adsorbed per cell, calculated from counts in the ultrathin sections, approached the observed maximal number of adsorbed phages per cell. This suggested that the receptors were exposed only at the sites of wall-membrane association, which comprised only about 6% of the total cell surface (6, 7). Possibly, however, the fixation, dehydration, and embedding procedures removed phages adsorbed to areas other than those over wall-membrane adhesions (7). It is known that a mild procedure like washing the bacteria in a $10^{-2}M$ phosphate buffer, pH 7.2, 25°C will remove outer membrane complexes able to irreversibly inactivate phages P22, FO, 6SR, Br2, and C21 (80). The outer membrane, with its receptor containing LPS (for phages T3, T4, T7, ϕX174) and protein (for phages T2, T5, T6) components, is, as far as we know, not covalently linked to the peptidoglycan.

A slightly different interpretation of Bayer's observations is that irreversible attachment (and perhaps triggering) can occur to the LPS or protein components at sites other than wall-membrane adhesions but that infection occurs only when the phages attach at an adhesion area, which is perhaps the site of synthesis of outer membrane. Some observations support such an interpretation: 1. only 10–25% of the FO, 6SR, and Br2 phage particles that attached irreversibly to logarithmically growing cells, under optimal conditions, were found to result in a lytic cycle (79, 81); 2. 30% of attached ϕX174 detached spontaneously from *E. coli* C in eclipsed form and an additional 50% could be washed away leaving only 20% firmly bound to the bacteria (114); and 3. the maximal number of 6SR phages attached per bacterium was estimated to be 1450 (70). This means that an average of seven phages should be attached at each wall-membrane adhesion, which is sterically impossible

if the latter make up only 6% of the total surface. This modified theory predicts that phages with or without empty heads would be seen attached at nonadhesion sites; this was observed for less than 25% of the phages (6, 7). More experimental work is needed, however, before the phage receptors can be properly localized on the bacterial surface.

Molecular Properties of Receptors in the LPS

An important and as yet unsolved question regarding phages whose critical sites are in polysaccharide side chains (either O side chains or core side chains) is whether the polysaccharide chain alone constitutes the site for attachment or if lipid A is involved. The function of the lipid may be to stabilize the configuration of a sufficient number of attachment sites to trigger ejection. Few attempts have been made to answer these questions perhaps because most investigators have looked only for phage inactivation by extracts. Extracted LPS is very polydisperse, and estimates of its molecular weight indicate that it may vary from 1 to 20×10^6 (145). The LPS has a marked tendency to aggregate in both polar and nonpolar solvents, and the isolated LPS represents a molecular aggregate. Available data indicate that the average LPS molecule in *Salmonella* contains approximately three polysaccharide side chains extending from the lipid A part (135). This would give a molecular weight of approximately 1.2×10^4 for the LPS molecule of a rough mutant with a complete core and approximately 3.2×10^4 for a smooth strain with ten repeating units per O side chain (135). Unfortunately there are no methods available for disaggregating the LPS molecules and measuring their possible phage-inactivating capacity in aqueous solution; these measurements have to be performed either on the LPS aggregate or on fractions obtained by acid or alkaline hydrolysis or by the action of detergents. Alkaline hydrolysis of LPS splits some of the ester-linked fatty acid residues from the glucosamine residues in the lipid A and reduces the aggregate molecular weight from 1 to 20×10^6 to approximately 9×10^4 for the LPS from a mutant with a complete core (98). Weak acid hydrolysis cleaves the molecule in the KDO region, which links the heptose part of the core to the glucosamine of lipid A to yield the core oligosaccharide side chain with an approximate molecular weight of $1 \text{ to } 3 \times 10^3$ (98).

Phage Attachment to Receptor Sites in the LPS

The following is an attempt to summarize what is known about the attachment to the receptor sites for the large tadpole-shaped DNA phages with a contractile sheath (T2, T4, FO), the DNA phages that have a small noncontractile tail (ϵ^{15}, P22), and the single-stranded DNA phages that attach with an apical capsomere (ϕX174-like group).

PHAGES WITH A CONTRACTILE TAIL SHEATH (T2, T4, FO) The sequence of events, from a phage morphological viewpoint, involved in attachment and penetration of T2 and T4 to *E. coli* has been established by Simon & Anderson (148), and is probably the same for other phages of this group. The phage attaches to the cell

surface with the aid of the tips of the long tail fibers, which apparently recognize the attachment sites in the LPS (177, 180). The adsorbed phage becomes oriented with the base plate parallel to the surface. The phage comes closer to the cell surface and the short tailpins make contact. In subsequent steps, not fully understood, the conformation of the base plate is changed, the tail sheath contracts and the base plate retracts from the surface. The base plate now appears anchored by short tail fibers, which are assumed to be relaxed tailpins (148).

Thus there are two phage organelles that must attach to the cell to allow DNA penetration: the long tail fibers and the short tailpins. These events take place in the interaction of T4 with *Shigella sonnei* LPS (64) and of FO phage with *Salmonella minnesota* LPS (78), which indicates that the extracted LPS contains the sites for both the tail fibers and the tailpins. The attachment to the receptor via the long tail fibers probably represents the reversible step in phage attachment. T4 phage mutated in genes 11 and 12 attached to *E. coli* B and oriented the base plate parallel to the surface as in normal infection (150); the phage mutant was, however, unable to go through the step involving sheath contraction. The mutant phage could be eluted, and by mixture with the lysate from another T4 mutant be complemented to form an infectious particle (150).

Another T4 mutant, affected in gene 12 only, could be complemented to an infectious particle before but not after adsorption to *E. coli* B bacteria (150). The tail sheath of this mutant contracted upon contact with the cell, but the phage could still be eluted, apparently because the tailpins did not anchor the phage (150). The anchoring of the tailpins in the LPS would then represent the irreversible step in attachment of these phages.

It is not known whether the tail fibers and tailpins attach to the same or to different structures in the LPS molecule. For irreversible attachment these phages require the aggregated LPS complex. Neither alkali- nor acid-hydrolyzed LPS inactivates the phages (85). This explains why the first attempts of Burnet to isolate material with phage-receptor activity failed, since one of the steps involved alkaline hydrolysis (19). A radioactive-labeled fraction of an alkali-hydrolyzed LPS from a mutant of *Salmonella* with the complete core attached to the FO phage, whereas a similarly prepared fraction from a mutant without the terminal N-acetyl-D-glucosamine residue did not attach (80). Whether this attachment took place to the tail fibers or the tailpins is currently under investigation. These data indicate that a complex with a molecular weight of more than 9×10^4, and thus containing several LPS molecules, is required for the irreversible attachment of the FO phage. It also may explain why LPS treated with ultrasonics or sodium deoxycholate does not inactivate the FO phage (78) and why LPS treated with polymyxin B failed to inactivate phages T4 and C21 (72). All these treatments result in the breakdown of the LPS into small molecular fragments; and the deoxycholate and the polymyxin may have interfered with attachment by binding to the LPS. The attachment step mediated by the long tail fibers is probably nonenzymatic since attachment takes place at 0°C as well as at 37°C (1, 44, 154, 162). The irreversible step on the other hand might be enzymatic since it is a temperature-dependent process (1, 44, 154, 162).

PHAGES WITH A SHORT NONCONTRACTILE TAIL (ϵ^{15}, P22, Ω8) Recent studies on the attachment of these phages to bacteria and LPS indicate that an endoglycosidase located in the phage tail is involved (62, 68, 159). Attachment of P22 (or of tail parts) to whole cells of *S. typhimurium* is followed by spontaneous detachment of the phages (or tail parts) from the receptors (62). Concomitantly the receptor sites in the O side chain are destroyed as is shown by the inability of the bacteria for the next two generations to adsorb newly added phage (62). This is done by a P22 phage endoglycosidase which hydrolyses the Rha $1 \rightarrow 3$ Gal linkage within the repeating unit (Figure 1) (80). Two independent studies on the process of attachment of phage ϵ^{15}, which attaches to the O side chains of *Salmonella* of serogroup E1 (see above), have shown that here also the destruction of receptor ability is mediated by an endoglycosidase which hydrolyzes the Rha $1 \rightarrow 3$ Gal linkage within the repeating unit (68, 159). The enzyme was found both associated with the tail parts and in solution in the phage lysate (68, 159). Phage attachment to LPS in absence of divalent cations was reversible, but on addition of manganese ions the attachment became irreversible and the phage DNA became susceptible to DNase (159). The enzyme showed the same substrate specificity as the phage; i.e. it attacked side chains in which the linkage between the repeating units was Gal $1 \rightarrow 6$ Man (as in non-ϵ^{15}-converted bacteria) and not side chains in which the corresponding linkage was in β configuration (as in ϵ^{15}-converted bacteria). It has been proposed that the purpose of the hydrolase is to allow the phage to penetrate the O antigen side chains to reach a suitable site for injection of phage DNA (159). Coliphage Ω8 similarly splits the O polysaccharide chain in *E. coli* O8:K27(−):H⁻ bacteria by hydrolyzing the Man $1 \rightarrow 3$ Man linkage between successive repeating units (132a). The mechanism of attachment for these phages has striking similarities with the attachment and penetration of the capsular layer by capsulotrophic bacteriophages (see below).

PHAGES WITH APICAL CAPSOMERES (ϕX174 GROUP) These phages attach to the receptor via one or more of their 12 vertex capsomeres (7). The Br2 and 6SR phages attach irreversibly to extracted LPS and the interaction between ϕX174 and LPS from *E. coli* C makes the phage DNA susceptible to DNase (S. M. Jazwinski, R. Marco, and A. Kornberg, personal communication). Alkaline hydrolysis of the LPS from a complete-core *Salmonella* mutant, able to adsorb FO phage but not to inactivate it, retained the ability to irreversibly inactivate the phages Br2 and 6SR (80). The molecular weight of the alkali-treated fraction is a hundredfold smaller than that of the extracted LPS, so that apparently a smaller molecular complex is sufficient to inactivate this group of phages. This finding is not unexpected when one considers the difference in size of the base plate in a tadpole-shaped phage and an apical capsomere in a phage of the ϕX group. It has recently been demonstrated that the isolated parental replicative form of the ϕX174 phage has one or a few molecules of a unique phage protein associated with it (63). It is tempting to speculate that this protein is situated in one of the vertices of the phage particle, and like the maturation or A proteins of the isometric RNA and filamentous DNA

phages (see below), is responsible for attachment to the bacterial receptor and the subsequent penetration of the cell.

RECEPTORS IN THE CELL WALL OF GRAM-POSITIVE BACTERIA

Gram-positive bacteria lack, as far as is known, outer membrane which in Gram-negative bacteria may represent as much as 90% of the cell wall dry weight (46). The peptidoglycan is instead the dominating component of the Gram-positive cell wall, representing from 50–90% of the dry weight (46). The peptidoglycan in Gram-negative bacteria has not been found to harbor phage receptors, probably a consequence of its being hidden deep in the cell wall, whereas that of Gram-positive bacteria is frequently associated with receptor activity. The peptidoglycan is built by linear glycan strands, N-acetyl-D-glucosamine, and N-acetylmuramic acid residues in β-1,4 glycosidic bond, cross-linked through peptides (46, 118). In staphylococci all, or nearly all, of the carboxyl groups of the N-acetylmuramic acid residues are involved in amide linkages to terminal L-alanine residues of the peptide component (46, 118). The peptide is composed of subunits; in *Staphylococcus aureus* tetrapeptides, L-alanyl-γ-D-isoglutaminyl-L-lysyl-D-alanine units, extending from the muramic acid residues are cross-linked by pentaglycine subunits extending from the terminal D-alanine residue of one subunit to the ε-amino group of the lysine residue of another peptide subunit (46, 118). In *S. aureus* about 50% of the muramic acid residues are substituted on C-6 by O-acetyls (46). Other structural components are found in the Gram-positive cell wall, some of them covalently linked to the peptidoglycan, others associated with the wall in weaker bondings (46). With the exception of the T layer from *Bacillus brevis* (51) none of these polymers have been isolated as distinct anatomical structures (46); consequently their integrity is dependent on the peptidoglycan. These polymers include the teichoic acids found in *Staphylococcus, Bacillus,* and *Lactobacillus,* teichuronic acids in *Bacillus,* capsules in *Staphylococcus* and *Streptococcus,* proteins in *Bacillus* and *Streptococcus,* and C-carbohydrates in *Streptococcus* (46). Besides showing immunochemical specificity these components are, or are part of, the bacteriophage receptors in Gram-positive bacteria. Some of them, like the microcapsule in *S. aureus,* may, however, make the bacteria resistant to bacteriophage infection by covering receptor sites (184).

Phages representative of four of the six morphological groups (10) attack Gram-positive bacteria; they include the large tadpole-shaped DNA-containing bacteriophages with or without a contractile tail sheath, phages with a short noncontractile tail, and phages without tail and with small capsomeres.

Receptors in the Teichoic Acid-Peptidoglycan Complex

Shortly after the demonstration in 1934 that bacteriophage-inactivating material could be extracted from Gram-negative bacteria (20, 77) autolysates from *S. aureus* were shown to inactivate staphylococcal phages (130). It was also shown that, quite unexpectedly, both *Bacillus subtilis* and enterococci (*Streptococcus faecalis*), although not lysed by the staphylococcal phages, were able to inactivate them (129, 131). Subsequently it was demonstrated that several of the *S. aureus* typing phages could attach to most of the *S. aureus* strains tested, even though only some of them were lysed (110, 136). This indicates that there are structures in common among these species, more frequently than has been found in the species of Gram-negative bacteria. The analytical work on the structural components in the Gram-positive cell wall performed during the last decade (46) has given a better understanding of the receptor structures in *Staphylococcus* and *Bacillus* (24, 27, 47, 111, 146, 186) and their common features.

Exposed at the surface of *S. aureus* is a teichoic acid covalently linked to the muramic acid residue in the peptidoglycan (46). The teichoic acid is a linear polymer of D-ribitol units bridged by 1,5-phosphodiester linkages; each of the ribitol units is substituted at C-4 by either an α- or a β-linked N-acetyl-D-glucosamine residue (46). About 50% of the D-ribitol residues have D-alanine residues ester-linked to C-2 or C-3. The anomeric linkage of the N-acetyl-D-glucosamine residues is strain specific; some have exclusively β-linkages, other exclusively α-linkages, whereas others have varying proportions of both α- and β-linkages (46). Cell walls of *S. aureus* were shown to inactivate several bacteriophages but teichoic acid and glycopeptide, prepared by trichloroacetic acid (TCA) extraction from the cell walls, were devoid of phage-inactivating activity (110).

Mutants of *S. aureus* in which the N-acetyl-D-glucosamine-containing ribitol teichoic acid was replaced by a D-glucose-containing glycerol teichoic became phage resistant (181), an observation that pointed to the importance of teichoic acid as receptor for the phages concerned. Successful attempts to solubilize receptor-active material from cell walls were made in studies in which specific bonds in either the peptide subunits, the glycan strands, or the teichoic acid were hydrolyzed and the effect on the phage-inactivating capacity of the fractions obtained after gel filtration and chromatography was followed (27, 111). For irreversible inactivation of phage 3C the fraction had to be a complex of teichoic acid linked to the disaccharide N-acetyl-D-glucosamine 1 → 3 4 N-acetylmuramic acid with the tetrapeptide subunit in amide linkage to the muramic acid residue (111). The amount of material required to inactivate the 3C phage, calculated as organic phosphorus from the teichoic acid, was, however, a hundredfold higher than found with cell walls (111). Enzymatic hydrolysis of the amide bond almost completely abolished the phage-inactivating capacity (111). Fractions containing complexes with either longer glycan strands or the pentaglycine bridges were not necessary to inactivate phage 3C (111). None of these fractions inactivated irreversibly any of the 3B, 42D, or 53 phages, even if the *Staphylococcus aureus* strain investigated was lysed by phage 3B (111). Reversible attachment of 3C and of phages 71 and 77 was observed to a complex of teichoic acid linked to the entire glycan strand, obtained from the same strain of *S. aureus* by hydrolyzing both the amide linkage and the peptide linkages in the pentaglycine subunit (27). Treatment of this fraction with an endo-N-acetyl-D-glucosaminidase abolished the reversible attachment, indicating the importance of the supporting peptidoglycan network for the configuration of the teichoic acid (27).

The N-acetyl-D-glucosamine residues in the teichoic acid seem to be indispensable for the receptor since phage 52A-, 79-, and 80-resistant mutants obtained after nitrosoguanidine treatment of *S. aureus* lacked only the amino sugar (24). Treatment of cell walls from a strain with predominantly β-linked N-acetyl-D-glucosamine residues in the teichoic acid, with an exo-β-N-acetyl-D-glucosaminidase also reduced the phage 3C inactivating capacity (27). Isolated cell walls with either only α-, only β-, or both α- and β-linked amino sugar residues did not differ in their ability to inactivate phages 52A, 3C, 42D, and 53. It was concluded that the anomeric linkage of the N-acetyl-D-glucosamine is not important for the receptor activity (24, 111). *S. aureus* strains (phage type 187) that do not adsorb the above-mentioned phages were recently found to have a teichoic acid in which the N-acetyl-D-glucosamine residue had been replaced by N-acetyl-D-galactosamine (69). Alkaline treatment of *S. aureus* cell walls removed the O-acetyl groups on C-6 of the muramic acid residues and the D-alanine residues on C-2 and C-3 of D-ribose in the teichoic acid and destroyed their inactivating capacity for phage 52A (146). Selective removal of the ester-linked D-alanine residues by hydroxylamine under neutral conditions did not alter the receptor activity, which indicates that the O-acetyl groups on the muramic acid residues, as well as the amino sugar in the teichoic acid, are critical parts of the phage 52A receptor (146).

Strains belonging to the genus *Bacillus* have a cell wall with peptidoglycan and teichoic acid components, albeit variations may occur, built according to the same principle as described for *S. aureus* (46). The teichoic acid of *Bacillus subtilis* differs from that of *S. aureus* only in that D-glucose instead of N-acetyl-D-glucosamine is 1, 4 linked to the D-ribitol units (46). The D-glucose residue seems to be as important for the receptor of *B. subtilis* phages as the amino sugar for the staphylococcal phages. None of the subtilis phages ϕ1, ϕ25, ϕ29, SP3, SP10, SPO_2, and μ, which represent Bradley's groups A, B, and C (10), adsorbed to mutants of *B. subtilis* which lacked the D-glucose residue of the teichoic acid (47, 186). Enzymatic hydrolysis of the amide linkage between the muramic acid residue and the peptide subunit destroyed the phage-inactivating capacity (186). No soluble receptor-containing fraction was isolated (186).

Cultivation of *B. subtilis* W-23 under phosphorous limitation results in production of teichuronic acid (i.e. a polymer of glucuronic acid and galactosamine) instead of teichoic acid (3). This change results in loss of ability of the cells to inactivate phage ϕSP50, which is inferred to require a cell wall with glucosylated teichoic acid for inactivation (3). Restoration of normal growth conditions resulted in the reappearance of ϕSP50 receptor activity (3). Lysogenization with *B. subtilis* phages can render the bacteria unable to adsorb the lysogenizing phage (47, 66), but the presumed structural change in the cell wall, or membrane, was not established in either of the reported observations.

Thus for some *S. aureus* phages a soluble macromolecular complex containing teichoic acid covalently linked to peptidoglycan can be isolated from the cell wall and found to inactivate reversibly or irreversibly the phages. In both *S. aureus* and *B. subtilis* the presence of either N-acetyl-D-glucosamine (24, 27) or D-glucose (47, 186) residues in the teichoic acid seem to be indispensable for the receptor, whereas

the D-alanine residues seem dispensable at least in *S. aureus* (146). Even if the teichoic acid as such contains the sites to which the phages attach primarily, not even reversible attachment to isolated teichoic acid could be demonstrated (27). Reversible attachment seems to occur only to a complex of teichoic acid covalently linked to a glycan strand (27). Either the tested teichoic acids (usually obtained by TCA extraction and precipitation) have been altered during the isolation procedure or the methods used for the detection of phage-receptor interaction have not been sensitive enough. Alternatively the primary attachment of the phages may involve both the teichoic acid and groups on the glycan strand, such as the O-acetyl groups on the N-acetylmuramic acid residues in *S. aureus* needed for inactivation of phage 52A (146). For irreversible attachment of the staphylococcus phage 3C, a soluble complex of teichoic acid, glycan, and the peptide subunit in amide linkage was sufficient (27, 111). This complex, however, did not inactivate other staphylococcus phages such as 3B, 42D, and 53 (111). The observation that isolated peptidoglycan inactivated staphylococcus phage 77 irreversibly (137) is contradictory to the findings reported above (27, 111) and cannot be explained at present.

The original observations by Rakieten et al (129, 130) that *S. aureus* bacteriophages are inactivated by both *S. aureus* and *B. subtilis* bacteria and autolysates is thus readily explained by the structural similarity of the cell walls of these species. Except for minor and probably unimportant differences in the peptide subunits of the peptidoglycan the only other difference seems to be in the teichoic acid; there is an N-acetyl-D-glucosamine residue in *Staphylococcus aureus* and a D-glucose residue in *B. subtilis*, both 1,4 linked to the D-ribitol residue (46). The absence of the N-acetyl group on C-2 of D-glucose is apparently not important for the receptor specificity as measured in qualitative terms, whereas epimerization of the hydroxyl group on C-4 of D-glucose make the bacteria resistant (69). Rakieten also observed that enterococci (*Streptococci* group D) could inactivate some *S. aureus* phages (131). The teichoic acid of these bacteria differs from that of *Staphylococcus* and *Bacillus* both in structure and probably also in location in the cell wall (46); in the few strains studied it was made probable that it was located between the peptidoglycan and the cytoplasmic membrane (46) and thus not so easily accessible as the teichoic acid of *Staphylococcus* and *Bacillus* which is exposed at the surface. Structurally it is a 1,3-linked glycerol phosphate polymer substituted at C-2 of glycerol with kojibiose (2-O-α-D-glycosyl-D-glucose) and kojitriose. Besides the teichoic acid two other polysaccharides are found in the cell wall of *Streptococcus faecalis* (120): one containing D-glucose and D-galactose and the other L-rhamnose, D-glucose, D-galactose, and N-acetyl-D-galactosamine (the C-carbohydrate). It is not known which, if any, of these structures interact with the staphylococcal bacteriophages.

Receptors in the C-Carbohydrate-Peptidoglycan Complex

The streptococcal cell wall contains a polysaccharide, termed C-carbohydrate, covalently linked to the muramic acid of the peptidoglycan (46). The C-carbohydrate contains the antigens for the serological grouping of streptococci [with the exception for groups D (*Streptococcus faecalis*) and N (*Streptococcus lactis, S. cremoris*)

(46)] and is (or is part of) the receptor for some streptococcal bacteriophages (21, 26, 39, 74, 75). The streptococcal bacteriophages, isolated from lysogenic strains, that have been studied are mostly group specific, i.e. they lyse only strains of a single serogroup. However, A, C, and G bacteriophages can attach to bacteria of all three groups (26, 39, 74). Soluble receptors have been isolated only for the group C bacteriophage C1 (75) and for the group A temperate bacteriophage B940 (39). With the aid of a *Streptomyces albus* muralytic enzyme or of phage-induced lysin, also with muralytic activity, a C-carbohydrate-containing complex was isolated, 200 μg of which inactivated $\sim 10^9$ plaque-forming units of phage C 1 (75). The receptor had a value of 1.1–1.2S and consisted most probably of the C-carbohydrate linked to at least N-acetylmuramic acid-N-acetyl-D-glucosamine disaccharides cross-linked by peptide chains (75). As in the case of the *Staphylococcus* and *Bacillus* bacteriophages this macromolecule was necessary for irreversible inactivation; C-carbohydrate prepared by acid hydrolysis and devoid of peptidoglycan components did not inactivate the phage (75). The phage B940 receptor was prepared in the same way (39). For virulent group A bacteriophages such as A6, A12, and A25 irreversible attachment has been demonstrated only to living cells (39, 74). Heat-killed cells, cell wall fractions, and membranes did not inactivate irreversibly, but in some instances a reversible attachment was found (74). This attachment has to be considered specific since the phages concerned did not attach to *Staphylococcus* or *Bacillus megaterium* strains (39); this interesting observation has not been pursued. The reason that heat-killed cells, etc failed to inactivate these phages irreversibly may be that a living bacterium is necessary for the phage to eclipse or that the various treatments altered the conformation of the structures in the receptor, i.e. by denaturation or action of autolytic enzymes, so that inactivation did not take place.

The C-carbohydrate appears to be a branched polysaccharide which 1. in group A has a chain of α1,2-linked rhamnosyl residues nonstoichiometrically substituted on C-3 by β-linked terminal nonreducing N-acetyl-D-glucosamine residues (46), 2. in group C has the same rhamnose backbone but N-acetyl-D-galactosamine residues α-linked (46), and 3. in group G appears to have the rhamnosyl core in α1,4 linkage (25). The rhamnose residues of group G are substituted by D-galactose and N-acetyl-D-glucosamine (25, 46). It can be reasonably surmised that the phage attachment of the A, C, and G phages to A, C, and G streptococci is due to the presence of the rhamnose backbone even if for some phages one of the substituents, such as N-acetyl-D-glucosamine for phage A25 (39), may be important. The presence of a capsule of hyaluronic acid makes group A streptococci resistant to virulent phage, presumably by blocking the access to their receptor sites; it does not confer resistance to the temperate A phages, which contain a hyaluronidase (74). The presence of M, R, and T antigens, which are proteins and exposed at the surface, does not interfere with attachment of the streptococcal A, C, and G bacteriophages (39, 74).

Receptors in Other Peptidoglycan-Containing Complexes

The N1 bacteriophage, morphologically of Bradley's group B (10), lyses *Micrococcus lysodeikticus* (93). The attachment to whole cells is irreversible, and the presence of 10^{-2} KCN in the adsorption medium does not affect the irreversible process; thus metabolic activity of the cell is not needed for eclipse of N1 phage. Attachment to cell walls, isolated by differential centrifugation from disintegrated lyophilized bacteria, was only reversible however (94). The extent of reversible inactivation caused by cell walls was about the same as the irreversible inactivation caused by whole cells. The cell wall structure containing the receptor was not identified; neither heating to 100°C for 60 min, nor trypsin digestion, nor extraction with 2% sodium dodecylsulfate had any effect on the reversible attachment. But lysozyme treatment almost completely destroyed inactivating capacity (94), from which it can be surmised that the N1 receptor, like those for *Staphylococcus, Streptococcus,* and *Bacillus* phages, is a complex of polysaccharide covalently linked to the peptidoglycan. A mutant resistant to phage N1 differed from the parent strain only in a lower glucose content in the cell wall (94).

Receptors in a Surface Protein

A wide variety of bacteria belonging to *Bacillus, Halobacterium, Micrococcus, Spirillum* sp., and others have been found to have a regularly structured protein layer on the outer surface. A protein layer with a tetragonal symmetry (T layer) was isolated from cell walls of *Bacillus brevis* strain P1 and shown to be composed of subunits with a molecular weight of 140,000 (51). The subunits, held together by noncovalent bonds in the intact T layer, were composed of 99.3% protein and 0.7% carbohydrate. The T layer is held to the surface, probably to the peptidoglycan, by noncovalent bonds and can be removed as a sheet or can reassemble into a sheet from isolated subunits. Five out of six phages, isolated in a search for phages which have their receptor in the T layer, were inactivated by cell walls and by isolated (or reassembled) T layer of *B. brevis* strain P1 (51). The electron micrographs showed that the interaction between T layer and phage in some instances was accompanied by contraction of the tail sheath, even though DNA was not ejected. It is therefore reasonable to assume that the T layer causes an irreversible inactivation of the phages, though this point was not studied directly (51). Isolation of *B. brevis* mutants whose T layer inactivated some but not all of the five phages concerned, and with altered T-layer protein (determined by sodium dodecyl sulfate polyacrylamide gel electrophoresis) indicates that the T layer contains more than one specific receptor site. Other than the inactivation of the T2 and T6 phages by isolated protein from the outer membrane of *E. coli* B (108) this inactivation of five phages by the T layer of *B. brevis* P1 is the only report of phage inactivation by a cell wall protein.

Receptors in the Cytoplasmic Membrane

Phage *m13* is active against streptococci of serogroup N (*Streptococcus lactis, S. cremoris*). This phage, like most other streptococcal bacteriophages, has a long noncontractile tail lacking sheath, base plate, and other tail appendages (116). A soluble receptor, which inactivates *m13* irreversibly, was isolated from the cytoplasmic membrane fraction of disintegrated bacteria. The receptor activity was associated with a lipoprotein fraction obtained by sodium deoxycholate extraction of the membranes followed by gel filtration in the presence of the detergent (115). This fraction, with an estimated molecular weight of 2 to 8 X 10^5, contained 51% protein,

39% lipid, and 2% carbohydrate. The receptor activity is probably associated with the lipoprotein part since it was resistant to periodate oxidation (115). A soluble receptor of *Streptococcus faecium*, isolated by differential centrifugation of ultrasonically disrupted lysozyme spheroplasts, inactivated phage P3 irreversibly and was susceptible to periodate oxidation (167). Although this receptor was also susceptible to proteolytic enzymes it can be assumed that the specific P3 receptor activity resided in the polysaccharide parts of the cell wall and not the cytoplasmic membrane, and that the proteins were necessary to give the macromolecular conformation necessary for irreversible inactivation of the phage (see above, on staphylococcal phage receptors). The interpretation that the *Streptococcus lactis* phage *m13* receptor is located in the cytoplasmic membrane (115, 116) and also serves as site for primary attachment of the phage was supported by a morphological investigation (52). An electron micrographic study of *Streptococcus lactis* cell envelopes showed that the plasma membrane protrudes through conical holes in the cell wall (52) and thus would be accessible to the phage.

RECEPTORS IN THE CAPSULAR OR SLIME LAYER

Many bacteria are surrounded by a more or less defined capsular or slime layer (96). This capsular layer, by its mere presence, may block the access of bacteriophage to the receptor present in an underlying cell wall structure, such as the outer membrane of Gram-negative bacteria (23, 127) or the glycopeptide, with teichoic acid (184) or C-carbohydrate (74) of Gram-positive bacteria. Alternatively, it may serve for attachment of some phages that do not attach to nonencapsulated bacteria (23, 123). Bacteriophages that lyse capsulated bacteria often give rise to plaques surrounded by a translucent halo (37, 123) caused by the diffusion of a phage-induced lysin from lysed cells which hydrolyzes the capsular material and exposes the underlying outer membrane or cell wall.

Vi-Antigen as Phage Receptor

The Vi-antigen found in a few species of *Salmonella, Citrobacter,* and *E. coli* is a polymer of α1, 4-linked N-acetyl-D-galactosaminuronic acid residues that are partly O acetylated (96). The attachment of Vi-phage 1, which morphologically belongs to group B of Bradley (10), was elucidated in a series of investigations (160, 161). The phage attaches irreversibly to isolated cell walls. The use of a purified Vi-antigen adsorbed onto an erythrocyte stroma made it possible to study the reversible attachment step only, without the phage going into eclipse (161). Attachment to the Vi-antigen on red cell stromata readily takes place at 0°C in a medium containing 0.1 *M* ammonium acetate. If the temperature is raised the Vi-polysaccharide is deacetylated by the phage enzyme and the phage detaches without loss of infectivity (160, 161), a situation analogous to the attachment of influenza virus. Since the enzymatic activity is inhibited by chelating agents like EDTA, divalent cations are assumed to be important for the temperature-dependent enzymatic step. The phage enzyme does not depolymerize the Vi-antigen, which has a molecular weight in the range of 10^6, but causes the loss of almost all acetyl groups (160, 161).

Phage-deacetylated Vi-polysaccharide does not adsorb newly added Vi II-phage; reacetylation of the phage-deacetylated polysaccharide restores almost all of the phage-inactivating capacity (160, 161). The enzyme is firmly bound to the phage and may be located in the spikes which extend from the distal end of the tail. For irreversible attachment, other cell wall components seem to be required (160, 161). The influence of outer membrane components in association with the Vi-antigen on the attachment and eclipse process has, however, not been studied.

Capsular Receptors in Other Gram-Negative Bacteria

Phage infection in several species provided with a capsule induces the synthesis of capsular depolymerases (5, 37, 99, 123, 157, 187). The enzyme can be isolated from a crude phage lysate, partly in soluble form and partly phage associated (5, 156, 187). These enzymes are endohydrolases that show substrate specificity and often are active only against the exopolysaccharide of the host organism. This activity is not always paralleled by the specificity of phage infection; only 1 of 18 strains whose capsules were hydrolyzed by the phage enzyme was susceptible to phage infection (4). In a few systems the enzyme has been purified to homogeneity and its mode of action on a structurally characterized capsular polysaccharide elucidated (155, 156, 187).

The phage-bound and soluble enzymes of phage K-2, which depolymerize the capsule of an *Aerobacter aerogenes* strain, seemed identical in catalytic and molecular properties (187). The polysaccharide concerned is composed of linear chains of tetrasaccharide repeating units

$$\begin{array}{c} \text{GlcUA} \\ \beta \downarrow \; \tfrac{1}{2} \\ \text{-}\overline{\alpha}\text{-}3\ \text{Gal}\ 1\text{-}\overline{\alpha}\text{-}3\ \text{Man}\ 1\text{-}\overline{\alpha}\text{-}3\ \text{Gal}\ 1\text{-}\overline{\alpha}\text{-} \end{array}$$

The enzyme, a glycanohydrolase, attacks the polymer at random points hydrolyzing the galactosyl 1-$\overline{\alpha}$-3 galactose linkage between repeating units (187). The phage-bound and soluble enzymes of the *E. coli* phage K29 and *Klebsiella* phage K11 have endoglucosidase activity which hydrolyzes linkages in the capsular polysaccharides from *E. coli* 09:K29 and *Klebsiella* 03:K11, respectively (155, 156). It was suggested that the K29 and K11 phage-enzyme activities were associated with the tail spikes of these phages, which belong to Bradley's morphological group C (155). Most phages that display a lytic activity against capsular polysaccharides belong to Bradley's group C; i.e. have a very short noncontractile tail. The e^{14} phage that acts on *Salmonella* group E1 bacteria (see above) has the same morphology and its tail spikes carry an endohydrolase which breaks down its receptor (68, 159).

The capsule-specific phages do not seem to be irreversibly inactivated by isolated capsular antigen (156, 161). This would suggest that the capsular layer serves as site of a reversible attachment only and that other cell wall components are required for a subsequent irreversible attachment step. Such a theory seems plausible because triggering of the release of nucleic acid at a distance up to 400 nm from the cell wall might cause a very high frequency of abortive infection. Measurements of the fraction of attached phages that produce infection have apparently not been under-

taken but it seems likely that the phage enzyme merely aids in the penetration of the capsule. There is one exception to this statement (5): slime material was isolated from a *Pseudomonas aeruginosa* strain by extraction with saline and purified by ethanol:aceton precipitation, gel chromatography, and ultracentrifugation; this material irreversibly inactivated phage 2 and also caused the triggering of DNA ejection from the phage heads (5). In spite of the report that no LPS was detected it may be reasonably surmized that the slime polysaccharide was contaminated by outer-membrane components since 1. it was isolated from an autolysate by saline extraction, 2. it had a high nitrogen content, and 3. the material appeared as round discs in the electron micrographs—a structure often seen in outer-membrane preparations whereas slime polysaccharide by itself would not have been as electron dense.

Thus the capsulolytic enzymes appear to assist in the penetration of the capsule; the enzyme may also be concerned in the positioning of the phage on the surface by reducing the three-dimensional process of phage-receptor search to a two-dimensional process. However, a more careful study of the ionic requirements for attachment could reveal, as was found with the interaction between ϵ^{15} and its LPS receptor (159), that addition of a specific cation would render the reversible interaction irreversible.

RECEPTORS IN ASSOCIATION WITH FLAGELLA

Some bacteriophages attack only motile strains, of either Gram-positive or Gram-negative species. In spite of their probably widespread occurrence (36) only a few have been isolated. The best studied is x1, isolated by Sertic as phage VIII.113 almost four decades ago and found to lyse only motile strains of *Salmonella* (144). Since then x1 has been found to have a very broad host range; it lyses *Salmonella arizona* (104), *E. coli* (59), *Serratia marcescens* (59), *Proteus mirabilis*, and *P. rettgeri* (2). Six other phages, labeled x2 through x7 (2, 36), have been isolated and found to lyse motile enteric bacteria. For Gram-positive bacteria two flagellotrophic phages have been reported; PBS1 which lyses motile strains of *Bacillus subtilis* (67) and PBP1 which is specific for motile strains of *B. pumilus* (92). All of the hitherto studied flagellotrophic phages belong to class B of Bradley (10); they contain double-stranded DNA within a hexagonal head, measuring about 65 nm between its parallel surfaces, and have a noncontractile tail about 250 nm long and 15 nm wide with a tapering end terminated with a tail fiber about 200 nm long (2, 36, 138).

The flagellum, as studied in *E. coli* and *B. subtilis*, is composed of three components: a basal body by which it is anchored in the cell envelope, a hook, and a filament (32). The filament is supposed to be a helical structure composed of subunits of flagellin with a molecular weight of about 40,000 (58). Bacterial mutants changed in flagellar morphology, and sometimes also in phage sensitivity, have been isolated; there are mutants with straight, curly, or nonmotile flagella (58). It is believed that the flagellin subunit is composed of pure protein although the possibility of the presence of minor nonprotein components cannot be excluded (58). Although the makeup of amino acids in flagellin preparations from various species differ, some common features are striking. Aspartic acid, alanine, glutamic acid, and

threonine account for more than 50% of the amino acids in the flagellin molecule. Proline and histidine are present in small amounts or absent, whereas cysteine and tryptophan are absent in all flagellin preparations examined (58). The other amino acids are present in varying amounts (58). Comparative amino acid analysis of flagellins of antigenically distinct flagella from *Salmonella* showed that the antigenic difference, not unexpectedly, is associated with a difference in amino acid composition between flagellin molecules (103). Since the x1 phage has been found to attack genera as diverse as *Escherichia, Salmonella, Serratia,* and *Proteus* (2, 59, 104, 144), one would also like to find the similarities in the flagellin composition and structure that the x1 phage recognizes. The only relevant observation is the report that flagellin prepared from various strains of *Salmonella* have two different groups of antigenic determinants: one is species specific (according to the Kauffmann-White scheme) while the other is common to all strains tested (125).

The primary attachment of the x1 phage (104, 139) and the PBS1 phage (128) takes place with the aid of the tail fiber which appears to wind around the filament of the flagellum. This step is apparently reversible (104). Electron micrographs show that phages that have attached to the filaments still have their heads full of DNA (139). It appears that the attachment becomes irreversible only after the phage has traveled along the filament to the basal body (139). Thus the receptor is, or is in association with, the basal body of the flagellum and not the filament as was originally surmised (104). There are thus probably two receptors for the phage to recognize: one for the reversible attachment to the flagellar filament and one for the irreversible attachment at the base of the flagellum. The function of the flagellar filament could then be to reduce the three-dimensional diffusion process of the reactants to a one-dimensional one, the traveling of the phage down the flagellum. It must be stressed that the filament, hook, and basal body are not only functionally distinct, but differ also in immunological and physical respects (32).

The x1 phage attaches to the filament even if the flagellum is nonmotile due either to a genetic defect or to paralysis of the bacteria by heat, cold, anaerobic conditions, or chemicals (104, 139); under these conditions, however, the phage does not infect the bacteria (139). Several phages can be seen on each filament indicating the presence of several attachment sites per flagellum (104, 139). Shearing off the flagella reduces the attachment rate but filaments as short as 70 nm still adsorb phage (139). Neither the x1 phage (104, 139) nor the PBS1 phage (128) has been found to attach to isolated flagella. One may speculate that this is because the isolated filament has a different conformation of its subunits than the filament attached to live bacteria.

Moving flagella (or flagellar bundles) look like rotating spirals (58). The mechanism behind the transmission of the movement is not completely understood, but it is apparent that this movement is required for the phage to travel along the filament. The finding that bacterial mutants of *E. coli* and *Bacillus subtilis* possessing straight flagella, and nonmotile, are susceptible to x1 (60) and PBS1 (101), respectively, is not a contradiction to this statement. Owing to the loss of the spiral structure, movement of the flagella does not cause locomotion of the bacteria.

Although x1 has a broad host range it does not lyse *Salmonella* species with H-antigen specificities belonging to the e,h,g, . . . , or l, . . . series (104). Transduction of a g, . . . antigen into a susceptible strain makes it phage resistant (104),

indicating that the resistance results either from the absence of the attachment site or from its being covered. A host-range mutant of x1, phage M8, lysed *Salmonella* strains with the g, . . . , antigens and still retained activity against strains with other flagellar antigens (185). Whether phage M8 could lyse strains with the e,h, or l, . . . , antigens was not tested. The flagellins isolated from flagella with three different g, . . . , antigens differed from other *Salmonella* flagellins in lacking histidine (103). The importance of this difference cannot be understood until the structure of flagellin from different strains has been established.

The irreversible attachment of the phage apparently takes part at the base of the flagella (139). The hook does not seem to be involved in the attachment since mutants lacking the filament but exposing the hook or polyhooks on the surface have been isolated as phage x1-resistant mutants (124, 166). Electron micrographs indicate that x1 attaches irreversibly with the long axis of the tail parallel to the basal body (139). Up to five phages were seen attached at the base of one flagellum (139). It is possible, at least for the x1 phage, that the irreversible attachment occurred upon contact with the L ring of the basal body (32). Since the diameter of the L ring, 22.5 nm, is only slightly wider than the diameter of the hook, 17 nm (32), it seems unlikely that the tail of x1, which is 15 nm wide (138), should find its receptor exclusively on the L ring which protrudes only about 3 um from the hook. Another possibility is that the receptor is composed of a complex between the basal body and the cell wall. It is at present hard to surmise what cell wall component would be part of the receptor when one considers the widespread differences between the different genera lysed by x1 and the fact that x1 is not inactivated by nonflagellated bacteria. An alternative mechanism of x1 attachment is that the interaction with the flagellar filament activates the phage so that the collision with the base results in irreversible attachment.

Cell wall constituents can cause resistance to x1 infection; the presence of Vi-antigen on the surface of *Salmonella typhi* makes some strains x1 resistant although they are motile, an observation made by Sertic & Boulgakov in 1936 (144) and confirmed in later investigations (104).

RECEPTORS IN ASSOCIATION WITH PILI

Pili, defined as any filamentous appendage other than flagella extending from the bacterial surface, appear as flexible rods of various lengths on Gram-negative bacteria. Two different classes of bacteriophages have been attributed to have their receptors on, or in association with, pili; the isometric RNA phages and the filamentous DNA phages, class E and class F of Bradley (10), respectively.

More than ten morphological classes of pili have been described (13, 15, 16), but with a single exception only the sex pili are supposed to harbor phage receptors. Two main classes of sex pili have been described in *E. coli* and its relatives: 1. the F pili determined by the F factor and some R and colicine factors, and 2. I pili determined by colicine I factors or other derepressed R factors. Sex pili of each class are involved in the formation of mating pairs between donor and recipient cells and probably also

in the transmission of nucleic acid during mating (for reviews see 14, 15, 17). The pili probably also serve in the transmission of nucleic acid from the male-specific bacteriophages which attach to them. There may be exceptions to the above generalizations, however, in the case of the isometric RNA and filamentous DNA phages of *Pseudomonas aeruginosa*. These phages attach to pili which apparently are not involved in the transfer of bacterial nucleic acid (54, 55, 109). The inability of the male-specific bacteriophages to infect female bacteria results only from the lack of an attachment organelle for the phages, because spheroplasts of female cells are as susceptible to infection by isolated phage RNA as are spheroplasts of pilus-bearing male cells (176).

Pili seem to arise from random sites at the cell surface and are most probably anchored in the cytoplasmic membrane because spheroplasts retain the pili of their rod-shaped precursor. F^+ strains have an average of about one pilus per cell; some cells have none, whereas others have more than one pilus (14, 16). Pili can be easily removed from the cell surface by blender treatment and can then be isolated from the cell-free supernatant. Even without such treatment considerable amounts of pili are found in the supernatant of shaken broth cultures. Highly purified F-pili preparations, homogenous by both chemical and physical criteria, were recently studied in detail (14, 15). The F pili are composed of polymerized phosphoglycoprotein subunits of molecular weight 11,800. The pilin subunit is unusual with respect to amino acid composition; four of the commonly occurring amino acids—cysteine, proline, histidine, and arginine—are missing (14). The amino acid sequence is not known. The pilin molecule also contains two phosphate molecules and one D-glucose molecule covalently linked to it. It is not known where the phosphate and D-glucose molecules are attached or whether they are exposed at the surface of the pilus. The pilus itself has been envisaged as composed of two parallel protein rods each built by the F-pilin monomers (14). The F-pili have a diameter of 8.5 nm and may be several μm long. No structural studies on I pili or the *Pseudomonas aeruginosa* pili, which adsorb phages, have been reported.

Several male-specific isometric RNA phages have been described since the first reported isolations in 1960 (89, 90). Among the most intensively studied are R17, M12, fr, $Q\beta$, f2, and f4 specific for *E. coli*. They all have a diameter of about 27 nm. The phages studied contain 180 identical protein subunits, each built up of 129 amino acids (53). Attachment of the male-specific phages to F pili was demonstrated by Crawford & Gesteland in 1964; their electron micrographs showed R17 phage particles covering the entire length of the F pili of an *E. coli* strain (28). Each F pilus can adsorb several hundred phage particles; the actual number depends on the length of the pilus. The question as to whether any one of the apparently identical 180 capsomeres of the phage capsid could attach to the receptor, or if one (or several) of them was specialized for attachment, was resolved by the discovery that another phage capsid component, the A or maturation protein, was required for constitution of an infectious phage particle (134). There is only one A protein molecule of molecular weight ca 38,000 (152) per phage particle (153). The A protein, besides serving in the attachment also, enters the cell together with the

nucleic acid (73). The physical properties of the isolated A protein—it is difficult to obtain in pure form, is strongly hydrophobic, and adheres to membranes (152)—has made it unsuitable for a study of the direct interaction between the A protein and intact F pili or the F-pilin monomer.

Among the filamentous DNA bacteriophages there are two different classes discernible: the Ff phages which attach onto the tips of F pili (102) and the If phages which attach onto the tips of I pili (107). These phages differ in length, the Ff phages being about 850 nm long and the If phages about 1300 nm long (102). There are only a few attachment sites per bacterium for the DNA phages; by measuring the attachment of labeled phage (56, 163) the maximal number has been estimated to be three per bacterium. Most pili have only one phage attached to the tip, but sometimes two and once three phages have been seen on one pilus (22). The higher estimated number of receptor sites per bacterium is certainly a consequence of the presence of more than one pilus on some cells. More than 30 filamentous DNA phages had been described by 1969 (102); the best studied are M13, fd, Ec9, and HR among the Ff class, and If1 and If2 among the If class. As with the RNA phages, the attachment of the DNA phages to the receptor has been implicated to the specific A protein (102). There are only a few molecules of A protein per phage with a molecular weight of 70,000 (102).

An accurate determination of the kinetics of attachment of these phages is much more difficult than similar determinations for phages having their receptors in the cell wall. This is true for both the centrifugation and the filtration methods (see section on methodological aspects). The probable bases for these difficulties are as follows: 1. The phage population is heterogeneous; only a fraction attaches to the pili and of these less than half are able to infect (122). 2. Not all bacteria have pili; indeed at any given moment a maximum of 85% of the cells carry F pili (16), and up to 90% of the pili present in a culture are detached from the cells (16). 3. Phages attached to F pili may adsorb to the filter (29, 88). 4. When the attachment is performed at 37°C the empty phage capsid separates from the pili after injection of the phage RNA (34, 122), whereas the A protein enters the cell with the RNA (73). The estimation of adsorption of phage to pili on bacteria can therefore be used only as a qualitative assay. The use of free F pili is preferred, even though this method also suffers from methodological difficulties such as aggregation of F pili and the passage of phage-covered F pili (or fragments) through the filter (16). These difficulties can, however, be taken into account when evaluating the experimental data.

Maximal attachment of both the isometric RNA and the filamentous DNA phages takes place in 0.1 *M* NaCl solutions or in solutions with a similar ionic strength (29, 163). Divalent cations are not required for attachment of either sort of phage but are needed for the penetration step in the case of the isometric RNA phages (121). Studies of the attachment step are preferably done at low temperatures: 0 to +4°C. Under these conditions the attachment is reversible, i.e. the phage does not go into eclipse, and consequently the phage can be neutralized by antiphage antiserum and eluted by solutions of low ionic strength. Attachment to isolated pili or fragments thereof is always reversible, which is taken to indicate that the metabolic activity of the bacterial cell is necessary for the phage to eclipse (14–16). The

experimental work carried out by Brinton & Beer (16) indicates that the interaction of R17 phage with F pili is weak, with an equilibrium constant of about 5×10^{-9} ml/phage at 0°C in the calcium-supplemented Z medium (90). At 37°C the equilibrium constant was only twice as large; thus the attachment is only slightly temperature dependent (16).

The structure of the receptor site on the F pili is unknown. The smallest fragment of F pili seen interacting with RNA phages in electron micrographs is about 100 nm long (165, 174); this probably means that the A protein of the phage attaches to more than one F-pilin molecule. F pili are degraded by organic solvents and by trypsin (16, 174) but the receptor activity of these fragments is unknown. The discovery by Brinton and co-workers (14, 15) that the pilin molecule contains covalently linked D-glucose and phosphate molecules may initiate experiments to study whether any or both of these molecules form part of the receptor. Zn^{2+} prevents attachment of the male-specific DNA phages (119, 163) (but not of the male-specific RNA phages) and also prevents formation of mating pairs (14, 16), perhaps by interacting with the phosphate groups. As early as 1961 it was demonstrated that treatment with periodate, in concentrations which did not significantly decrease the viability of the culture, prevented both formation of mating pairs (151) and the attachment of male-specific RNA phages (33). It is tempting to speculate that this was due to oxidation of the D-glucose residue; however, it is also possible that periodate treatment interferes with the assembly and outgrowth of F pili at the same time as old pili are spontaneously detached from the cells. Phenethyl alcohol treatment was reported to abolish attachment of both classes of phages to inferred pili-bearing cells but not to free F pili (175), and levallorphan was reported to decrease phage attachment to pili-bearing whole cells (126). These agents also may prevent assembly and outgrowth of F pili.

The plasmid has been shown to have 11 cistrons; of these probably 1 codes for the F-pilin protein subunit and 1 each for its glucosylation and phosphorylation (179). Now that the structure of the F-pilin molecule has been to some extent elucidated (14, 15) it will be possible to study the reason for the inability of some mutants to adsorb certain male-specific phages, despite their possession of F pili. These mutants comprise strains that are resistant to all tested male-specific RNA phages but susceptible to male-specific DNA phages (105, 147) and others which are resistant to one RNA phage, MS2, but susceptible to another, $Q\beta$ (and to DNA phages) (106).

The male-specific DNA phages are inferred to attach at the tips of the pili with the aid of the A protein (102), which also enters the cell and is found to form a complex with the phage DNA when it has been converted to a duplex replicative form (63). Nothing is known about the structural features of the part of the F-pilin molecule(s) which forms the attachment site for the male-specific DNA phages and attaches the donor bacterium to the recipient cell. F-pili mutants resistant to male-specific DNA phages have not been reported (14, 15).

RNA phages have also been isolated from *Pseudomonas aeruginosa* (38, 54, 55) and *Caulobacter* (142). However, nothing is known about their receptors other than they attach to pili.

CONCLUDING REMARKS

Almost every structure exposed on the surface of a bacterial cell or extending from it can act as (or include) phage receptors. Phages provided with different organelles for attachment differ in their mode of attachment to the cell. Three mechanisms for attachment can be discernible at this stage, even if other mechanisms can by no means be excluded: 1. attachment of the large tadpole-shaped DNA phages provided with both tail fibers and tailpins extending from the base plate; 2. attachment of the phages with a short noncontractile tail associated with an endoglycosidase; and 3. attachment of the isometric RNA and filamentous single-stranded DNA phages with the aid of the maturation or A protein.

In the first case, Mechanism 1, the tail fibers of the large DNA phages recognize the attachment sites, be they polysaccharide side chains in a LPS of a Gram-negative bacterium or complexes of teichoic acid covalently linked to a glycan strand in a Gram-positive bacterium. This step probably represents reversible attachment. For irreversible attachment the tail spikes, or similar base plate organelles, have to interact with the receptor. Nothing is known about the structural features of the receptor with which the tail spikes interact or whether the interaction is enzymatic. It seems clear, however, that for irreversible attachment to occur the receptor must be a macromolecular complex such as an extracted LPS aggregate from Gram-negative bacteria or a complex of teichoic acid and peptidoglycan from Gram-positive bacteria. The mechanism of attachment is the most complicated one, calling for the cooperation between tail fibers and tail spikes.

In Mechanism 2 the phages with a short noncontractile tail, like ϵ^{15} and P22, attach to the LPS receptor and are provided with an endoglycosidase that partially degrades the receptor (68, 80, 159). Attachment of the phage to the O side chain of lipid-free polysaccharide is reversible, whereas the reaction to the molecular aggregate of extracted LPS is irreversible, but only in the presence of manganese ions (159). Similarly the capsulotrophic phages attach to and degrade the capsular layer. Isolated capsular material does not inactivate the phages or only to a very limited extent (156, 160, 161) raising doubt that the capsule represents the receptor. However, in some systems failure of capsular material to inactivate may result from failure to provide some required ionic condition.

In Mechanism 3 the isometric RNA and filamentous DNA phages attach to the receptor, inferred to be situated on the sex pili, with the aid of the A protein (102, 134). The phage is uncoated and the A protein enters the cell together with the nucleic acid (63, 73). The RNA phages attach reversibly to isolated pili or at low temperatures to pili on bacteria (14, 16). The attachment to pili present on live bacteria becomes irreversible at higher temperatures (14, 16). The filamentous DNA phages cannot be eluted when they have attached to pili on bacteria at 0°C; the fact that antiphage antiserum could still block the infective process (which it cannot at 37°C) (163) indicates that the first attachment step also for this class of phages is reversible. The attachment to pili on bacteria, but not to free pili, becomes irreversible at 37°C (163).

There are some phage-receptor systems that still cannot be placed under any of these tentative headings for the mechanism of attachment: the interaction of the ϕX174-like group of bacteriophages with the receptor in the LPS and the interaction between the flagellotrophic phages with the complex of flagella and cell wall. Even when we can define the structural component of the bacterium, e.g. LPS, teichoic acid-peptidoglycan complex, pili—which constitutes the receptor of a given phage—we are faced with the problem of isolating this receptor-containing structure from the bacteria in a soluble and receptor active form. Lipopolysaccharides, which are distinct anatomical structures in the cell envelope, are relatively easily obtained in a soluble form and show almost the same receptor activity as when it is in the cell (79). For other receptor-containing structures, like the complexes of teichoic acid with peptidoglycan (27, 111) and C-carbohydrate with peptidoglycan (39, 75), it has usually not been possible to isolate a soluble receptor able to irreversibly inactivate the phages. A probable reason for this is that the teichoic acid and C-carbohydrates are not distinct anatomical structures of the cell wall but their conformation, and consequently that of the phage attachment sites, is dependent on the underlying rigid peptidoglycan network. Solubilization has involved hydrolysis of bindings in the peptidoglycan, and one has often been able to observe only reversible attachment (27, 39, 74). For future research on phage receptors it is necessary not only to extend our structural studies of receptor-containing structures but also to make use of the increasing number of phage mutants available in order to study the interaction of soluble receptors (and its subunits) with isolated phage parts like tail fibers (half fibers) and apical capsomeres. This will make it possible to define the sites involved in the primary, reversible, attachment step.

Even if we still do not know much about the structures of the receptors the mere knowledge of where in the cell they are localized or what genetic information is required for their synthesis can be successfully employed for the study of the behavior of phages in bacteria that are phage resistant because of lack of the receptor. Thus Watson & Paigen (171) found that the LPS with the receptor sites for the coliphage U3, which belongs to the ϕX174-like group, could be transferred to spheroplasts of phage-resistant cells and made them phage sensitive, a discovery which opens up new avenues to investigations not only of phage genetics but also of the function and biosynthesis of cell walls. The use of intergeneric hybrids, where *Shigella flexneri* had inherited *E. coli* genes necessary for the synthesis of the phage λ receptor, is another example of how the knowledge of the requirements to synthesize a phage receptor can be used, in this case to facilitate a study of the behavior of phage λ in *Sh. flexneri* (45).

ACKNOWLEDGMENTS

I am greatly indebted to Dr. B. A. D. Stocker for valuable discussions during the preparation of this manuscript. I am also thankful to Drs. C. C. Brinton Jr., K. Jann, O. Lüderitz, G. Schmidt, and A. Wright for their permission to cite unpublished

data. This research has been supported by The Swedish Medical Research Council grant No. B68-40X-656 and an NIH International Fellowship No. F05 TW 1912.

Literature Cited

1. Adams, M. 1959. *Bacteriophages.* New York: Interscience
2. Appelbaum, P. C., Hugo, N., Coetzee, J. N. 1971. *J. Gen. Virol.* 13:153–62
3. Archibald, A. R., Coapes, H. E. 1971. *Biochem. J.* 125:667–69
4. Bartell, P. F., Orr, T. E., Lam, G. K. H. 1966. *J. Bacteriol.* 92:56–62
5. Bartell, P. F., Orr, T. E., Reese, J. F., Imaeda, T. 1971. *J. Virol.* 8:311–17
6. Bayer, M. E. 1968. *J. Virol.* 2:346–56
7. Bayer, M. E., Starkey, T. W. 1972. *Virology* 49:236–56
8. Bertani, L. E., Bertani, G. 1971. *Advan. Genet.* 16:199–237
9. Beimer, J., Beimer-Jochmans, M. P., Dirrx, J., Deregel, D. 1965. *Bull. Acad. Roy. Med. Belg.* 5:749–90
10. Bradley, D. E. 1967. *Bacteriol. Rev.* 31:230–314
11. Bradley, D. E. 1970. *Can. J. Microbiol.* 16:965–71
12. Braun, V., Bosch, V. 1972. *Proc. Nat. Acad. Sci. USA* 69:970–74
13. Brinton, C. C. Jr. 1965. *Trans. N.Y. Acad. Sci.* 27:1003–54
14. Brinton, C. C. Jr. 1971. *Crit. Rev. Microbiol.* 1:105–60
15. Brinton, C. C. Jr. 1973. *Bacteriol. Rev.* In press
16. Brinton, C. C. Jr., Beer, H. 1967. *The Molecular Biology of Viruses*, 251–89. New York: Academic
17. Brinton, C. C. Jr., Gemski, P. Jr., Carnahan, J. 1964. *Proc. Nat. Acad. Sci. USA* 52:776–83
18. Brown, D. T., MacKenzie, J. M., Bayer, M. E. 1971. *J. Virol.* 7:836–46
19. Burnet, F. M. 1927. *Brit. J. Exp. Pathol.* 8:121–29
20. Burnet, F. M. 1934. *J. Pathol. Bacteriol.* 38:285–99
21. Campbell, G. L., Friend, P. L. 1972. *Absrr. Am. Soc. Microbiol.* 72:44
22. Caro, L. G., Schnös, M. 1966. *Proc. Nat. Acad. Sci. USA* 56:126–32
23. Chakrabarty, A. M., Niblack, J. F., Gunsulus, I. C. 1967. *Virology* 32:522–34
24. Chatterjee, A. N. 1969. *J. Bacteriol.* 98:519–27
25. Chiongio, D. T., Hayashi, J. A. 1969. *Arch. Biochem. Biophys.* 130:39–47
26. Colón, A. E., Cole, R. M., Leonard, C. G. 1971. *J. Virol.* 8: 103–10
27. Coyette, J., Ghuysen, J. M. 1968. *Biochemistry* 7:2385–89
28. Crawford, E. M., Gesteland, R. F. 1964. *Virology* 22:165–67
29. Danziger, R. E. Paranchych, W. 1970. *Virology* 40:547–53
30. Delbrück, M. 1940. *J. Gen. Physiol.* 23:631–42
31. DePamphilis, M. L. 1971. *J. Virol.* 7: 683–86
32. DePamphilis, M. L., Adler, J. 1971. *J. Bacteriol.* 105:376–83; 384–95; 396–407
33. Dettori, R., Maccacaro, G. A., Piccinin, G. L. 1961. *Giorn. Microbiol.* 9: 141–50
34. Edgell, M. H., Ginoza, W. 1965. *Virology* 27:23–27
35. Edgell, M. H., Hutchison, C. A. III., Sinsheimer, R. L. 1969. *J. Mol. Biol.* 42:547–57
36. Edwards, S., Meynell, G. G. 1967. *J. Gen. Virol.* 2:443–44
37. Eklund, C., Wyss, O. 1962. *J. Bacteriol.* 84:1209–15
38. Fearry, T. W., Fisher, E. Jr., Fisher, T. N. 1964. *J. Bacteriol.* 87:196–208
39. Fischetti, V. A., Zabriskie, J. B. 1968. *J. Exp. Med.* 127:489–505
40. Franklin, N. C. 1969. *Virology* 38: 189–91
41. Freer, J. H., Salton, M. R. J. 1971. *Microbial Toxins IV*, 67–126. New York: Academic
42. Fujimura, R., Kuesberg, P. 1962. *Biophys. J.* 2:43–49
43. Fukasawa, T., Saito, S. 1964. *J. Mol. Biol.* 8:175–83
44. Garen, A., Kozloff, L. M. 1959. *The Viruses*, 2:203–36. New York: Academic
45. Gemski, P. Jr., Alexeichik, J. A., Baron, L. S. 1972. *J. Virol.* 10:668–74
46. Ghuysen, J.-M., Stromінger, J. L., Tipper, D. J. 1968. *Comp. Biochem.* 26A:53–104
47. Glaser, L., Ionesco, H., Schaeffer, P. 1966. *Biochim. Biophys. Acta* 124: 415–17
48. Godard, C., Beumer-Jochmans, M. P., Beumer, J. 1971. *Ann. Inst. Pasteur* 120:475–89
49. Hagiwara, S., Uetake, H., Takeda, K. 1956. *Ann. Rep. Inst. Virus Res. Kyoto Univ.* 9:126–29
50. Hattman, S., Fukasawa, T. 1963. *Proc. Nat. Acad. Sci. USA* 50:297–300
51. Henry, C. M. 1972. *Studies on the tetragonal self-assembling protein layer of Bacillus brevis Pt.* PhD thesis. Univ. Pittsburgh, Pittsburgh, Pennsylvania. 172 pp.
52. Hirst, A., Stubbs, J. M. 1969. *J. Bacteriol.* 97:1466–79
53. Hohn, T., Hohn, B. 1970. *Advan. Virus Res.* 16:43–98
54. Holloway, B. W. 1969. *Bacteriol. Rev.* 33:419–43
55. Holloway, B. W., Krishnapillai, V., Stanisich, V. 1971. *Ann. Rev. Genet.* 5:425–46
56. Hsu, Y. C. 1968. *Bacteriol. Rev.* 32: 387–407
57. Hämmerling, G., Lüderitz, O., Westphal, O., Märeli, P. H. 1971. *Eur. J. Biochem.* 22:331–44
58. Iino, T. 1969. *Bacteriol. Rev.* 33: 454–75
59. Iino, T., Mitani, M. 1967. *J. Virol.* 1: 445–47
60. Iino, T., Mitani, M. 1967. *J. Gen. Microbiol.* 49:81–88
61. Israel, J. V., Anderson, T. F., Levine, M. 1967. *Proc. Nat. Acad. Sci. USA* 57:284–91
62. Israel, V., Rosen, H., Levine, M. 1972. *J. Virol.* 10:1152–58
62a. Jann, K., Schmidt, G., Wallenfels, B., Freund-Möllbert, E. 1971. *J. Gen. Microbiol.* 67:289–97
63. Jazwinski, S. M., Marco, R., Kornberg, A. 1973. *Proc. Nat. Acad. Sci. USA* 70:205–9
64. Jesaitis, M. A., Goebel, W. F. 1953. *Cold Spring Harbor Symp. Quant. Biol.* 18:205–8
65. Johnston, J. H., Johnston, R. J., Simmons, D. A. R. 1967. *Biochem. J.* 105: 79–87
66. Jonasson, J., Rutberg, L., Young, F. E. 1969. *J. Virol.* 4:309–10
67. Joys, T. M. 1965. *J. Bacteriol.* 90: 1575–77
68. Kanegasaki, S., Wright, A. 1973. *J. Virol.* 52:160–73
69. Karakawa, W. W., Kane, J. A. 1971. *J. Immunol.* 106:900–6
70. Kay, D. 1962. *J. Gen. Microbiol.* 27: 201–7
71. Kita, H., Nikaido, H. 1973. *J. Bacteriol.* 113:672–79
72. Koike, M., Iida, K. 1971. *J. Bacteriol.* 108:1402–11
73. Krahn, P. M., O'Callaghan, R. J., Paranchych, W. 1972. *Virology* 47: 628–37
74. Krause, R. M. 1957. *J. Exp. Med.* 106: 365–83
75. Ibid 1958. 108:803–21
76. Lehmann, V., Lüderitz, O. Personal communication
77. Levine, P., Frisch, A. W. 1934. *J. Exp. Med.* 59:213–28
78. Lindberg, A. A. 1967. *J. Gen. Microbiol.* 48:225–33
79. Lindberg, A. A. 1971. *Bacteriophage attachment and inactivation in relation to chemical composition of Salmonella lipopolysaccharides.* Thesis. Karolinska Institutet, Stockholm, Sweden. 47 pp.
80. Lindberg, A. A. Unpublished observations
81. Lindberg, A. A., Hellerqvist, C.-G. 1971. *J. Bacteriol.* 105:57–64
82. Lindberg, A. A., Hellerqvist, C.-G., Motta, G., Mäkelä, P. H. Unpublished observations
83. Lindberg, A. A., Hellerqvist, C.-G., Rydén, U. Unpublished observations
84. Lindberg, A. A., Holme, T. 1969. *J. Bacteriol.* 99:513–19
85. Lindberg, A. A., Holme, T. 1969. *Colloq. Int. Centre Nat. Rech. Sci.* 174: 141–54
86. Lindberg, A. A., Holme, T., Hellerqvist, C.-G., Svensson, S. 1970. *J. Bacteriol.* 102:540–47
87. Lindberg, A. A., Sarvas, M., Mäkelä, P. H. 1970. *Infect. Immunity* 1:88–97
88. Lodish, H. F., Zinder, N. D. 1965. *Biochem. Biophys. Res. Commun.* 19: 269–78
89. Loeb, T. 1960. *Science* 131:932–33
90. Loeb, T., Zinder, N. D. 1961. *Proc. Nat. Acad. Sci. USA* 47:282–89
91. Losick, R., Robbins, P. W. 1969. *Sci. Am.* 221:120–34
92. Lovett, P. S. 1972. *Virology* 47:743–52
93. Lovett, P. S., Shockman, G. D. 1970. *J. Virol.* 6:125–34
94. Lovett, P. S., Shockman, G. D. 1970. *J. Virol.* 6:135–44
95. Luria, S. E., Human, M. L. 1952. *J. Bacteriol.* 64:557–69
96. Lüderitz, O., Jann, K., Wheat, R. 1968. *Comp. Biochem.* 26A:105–228
97. Lüderitz, O., Staub, A. M., Westphal, O. 1966. *Bacteriol. Rev.* 30:192–255
98. Lüderitz, O., Westphal, O., Staub, A. M., Nikaido, H. 1971. *Microbial Toxins IV*, 145–233. New York: Academic
99. Maré, I. J., Smit, J. A. 1969. *J. Gen Virol.* 5:551–52
100. Mark, M. T. Personal communication
101. Martinez, R. J., Ichiki, A. T., Lundh, N. P., Tronick, S. R. 1968. *J. Mol. Biol.* 34:559–64

102. Marvin, D. A., Hohn, B. 1969. *Bacteriol. Rev.* 33:172–209
103. McDonough, M. W. 1965. *J. Mol. Biol.* 12:342–55
104. Meynell, E. W. 1961. *J. Gen. Microbiol.* 25:253–90
105. Meynell, E. W., Datta, N. 1967. *Nature* 214:885–87
106. Meynell, G. G., Aufreiter, E. 1969. *J. Gen. Microbiol.* 59:429–30
107. Meynell, G. G., Lawn, A. M. 1968. *Nature* 217:1184–86
108. Michael, J. G. 1968. *Proc. Soc. Exp. Biol. Med.* 128:434–38
109. Minamishima, Y., Takeya, K., Ohnishi, Y., Amako, K. 1968. *J. Virol.* 2:208–13
110. Morse, S. I. 1962. *J. Exp. Med.* 116: 247–57
111. Murayama, Y., Kotani, S., Kato, K. 1968. *Biken's J.* 11:269–91
112. Naide, Y., Nikaido, H., Mäkelä, P. H., Wilkinson, R. G., Stocker, B. A. D. 1965. *Proc. Nat. Acad. Sci. USA* 53: 147–53
113. Newbold, J. E., Sinsheimer, R. L. 1970. *J. Virol.* 5:427–31
114. Newbold, J. E., Sinsheimer, R. L. 1970. *J. Mol. Biol.* 49:49–66
115. Orum, J. D. 1971. *J. Gen. Virol.* 13: 59–71
116. Oram, J. D., Reiter, B. 1968. *J. Gen. Virol.* 3:103–19
117. Ornellas, E. P., Enomoto, M., Stocker, B. A. D. 1971. *Bacteriol. Proc.* 71:207
118. Osborn, M. J. 1969. *Ann. Rev. Biochem.* 38:501–38
119. Ou, J. T., Anderson, T. F. 1972. *J. Virol.* 10:869–71
120. Pazur, J. H., Anderson, J. S., Karakawa, W. W. 1971. *J. Biol. Chem.* 246:1793–98
121. Paranchych, W. 1966. *Virology* 28: 90–99
122. Paranchych, W., Krahn, P. M., Bradley, R. D. 1970. *Virology* 41:465–73
123. Park, B. H. 1956. *Virology* 2:711–18
124. Patterson Delafield, J., Martinez, R. J., Stocker, B. A. D., Yamaguchi, S. 1973. *Arch. Mikrobiol.* In press
125. Pye, J. 1968. *Ann. Rep. 1967–1968 Walter and Eliza Hall Inst. Med. Res., Melbourne, Australia*, p. 72
126. Raab, C., Röschenthaler, R. 1970. *Biochem. Biophys. Res. Commun.* 41: 1429–36
127. Radke, K. L., Siegel, E. C. 1971. *J. Bacteriol.* 106:432–37
128. Raimondo, L. M., Lundh, N. P., Martinez, R. J. 1968. *J. Virol.* 2:256–64
129. Rakieten, M. L., Rakieten, T. L. 1937. *J. Bacteriol.* 34:285–300
130. Rakieten, M. L., Rakieten, T. L., Doff, S. 1936. *J. Bacteriol.* 32:505–18
131. Rakieten, M. L., Tiffany, E. J. 1938. *J. Bacteriol.* 36:155–73
132. Rapin, A. M. C., Kalckar, H. M. 1971. *Microbial Toxins IV*, 267–307. New York: Academic
132a. Reske, K., Wallenfels, B., Jann, K. 1973. *Eur. J. Biochem.* In press
133. Robbins, P. W., Uchida, T. 1965. *J. Biol. Chem.* 240:375–83
134. Roberts, J. W., Steitz, J. E. A. 1967. *Proc. Nat. Acad. Sci. USA* 58:1416–21
135. Rothfield, L., Romeo, D. 1971. *Bacteriol. Rev.* 35:14–38
136. Rountree, P. M. 1947. *Aust. J. Exp. Biol. Med. Sci.* 25:203–11
137. Rosato, R. R., Cameron, J. A. 1964. *Biochim. Biophys. Acta* 83:113–19
138. Schade, S. Z., Adler, J. 1967. *J. Virol.* 1: 591–98
139. Schade, S. Z., Adler, J., Ris, H. 1967. *J. Virol.* 1:599–609
140. Schlesinger, M. 1932. *Z. Hyg. Infektionskrankh.* 114:136–48; 149–60
141. Schmidt, G. 1972. *Zentralbl. Bakteriol. Parasitenk., Abt. I Orig. A* 220:472–76
142. Schmidt, J. M. 1966. *J. Gen. Microbiol.* 45:347–53
143. Schnaitman, C. A. 1971. *J. Bacteriol.* 108:553–63
144. Sertic, V., Boulgakov, N. A. 1936. *C. R. Soc. Biol.* 123:887–88
145. Shands, J. W. Jr. 1971. *Microbial Toxins IV*. 127–44. New York: Academic
146. Shaw, D. R. D., Chatterjee, A. N. 1971. *J. Bacteriol.* 108:584–85
147. Silverman, P. M., Rosenthal, S., Mobach, H., Valentine, R. C. 1968. *Virology* 36:142–46
148. Simon, L. D., Anderson, T. F. 1967. *Virology* 32:279–97
149. Simon, L. D., Anderson, T. F. 1967. *Virology* 32:298–305
150. Simon, L. D., Swan, J. G., Flatgaard, J. E. 1970. *Virology* 41:77–90
151. Sneath, P. H. A., Lederberg, J. 1961. *Proc. Nat. Acad. Sci. USA* 47:86–90
152. Steitz, J. A. 1968. *J. Mol. Biol.* 33: 923–36
153. Steitz, J. A. 1968. *J. Mol. Biol.* 33: 937–45
154. Sient, G. S. 1963. *Molecular Biology of Bacterial Viruses*. San Francisco: W. H. Freeman
155. Stirm, S., Bessler, W., Fehmel, F., Freund-Möllbert, E., Thurow, H. 1971. *Virology* 45:303–8
156. Stirm, S., Bessler, W., Fehmel, F., Freund-Möllbert, E. 1971. *J. Virol.* 8: 343–46

157. Stirm, S., Freund-Möllbert, E. 1971. *J. Virol.* 8:330–42
158. Stocker, B. A. D., Mäkelä, P. H. 1971. *Microbial Toxins IV*, 369–438. New York: Academic
159. Takeda, K., Uetake, H. 1971. *Ann. Rep. Inst. Virus Res. Kyoto Univ.* 14:55
160. Taylor, K. 1965. *Biochem. Biophys. Res. Commun.* 20:752–56
161. Taylor, K. 1966. *Acta Biochim. Polon.* 13:97–106
162. Tolmach, L. J. 1957. *Advan. Virus Res.* 4:63–110
163. Tzagoloff, H., Pratt, D. 1964. *Virology* 24:372–80
164. Uetake, H., Luria, S. E., Burrows, J. W. 1958. *Virology* 5:68–91
165. Valentine, R. C., Strand, M. 1965. *Science* 148:511–13
166. Vary, P. S., Stocker, B. A. D. 1973. *Genetics* 73:229–45
167. Vidaver, A. K., Brock, T. D. 1966. *Biochim. Biophys. Acta* 121:298–314
168. Wais, A. C., Goldberg, E. B. 1969. *Virology* 39:153–61
169. Watson, J. D. 1950. *J. Bacteriol.* 60: 697–718
170. Watson, G., Paigen, K. 1971. *J. Virol.* 8:669–74
171. Watson, G., Paigen, K. 1972. *Nature New Biol.* 239:120–22
172. Weidel, W. 1958. *Ann. Rev. Microbiol.* 12:27–48
173. Weltzien, H. U., Jesaitis, M. A. 1971. *J. Exp. Med.* 133:534–53
174. Wendt, L. W., Ippen, K. A., Valentine, R. 1966. *Biochem. Biophys. Res. Commun.* 23:375–80
175. Wendt, L., Mobach, H. W. 1969. *J. Bacteriol.* 97:640–46
176. Weppelman, R. M., Brinton, C. C. Jr. 1970. *Virology* 41:16–34
177. Wildy, P., Anderson, T. F. 1964. *J. Gen. Microbiol.* 34:273–83
178. Wilkinson, R. G., Gemski, P. Jr., Stocker, B. A. D. 1972. *J. Gen. Microbiol.* 70:527–54
179. Willetts, N., Achtman, M. 1972. *J. Bacteriol.* 110:843–51
180. Wilson, J. H., Luftig, R. B., Wood, W. B. 1970. *J. Mol. Biol.* 51:423–34
181. Wolin, M. J., Archbald, A. R., Baddiley, J. 1966. *Nature* 209:484–86
182. Wright, A. 1971. *J. Bacteriol.* 105: 927–36
183. Wright, A., Barzilai, N. 1971. *J. Bacteriol.* 105:937–39
184. Wu, T. C. M., Park, J. T. 1971. *J. Bacteriol.* 108:874–84
185. Yamaguchi, S. 1967. *J. Gen Virol.* 2: 187–90
186. Young, F. E. 1967. *Proc. Nat. Acad. Sci. USA* 58:2377–84
187. Yurewicz, E. C., Ghalamber, M. A., Duckworth, D. H., Heath, E. C. 1971. *J. Biol. Chem.* 246:5607–16
188. Zinder, N. D. 1958. *Virology* 5:291–326

J. Mol. Biol. (1972) 66, 445–469

↗ EDTA ?

Product of T4 Gene *12*

WILLIAM S. MASON† AND ROBERT HASELKORN

Department of Biophysics
University of Chicago, Chicago, Ill., U.S.A.

(*Received 6 October 1971*)

The product of gene *12* appears to be required for the proper functioning of the base plate of bacteriophage T4. Utilizing an *in vitro* assay for this gene product, a purification procedure has been devised. Gel filtration and sedimentation analyses show that the partially purified protein has a molecular weight of at least 157,000 daltons; in addition, a partially purified gene *12* product preparation activates purified gene *12*⁻ particles at a high efficiency. Since other experiments have shown that the gene *12* product is a structural component of the phage, we interpret the high efficiency of activation to mean that the gene *12* product is the only structural defect of gene *12*⁻ particles.

Autoradiography of infected cell extracts analyzed by electrophoresis on sodium dodecyl sulfate/acrylamide gels reveals that the gene *12* polypeptide has a molecular weight of 55,000 daltons; moreover, this labeled polypeptide is the only peptide of molecular weight greater than ~20,000 daltons which specifically binds to gene *12*⁻ particles. We suggest that the 55,000 molecular weight polypeptide is the major subunit of the active gene *12* product and that the active protein contains at least two such peptides. The possibility of additional low molecular weight subunits has not been eliminated.

Quantitative analysis of *in vitro* assembly, employing infected cell extracts, suggests that two gene *12* product molecules are capable of converting a gene *12*⁻ particle to an infective unit but a gene *12*⁻ particle possesses at least three binding sites for the gene *12* product.

This product appears to "bind" to the debris present in infected cell extracts; the product of gene *11* does not.

1. Introduction

Bacteriophage T4 heads, tails and tail fibers assemble by independent pathways, and the completed substructures are then assembled into viable phage (Wood, Edgar, King, Lielausis & Henninger, 1968). When a phage possesses a conditionally lethal mutation in gene *12*, infection under non-permissive conditions leads to the accumulation of non-infective phage-like particles (*12*⁻ particles). These particles appear normal by electron microscopy and carry normal amounts of tail fiber antigen (King, 1968); however, although able to absorb to the surface of host bacteria, gene *12*⁻ particles are unable to cause lysis from without, or to kill the bacterium (King, 1968; Simon, Swan & Flatgaard, 1970).

Edgar & Wood (1966) have shown that the gene *12* product can participate in *in vitro* assembly, apparently by acting upon the base plate or core-base plate (Edgar & Lielausis, 1968). Phage particles which have not been acted upon by the gene *12*

† Present address: Department of Microbiology, U.S.C. School of Medicine, Los Angeles, Calif. 90033, U.S.A.

product are defective in attachment of the "short tail fibers" to the cell surface and/or the co-ordination of base plate attachment with sheath contraction and DNA release (Simon *et al.*, 1970)—that is, the base plate seems to be defective.

Phage carrying a mutation in gene *11* synthesize phage particles (under non-permissive conditions) which are phenotypically similar to gene *12*$^-$ particles (King, 1968; Simon *et al.*, 1970). Yanagida & Ahmad-Zadeh (1970) have presented data suggesting that the gene *12* product is an antigenic component of the intact base plate, while under similar conditions gene *11* antigen is not detectable; in addition, *in vitro* studies have shown that gene *11*$^-$ phage particles are also gene *12*$^-$, whereas gene *12*$^-$ particles are gene *11*$^+$ (Edgar & Lielausis, 1968). It thus appears that the gene *12* product is a surface component of the base plate, possibly of the spikes (Simon *et al.*, 1970), whereas the gene *11* product might not be exposed to the surface on intact phage.

Snustad (1968) suggested that in mixed infection with T4$^+$ and gene *12*$^-$ (or gene *11*$^-$) phage the *in vivo* requirement for active gene *12* product (and gene *11* product) is stoichiometric rather than catalytic, also implying that the gene *12* product may be a structural subunit of the phage.

In this report *in vitro* assembly has been exploited to characterize further the gene *12* product. Since the gene *12* product acts on the phage tail, mutants defective in tail or in head and tail formation have been used as gene *12* product (12P) *donors* and gene *12*$^-$ particles as 12P *acceptors*. The hydrodynamic properties of the gene *12* product have been examined, a preliminary purification procedure has been devised, and a quantitative analysis of the *in vitro* assembly reaction has been applied to determine the stoichiometry of gene *12* product activation of *12*$^-$ particles.

For convenience and economy, we have followed the following convention in referring to the products of T4 genes: the single polypeptide product of gene *12*, identified, for example, on SDS/polyacrylamide gels, is called P12 (Laemmli, 1970). The biologically active complex, capable of converting *12*$^-$ particles to plaque-forming units, is called 12P.

2. Materials and Methods

(a) *Bacterial strains*

Escherichia coli strains B^E and CR63 served as the non-permissive and permissive hosts, respectively, for T4 amber mutants. When selective plating was necessary to distinguish between amber mutants an rII (*rd*/41) deletion was incorporated into the appropriate genome and S26R1E was used as the selective host (S26R1E is non-permissive for rII mutants, but suppresses amber mutants).

(b) *Phage strains*

The T4 *amber* mutants were derivatives of T4D and are from the collection of R. S. Edgar, who generously supplied us with the following amber mutants: *5*$^-$(N135); *6*$^-$(N102); *7*$^-$(B16); *8*$^-$(N132); *9*$^-$(E17); *10*$^-$(B255); *11*$^-$(N93); *12*$^-$(N69; N104; NG75); *23*$^-$(B17); *25*$^-$(N67); *26*$^-$(N131); *27*$^-$(N120); *28*$^-$(A452); *29*$^-$(B7); *51*$^-$(S29); *53*$^-$(H28); *34*$^-$(B25-A455); *37*$^-$(N52-B280); X4E (Edgar & Wood, 1966); XP18 (genes *5*$^-$, *6*$^-$, *7*$^-$, *8*$^-$, *9*$^-$, *10*$^-$ = B256-B251-B16-N132-E17-B255). X4E carries mutations in genes *34*, *35*, *37* and *38*; these genes all affect tail fiber proteins. Gene *23* is the principal head capsid protein; all other genes listed are involved in tail formation. Several multiple amber mutants were constructed: *12*$^-$(N69-N104), back-crossed three times with T4$^+$; *12*$^-$-*23*$^-$-*27*$^-$ $\pm$*rd* 41 (N69-N104-B17-N120 $\pm$*rd*/41); *23*$^-$-*27*$^-$ $\pm$*rd* (B17-N120 $\pm$*rd*/41); *12*$^-$-*27*$^-$ (N69-N104-N120); *23*$^-$-*27*$^-$-*34*$^-$-*37*$^-$. The rII mutant was selected by inability

to plate on S26RIE; *23⁻-27⁻-34⁻-37⁻* was selected by inability to complement (Edgar, Denhardt & Epstein, 1964) the respective double mutants in genes *34* and *37*.

(c) *Media and buffers*

Tryptone broth, used for bacterial growth and as a dilution medium for plating, contained 10 g Bacto-Tryptone (Difco) and 5 g NaCl in 1000 ml. of water. M9, used for radioactive labeling, contained 7 g $Na_2HPO_4 \cdot 2H_2O$, 3 g KH_2PO_4, 0·5 g NaCl, 1 g NH_4Cl, 4 g glucose, 0·5 m-moles $MgSO_4$, and 0·05 m-mole $CaCl_2$/l. Supplemented M9 medium (M9S), used in the preparation of phage lysates and extracts, contained 10 g of Casamino acids (Difco)/l. of M9 medium. Tryptone bottom agar contained 5 g NaCl, 10 g Bacto-Tryptone, and 15 g Bacto-Agar (Difco)/l. of water. Epstein–Hershey top agar (EHA) has been described (Steinberg & Edgar, 1962).

Hershey T2 buffer (HT2), used for resuspending phage pellets, has been described by Hershey & Chase (1952), and BUM buffer (0·0039 M-Na_2HPO_4, 0·0022 M-KH_2PO_4, 0·007 M-NaCl, 0·02 M-$MgSO_4$) by Edgar & Lielausis (1968). 0·061 M-phosphate buffer was 0·039 M-Na_2HPO_4, 0·022 M-KH_2PO_4.

(d) *Defective lysates and extracts*

E. coli B^s were grown to 4×10^8/ml. (at 37°C), infected at a multiplicity of infection of 5 and superinfected 5 min later (if indicated) at the same multiplicity of infection. Acceptor *lysates* were prepared by chilling the infected culture, which was then clarified by centrifugation and stored at 4 to 7°C (50 to 100 μg chloramphenicol/ml. was usually added to retard bacterial growth). Gene *12⁻* particle lysates retained activity for several months. Donor lysates were frozen quickly (in dry ice/acetone) if not intended for use the same day, stored at −20°C, and used within a few hr after being thawed. Lysates intended for use the same day were prepared simply by chilling an infected culture to 4°C.

Defective *extracts* were prepared essentially as described by Edgar & Lielausis (1968). Cells were resuspended in 0·02 to 0·01 the volume of the infected culture, and portions were quick-frozen and stored at −20°C.

(e) In vitro *complementation*

The basic procedure for *in vitro* complementation (assembly) has been described by Edgar & Lielausis (1968). Complementation was usually initiated by mixing equal volumes (0·05 or 0·1 ml.) of donor and acceptor (donor added to acceptor) at 4°C. Reaction mixtures were diluted in Tryptone broth for plating. The results are expressed as plaque-forming units/ml. of reaction mixture after subtracting the background due to acceptor alone (unless indicated); the donor background was generally negligible. The donor or acceptor dilution is the dilution before mixing. Complementation conditions are indicated as: amount donor — amount acceptor; length of 30°C incubation; buffer.

(f) *Centrifugation*

5 ml. and 27 ml. of 5 to 20% linear sucrose gradients were prepared in nitrocellulose tubes. Following centrifugation, 15-drop fractions (5-ml. gradients) or 33-drop fractions (27-ml. gradients) were collected from a needle inserted through the bottom of the tube; if pelleted material was present, the needle was inserted so that the opening was slightly above the pellet. Sedimentation coefficients were determined using the method of Martin & Ames (1961) with external sedimentation markers. Since different numbers of fractions were usually collected from each gradient of a set, the positions of peaks of activity are normalized with respect to the number of fractions collected from the gradient containing catalase. Peaks are indicated as weight averages ($\downarrow$) or as maximum activity ($\downarrow$). Clarification denotes a 10- to 15-min spin at 5000 rev./min. Continuous flow centrifugation employed a Sorvall continuous flow system (flow rate 200 to 400 ml./min) at 16,000 rev./min.

(g) *Purification of particles (12⁻; X4E) and phage*

Lysates were clarified and the phage (or particles) pelleted (e.g. 40 min at 26,000 rev./min, 30 rotor or 90 min at 12,900 rev./min, GSA rotor). The pellets were resuspended in HT2 buffer, and the resuspended phage clarified. For further purification, 2-ml. samples of phage or particles ($< 2{\cdot}5 \times 10^{12}$/ml.) were centrifuged for 15 min at 30,000 rev./min in

the SW50 rotor at 20 to 25°C through a CsCl step gradient containing 0·5-ml. samples of 70,60,50,40,30,20% CsCl (% saturation) in 0·01 M-Tris · HCl, pH 7·5 (the 20% layer contained 5% (v/v) glycerol). CsCl was removed from the phage band by successive dialyses against 1·0 M-NaCl/0·01 M-Tris (pH 7·5) and 0·1 M-NaCl/0·01 M-Tris, pH 7·5.

(h) *Labeling of infected bacteria*

E. coli B^{s} were grown to 4×10^{8}/ml. at 37°C, infected (with pelleted phage) at a multiplicity of infection of 5, and superinfected 8 min later. A ^{14}C-labeled amino-acid mixture was added at 20 min. At 30 to 35 min the cells were poured onto crushed ice, collected by centrifugation, and resuspended in 0·1 vol. of SDS sample buffer (Laemmli, 1970). Labeled extracts (10- to 50-fold concentrated) for *in vitro* complementation were prepared as described in section (d) above. Infected cells received 0·047 to 0·168 μCi/ml. of each of the following amino acids: L-arginine, L-leucine, L-lysine, L-valine, L-threonine and L-isoleucine. Incorporation into material insoluble in hot trichloroacetic acid was measured in a Beckman low beta Gas-flow Counter (17% efficiency).

(i) *Sodium dodecyl sulfate gel electrophoresis*

Polyacrylamide gel electrophoresis in SDS was carried out using the procedures described by Laemmli (1970) on 10% gels. Extracts in SDS sample buffer (Laemmli, 1970) were heated for 2 min at 100°C before electrophoresis; phage pellets were heated for 10 min. Sample volumes (per gel) were usually 50 to 100 μl. Electrophoresis (4 mA/gel) was continued until the tracking dye (bromothymol blue) had migrated 7 to 8 cm. Gels were fixed and stained according to Weber & Osborn (1969), except that the gels were allowed to destain by diffusion; in some cases the staining step was omitted. Polypeptide molecular weights were determined using the calibration procedure of Weber & Osborn (1969), with calibration standards used as external markers.

The procedure for slicing and drying gels has been described by Fairbanks, Levinthal & Reader (1965). Autoradiograms were prepared using Kodak No Screen X-ray film.

(j) *Filtration chromatography*

Sephadex G200, Sepharose 4B, and Sephadex K25/45 columns were products of Pharmacia Fine Chemicals, Inc. Gel columns (2·5 cm × 35 to 40 cm) were prepared, a suitable operating pressure was maintained with a mariotte bottle (5 to 10 cm buffer with G200; 12 to 15 cm buffer with Sepharose 4B), and columns were eluted with downward flow. Void volumes were determined with Blue Dextran 2000 (Pharmacia): 0·2% (w/v) for G200, 0·5% (w/v) for Sepharose 4B. Columns were further calibrated for the determination of Stokes radii using the procedure of Ackers & Steere (1967).

(k) *Protein assays*

Protein was assayed by the colorimetric method of Lowry, Rosebrough, Farr & Randall (1951); in some cases, bovine serum albumin and ovalbumin concentrations were determined by adding 10% trichloroacetic acid, vortexing briefly, incubating for 15 min at 30°C, measuring the absorbance at 300 nm, and comparing with a calibration standard (10 to 80 μg/ml.). In the colorimetric assay, protein concentrations have been expressed as mg equivalents of bovine serum albumin.

(l) *Partial purification of gene 12 product*

E. coli B^{s} were grown to 4×10^{8}/ml. (at 32°C), infected with XF18 at a multiplicity of infection of 5, and superinfected 5 min later. After 3·5 hr the bacteria and bacterial debris were chilled by passage through copper coils packed in ice-water and collected by continuous flow centrifugation at 300 to 400 ml./min. Portions were quick-frozen at this time (F1) to serve as 12P standards for later assays.

The pellets were resuspended, with sonication, in 0·061 M-phosphate buffer; 0·2 mg. DNase was added and after a 15-min incubation at 30°C the volume was brought to 1·1. with cold 0·061 M-phosphate (fraction 1). The bacterial debris were pelleted (60 min-9K-GSA)† and resuspended in 200 ml. of 0·061 M-phosphate/0·01 M-EDTA. After a 15-min

† Conditions of centrifugation are abbreviated by specifying time, speed in thousands of rev./min (K), and rotor in parentheses. SS34 and GSA are Sorvall rotors; all others are Spinco.

incubation at 30°C (fraction II) this fraction was clarified twice: 15 min-5*K*-GSA, then 40 min-26*K*-30 rotor (fraction III). Saturated ammonium sulfate was added to fraction III to 43% (12P salts out at 35 to 40% saturated ammonium sulfate) and the precipitate collected (40 min-16*K*-21 rotor). The precipitate was resuspended in 0·061 M-phosphate/0·01 M-EDTA (fraction IV). Fraction IV was made 50% in ammonium sulfate; the precipitate was collected (30 min-15*K*-SS34) and resuspended in 12 to 15 ml. of 0·061 M-phosphate/0·01 M-EDTA (i.e. the volume was adjusted so that the fraction floated on 5% sucrose (V)). Fraction V was layered on three 37-ml. 5 to 20% sucrose gradients (0·061 M-phosphate/0·01 M-EDTA) at 3 to 5 ml./gradient and centrifuged for 38 to 42 hr-23-5*K*-SW25 rotor (Fig. 1). The peak fractions were pooled (fraction VI), ammonium sulfate was

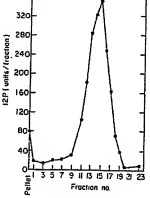

FIG. 1. Preparative sucrose gradient centrifugation of gene *12* product. See Materials and Methods, section (1).

added to 50% saturation, the precipitate was collected (30 min-10*K*-SS34), and resuspended in 0·061 M-phosphate/0·01 M-EDTA (fraction VII). Fraction VII has been further analyzed as described in Figs 6 and 7. The purification is summarized in Table 1.

(m) *Chemicals*

Ammonium sulfate and sucrose (special enzyme grade) were obtained from Mann Research Laboratories and Schwarz/Mann, respectively. CaCl (ultrapure) was a product of E. Merck Ag. Darmstadt (Germany).

Ovalbumin, hog pancreas α-amylase, and yeast alcohol dehydrogenase were obtained from the Sigma Chemical Company (St Louis); β-galactosidase, chymotrypsinogen A, malate dehydrogenase, and lysozyme were from the Worthington Biochemical Corporation; catalase was from C. F. Boehringer & Söhn (Germany); bovine serum albumin and bovine plasma albumin were from General Biochemicals (Chagrin Falls, Ohio) and the Armour Pharmaceutical Company (Kankakee, Ill.), respectively; equine heart cytochrome *c* was from Calbiochem.

Chloramphenicol was obtained from Parke, Davis, and Company; Tris-(hydroxymethyl)-amino methane from Aldrich Chemical Company (Milwaukee, Wisconsin); gelatin, U.S.P. from Fisher Scientific; ^{14}C-labeled amino acids from Schwarz Bioresearch, Inc. and New England Nuclear. All other chemicals were reagent grade.

(n) *Miscellaneous*

12P assays: gene *12* product donors were usually not diluted until immediately before mixing with 12P acceptor. Unless otherwise noted, the acceptor was a clarified N69-N104 gene *12*$^{-}$ particle lysate.

TABLE 1

A partial purification of the 12P

Fraction	Volume	Units 12P	Protein (mg)	Unit 12P/mg protein	Purification factor
		Experiment 1			
Ft	15 l.	≡15,000	4650	3·23	
lysate	15 l.	11,700	4650	2·52	≡1
I	1 l.	10,000	1250	8·0	3·18
II	200 ml.	5000	808	6·2	2·46
III	170 ml.	4550	70	65	25·8
IV	13 ml.	2830	28·6	99	39·3
V	14 ml.	2280	22·4	102	40·5
VI	20·4 ml.	1490	2·55	585	232
VII	6·6 ml.	1060	3·3	322	128
		Experiment 2			
Ft	12·25 l.	12,250	5900	2·08	
lysate	12·25 l.	10,000	5900	2·71	≡1
I	1 l.	7900	820	9·6	3·54
II	200 ml.	4200	392	10·7	3·95
III	180 ml.	4290	42	102	37·6
IV	33 ml.	2800			
V	10 ml.	2100	22·4	94	34·7
VI	18 ml.	1220	1·71	710	262
VII	6·7 ml.	1260	2·14	585	216

See Materials and Methods, section (1) for details.

EDTA concentrations are nominal for experiments in which EDTA was added to lysates or extracts to provide for the release of 12P from debris (additions were usually made from a 0·5 M-EDTA stock solution, and indicated molarities do not take into account volume changes).

Illustrations. A straight line with a slope of −2 has been drawn to fit the data (at limiting donor concentrations) for all of the *in vitro* complementation assays; moreover, this slope has been used for all quantitative estimates of gene *12* product activity.

3. Results

(a) *An assay for the activity of gene* 12 *product* (*12P*)

In order to determine appropriate conditions for the *in vitro* assay for 12P, a series of experiments employing both crude and clarified extracts of gene *12*⁻ and *23*⁻*-27*⁻*rdf* infected cells was performed. S26R1E was used for plating complemented gene *12*⁻ particles since this bacterium is non-permissive for any phage present in the gene *23*⁻*-27*⁻*rdf* extracts. The results of one experiment in which various dilutions of a gene *23*⁻*-27*⁻*rdf* extract were complemented with a single dilution of a gene *12*⁻ extract are presented in Figure 2. The straight lines are drawn with slopes of −2, giving a reasonable fit to the data when the gene *23*⁻*-27*⁻*rdf* extract is highly diluted. Since the −2 slope seemed to be reproducible it has been utilized to provide a quantitative assay for 12P. That is, one or more data points at a suitable high 12P dilution are assumed to conform to the −2 slope, permitting extrapolation (or interpolation) to an arbitrarily chosen complemented titer. The relative concentration of two different 12P samples is then the ratio of the dilutions required to complement the

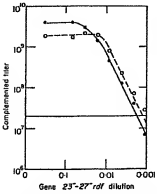

FIG. 2. *In vitro* complementation of gene *23⁻-27⁻rdf* extract with 30- and 60-fold dilutions of N69 extract.
Conditions: 0·1 ml.-0·1 ml., 2 hr at 30°C; BUM.
Plating bacteria: S26R1E.
—●—●—, N69/30; --○--○—, N69/60.

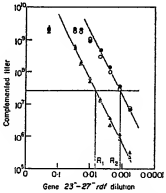

FIG. 3. Sedimentation of 12P with cell debris. Portions of N69 and gene *23⁻-27⁻ rdf* extracts were clarified and both crude and clarified extracts were diluted for *in vitro* complementation; the acceptor was used at a 50-fold dilution. The ratio R_1/R_2 is approximately 0·2 indicating that only 16% (1/6·2 × 100%) of the 12P activity remained in the donor supernatant following clarification.
Conditions: 0·1 ml.-0·1 ml.; 2 hr at 30°C; BUM.
Plating bacteria: S26R1E.
(●), N69—*23⁻-27⁻rdf*; (○), clarified N69—*23⁻-27⁻rdf*; (▲), N69—clarified *23⁻-27⁻rdf*; (△), clarified N69—clarified *23⁻-27⁻rdf*.

gene *12⁻* particles to the assigned titer (e.g. R_1/R_2 in Fig. 3). Unless noted, time has not been a limiting factor in the gene *12 in vitro* complementation reaction (R. Haselkorn and L. Deloria, unpublished data; Mason, 1971).

Since at all dilutions of gene *23⁻-27⁻rdf* extract the complemented titer was dependent upon the concentration of the gene *12⁻* extract, 12P concentrations must be determined at a fixed concentration of acceptor extract. Addition of an excess of

gene *12*$^-$*-23*$^-$*-27*$^-$*rdf* extract to the *in vitro* complementation mixes does not significantly alter the complemented titer (Mason, 1971), suggesting that the gene *12*$^-$ particle itself is the limiting factor in the contribution of gene *12* acceptor extract to *in vitro* assembly.

Three gene *12 amber* mutants (N69, NG75, and N104) were found to produce equivalent gene *12* acceptor lysates, suggesting that *in vitro* complementation is not significantly inhibited by the gene *12 amber* peptide fragments produced by any of these mutants. (N69 and N104 have been described by Edgar *et al.* (1964); NG75 recombines with both N69 and N104.) The gene *12* acceptor lysates are stable for several months at 4°C. T4 and gene *12*$^-$ particles purified through CsCl had specific activities of 0·92 and $1·02 \times 10^{11}$ particles per optical density unit at 265 nm, compared to $1·2 \times 10^{11}$ T4 phage per optical density unit reported by Winkler, Johns & Kellenberger (1962). The purified gene *12*$^-$ particles retained greater than 80% of their activity after six months at 4°C.

Several modifications of BUM buffer have been tested for their effect on *in vitro* complementation. Of these, BUM supplemented with bovine serum albumin (50 μg/ml.) was found to produce the highest complemented titer; the bovine serum albumin supplement appeared to stabilize the diluted 12P, since it was almost equally effective if used for 12P dilution alone or for diluting both the donor and acceptor extracts for *in vitro* complementation.

(b) *12-P donor activity of base plate mutant lysates*

Since gene *12* expression, *in vitro*, might be affected by the expression of other base plate gene products, a set of base plate mutants was tested for 12P donor activity, with the results shown in Table 2. In order to compare lysates, 12P activity was normalized with respect to the activity of T4 lysozyme, a gene product whose expression should be independent of the base plate genes. Experiments 1 and 3 in Table 2 show that, of the base plate genes, only gene *9* mutant infection displays a seriously depressed level of 12P activity, comparable to that of *rdf* (normal phage) or X4E (fiberless phage). We interpret the fact that the latter two show donor activity (experiment 2) to mean that 12P is normally made in excess with respect to assembled components capable of binding 12P irreversibly. The reduced 12P donor activity of the *9*$^-$ lysate could be due to irreversible association of 12P with structures containing 12P binding sites (Flatgaard, 1969). Alternatively, the gene *9 amber* mutation might be polar, and depress the expression of gene *12*.

For consistency, *27*$^-$ and XF18 have been used as 12P donors for the experiments described below.

(c) *Hydrodynamic properties of the gene* 12 *product activity in crude preparations*

Clarification of extracts containing 12P by low speed centrifugation removes most of the gene *12* complementing activity. This point is illustrated in Figure 3, which shows that low speed clarification of the acceptor extract does not affect the complemented titer whereas low speed clarification of the donor extract reduces the titer greater than 10-fold. Other experiments have shown that the 12P can be recovered quantitatively from the pellet fraction.

Lysates and extracts contain appreciable concentrations of Mg^{2+} ions which might promote the binding of 12P to cell wall or membrane debris. The effect of EDTA on low speed centrifugation of the 12P (suggested by M. R. Adelman) was therefore

TABLE 2

Production of gene 12 *product in base plate mutant infection*

Mutant gene	12P complementing activity / lysozyme activity
Experiment 1	
5	1·0
6	1·12
7	0·98
8	1·11
9	0·36
10	0·78
25	0·87
26	1·08
27	1·17
28	0·74
29	0·72
51	0·66
53	0·6
Experimont 2	
27	0·02
rdf	0·44
X4E	0·40
Experiment 3	
27	1·0
27rdf	0·87
9	0·81
11rdf	0·74
11-27rdf	0·82

B^s was infected at a multiplicity of infection of 5 (at 37°C) and cells were chilled upon lysis or at 30 to 35 min post-infection; portions were quick-frozen at the end of infection for subsequent lysozyme assays. When lysis was complete 12P assays were performed. Lysozyme was assayed according to the procedure of Sekiguchi & Cohen (1964).

Expt 1. The 12P acceptor was pelleted gene *12*$^-$ particles; a frozen portion of the gene *27*$^-$ lysate was assigned a 12P activity of 1·0. Frozen portions of a 30 min. 30°C-T4$^+$ lysate (cell count 5×10^8/ml.) served as a lysozyme standard (activity = 1·0).

Expt 2. 12P assays were carried out with N69-N104 or N69-N104 *rdf* acceptor lysates: *rdf* was complemented with N69-N104 and plated on S26R1E; X4E was complemented with N69-N104 *rdf* and plated on S26R1E and CR63; gene *27*$^-$ was complemented with both acceptors and plated on both hosts, since gene *27*$^-$ served as a 12P standard. X4E particles were not significantly activated by N69-N104 *rdf*. Gene *27*$^-$ served as a lysozyme standard (activity = 1·0).

Expt 3. As in experiment 1. The gene *27*$^-$ lysate had assigned 12P and lysozyme activities of 1·0. Plating bacteria were S26R1E.

studied. Addition of EDTA prevented the 12P from sedimenting at low speed; however, an excess of EDTA over Mg^{2+} was not required (Table 3). High monovalent salt concentration alone does not promote release of 12P from the pellet fraction. The results presented in Table 4 show that 1·0 M-KCl does not give efficient release while 1·0 M-KCl/0·01 M-EDTA releases 12P as efficiently as 0·01 M-EDTA; 0·001 M-EDTA is more effective in 0·061 M-phosphate than in 0·0061 M-phosphate, suggesting the importance of the ionic strength of the buffer system as well as the chelating action of EDTA in promoting 12P release.

The sedimentation coefficient of 12P has been determined in several of the buffers listed in Tables 3 and 4. The 12P (low molecular weight species) has a sedimentation

TABLE 3

Low-speed sedimentation of 12P: effect of EDTA

EDTA concentration in resuspended pellet (M)	12P Complementing activity	
	Total resuspended pellet	Low-speed supernatant
0	1·00	0·12
5×10^{-3}	0·97	0·59
$2{\cdot}5 \times 10^{-2}$	0·94	0·83
5×10^{-2}	0·87	0·90

The low-speed (15 min-5*K*-30 rotor) pellet of a lysate of gene 23⁻-27⁻ infected *E. coli* B^{E} was resuspended by homogenization in the original volume of BUM, and 0·5 M-EDTA was added to the concentrations indicated in the first column. The suspensions were incubated for 1 hr at 4°C and then centrifuged at low speed. The second and third columns list the 12P activity before and after the second low-speed centrifugation, relative to the total activity in the sample without EDTA.

TABLE 4

Release of 12P by KCl and EDTA

Buffer	Relative amount of 12P activity		
	Crude suspension	Supernatant	Pellet
Experiment 1			
0·061 M-phosphate	≡1	0·38	0·76
0·061 phos/10^{-2} M-EDTA	1·24	1·13	0·46
0·061 phos/10^{-2} M-EDTA	1·30	1·24	0·11
0·061 phos/0·1 M-KCl	1·0	0·2	0·84
0·061 phos/1·0 M-KCl	1·0	0·45	0·45
0·061 phos/1·0 M-KCl/10^{-2} M-EDTA	1·0	1·0	0·03
†0·061 phos/$CHCl_3$	1·18	0·15	1·18
Experiment 2			
0·0061 M-phosphate	≡1	0·28	0·62
0·0061 phos/10^{-3} M-EDTA	1·19	0·29	0·72
0·0061 phos/0·01 M-KCl	1·0	0·28	0·64
0·0061 phos/0·1 M-KCl	0·81	0·16	0·66
0·0061 phos/1·0 M-KCl	0·78	0·26	0·48

One liter of B^{E} was infected with XF18 (multiplicity of infection = 5) and super-infected 6 min later. After 3 hr, 0·2 mg DNase was added, the culture was chilled until lysis, divided into portions, and centrifuged for 15 min-5*K*-GSA. The pellets were resuspended in 0·061 or 0·0061 M-phosphate at 0·025 to 0·02 volume. Recovery of 12P activity at this step was 30 to 50%. 0·5 M-EDTA and 4·0 M-KCl (in the respective buffers) were added to the indicated concentrations, the suspensions were sonicated to produce the crude suspensions (column 2), portions were centrifuged for 10 min-5*K*-SS34, and the pellets resuspended to the original volume in 0·0061 M-phosphate/0·001 M-EDTA (column 4).

† 0·5 ml. of $CHCl_3$ was added to a 2·0-ml. system and the mixture was incubated for 15 min at room temperature. The undissolved chloroform was removed before centrifugation.

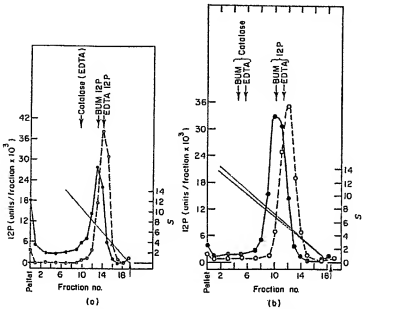

FIG. 4. Gradient centrifugation of 12P in various buffers.

(a) A gene *23*⁻*27*⁻ extract was diluted 3-fold with BUM and divided into 2 portions; 0·5 M-EDTA was added to one portion to 0·025 M and both were incubated for 15 min at 30°C. 0·1-ml. samples were then analyzed by centrifugation on 5 ml. of 5 to 20% sucrose gradients containing the appropriate buffer. Catalase (2 mg/ml. in BUM/EDTA) was run as an external sedimentation marker; the migration of catalase on 5 to 20% sucrose gradients was the same in BUM or BUM/EDTA. The gradients were run for 12 hr 35K-SW39 at 4 to 8°C and the recoveries of BUM 12P and BUM/EDTA 12P were 130% and 103%, respectively; the peak of 12P activity in BUM was estimated by averaging over fractions 11 to 15.

(b) As in (a), except the gradients also contained 1·0 M-KCl and the samples contained 0·9 M-KCl. The external catalase marker was centrifuged in a gradient containing KCl/BUM/EDTA; the migration of catalase in KCl/BUM and KCl/BUM/EDTA was compared in a separate centrifugation, with the relative migrations indicated in the Figure. Centrifugation was for 20 hr 35K-SW50 at 4°C and the recoveries of KCl/BUM and KCl/BUM/EDTA 12P were 120% and 105%, respectively.

—●—●—, BUM 12P; --○--○--, EDTA 12P.

coefficient ($S_{20,w}$) of 7·1 s in BUM, as compared to 6·3 s in BUM/EDTA (Fig. 4(a)). In 1·0 M-KCl/BUM and 1·0 M-KCl/BUM/EDTA the values are 6·7 s and 6·4 s, respectively (Fig. 4(b)).

In order to characterize the 12P further, an estimate of the 12P density was obtained by measuring its sedimentation rate relative to "typical" proteins in sucrose gradients supplemented with potassium tartrate (Fig. 5). Figure 5(a) shows the sedimentation profile of the 12P on a sucrose gradient supplemented with 28% (w/v) potassium tartrate: the sedimentation coefficient in the presence of BUM buffer was 7·4 s. Figure 5(b) demonstrates that the sedimentation of typical proteins is well behaved in 28% tartrate. From the data in Figures 4(a) and 5 it can be shown that the partial specific volume of 12P must be in the range 0·70 to 0·75, not significantly different from the density of typical proteins (Mason, 1971).

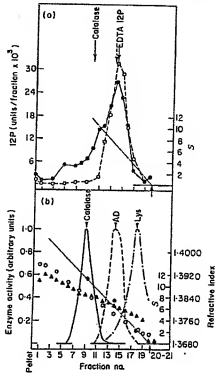

FIG. 5. Gradient centrifugation in sucrose gradients supplemented with 28% (w/v) potassium tartrate · ½ H_2O.

(a) The procedure is similar to that described in the legend to Fig. 4(a) except that the 5 to 20% sucrose gradients were also supplemented with potassium tartrate. Catalase (2 mg/ml. in BUM) was run as an external marker. The extract debris did not form a visible pellet but a sharp band of aggregated material appeared near the middle of each 12P gradient and was collected in fraction 11 (BUM gradient) and fraction 12 (BUM/EDTA gradient). The gradients were centrifuged for 60 hr-35*K*-SW50 at 3 to 5°C and the recovery of BUM/12P and BUM/EDTA/12P was 170% and 130%, respectively.

—●—●—, BUM 12P; – – ○– – ○–, BUM/EDTA/12P.

(b) 5 to 20% sucrose gradients containing BUM were supplemented with 28% (w/v) potassium tartrate · ½ H_2O. The migration of catalase (2 mg/ml.), lysozyme (5 mg) and yeast alcohol dehydrogenase (5 mg/ml.) were measured under the conditions described above. The refractive indices of gradient fractions before (▲) and after (○) centrifugation are indicated.

(d) *Sodium dodecyl sulfate gel electrophoresis: characterization of P12*

In this section we present the characterization of the polypeptide chains contained in 12P by electrophoresis in polyacrylamide gels containing SDS. Three experiments will be presented. First, two radioactive extracts differing only in their content of 12P have been compared by SDS gel electrophoresis; the single band differing in the two patterns is tentatively called P12. In the second experiment, the two labeled extracts were incubated with unlabeled gene *12*$^-$ particles, the acceptor particles purified, and their proteins examined by electrophoresis. A single band difference, corresponding in

position to P12, is again observed. For convenience this experiment is referred to as the "sweep" experiment. Finally, unlabeled donor extracts differing only in their content of 12P have been compared with respect to their ability to prevent association of radioactive 12P with gene *12*⁻ particles. In this "sweep-competition" experiment, only donor extracts containing 12P prevent the attachment of radioactive P12 to acceptors.

(1) Comparison of radioactive extracts. Extracts were prepared from cells infected with *27*⁻ and *12*⁻*-27*⁻ phage. Autoradiograms of SDS gel analyses of the two extracts are shown in Plate I, gels 1 and 2. The band called P12 is the only band present in the gene *27*⁻ extract which is clearly absent from the gene *12*⁻*-27*⁻ extract.

(2) Complementation with radioactive donor extracts—the sweep experiment. The radioactive extracts described in (1) were used to complement unlabeled gene *12*⁻ particles *in vitro*. The complemented particles were then purified, and the radioactive proteins associating with those particles were analyzed by SDS gel electrophoresis. The autoradiograms of the gels are shown in Plate I, gels 3 and 4. Again, the only apparent difference, on SDS gels, between particles complemented with gene *27*⁻ or *12*⁻*-27*⁻ is the radioactive band P12. Since P12 migrates to the same extent on SDS gels before and after association with gene *12*⁻ particles, the P12 polypeptide does not appear to be extensively modified as a consequence of association. (The bands common to gels 3 to 8 in Plate I are probably head proteins derived from particles present in the donor extract; see below.)

(3) Complementation with radioactive donor extracts—the sweep-competition experiment.

If the association of 12P with acceptors is irreversible, and if there are a limited number of sites to which P12 may bind, then unlabeled donor extract should prevent the association of labeled P12 with gene *12*⁻ particles. Therefore the sweep experiment was repeated with the simple modification described in Plate I. Before incubation with radioactive donor extracts, the gene *12*⁻ acceptor particles were incubated with either unlabeled gene *23*⁻*-27*⁻ extract or with unlabeled gene *12*⁻*-23*⁻*-27*⁻ extract. Since there are two radioactive extracts and two unlabeled extracts to be compared, four complemented acceptors were purified and analyzed on SDS gels. Comparison of gels 5 and 6 in Plate I shows that the unlabeled gene *23*⁻*-27*⁻ extract, but not the gene *12*⁻*-23*⁻*-27*⁻ extract, prevented the subsequent association of P12, from a radioactive gene *27*⁻ extract, with gene *12*⁻ acceptors. Gels 7 and 8 (Plate I) show that neither unlabeled extract promoted the association of a radioactive protein with gene *12*⁻ acceptors.

The interpretation of the experiment just described depends upon an important control: the concentration of T4 proteins in the two competitor extracts must be comparable for every protein except P12. The lysozyme activity was nearly identical in the two extracts; the same was true for the concentration of tail fibers, as measured by quantitative *in vitro* complementation. Therefore, the conclusion that only P12 in an unlabeled extract can prevent the subsequent association of radioactive P12 with gene *12*⁻ particles appears valid.

In both the sweep and sweep-competition experiments (Plate I) P12 contained only a minor fraction of the total radioactivity associating with the purified particles. Since some phage heads from the radioactive extracts probably were purified together with the complemented gene *12*⁻ particles, most of the radioactive bands on gels 3 to 8 (Plate I) must represent head polypeptides. A second sweep experiment employing

labeled head⁻/tail⁻ extracts was therefore performed. The results of this experimen (Plate II) again suggest that P12 is the only polypeptide of molecular weight greate than 20,000 daltons (the lower limit of resolution of the gels) that is specifically swep from gene *12*⁺ extracts and not from gene *12*⁻ extracts.

Because the experiments of this section have established P12 as a likely componen of 12P, it was worthwhile to establish the molecular weight of P12. The molecula weight of P12 was estimated by comparing its mobility on SDS gels with the mobility of several protein standards (bovine serum albumin, catalase, γ-globulin, α-amylase malate dehydrogenase, chymotrypsinogen, cytochrome *c*, P23*, and P18 (Laemmli 1970)), and found to have a molecular weight of 55,000 ± 5000 daltons.

(c) *Molecular weight of partially purified 12P*

A procedure has been described in Materials and Methods for obtaining 100-fold purified 12P (fraction VII). The elution volumes of fraction VII 12P from G200 and Sepharose 4B gel filtration columns have been used to estimate the Stokes radius of the 12P and molecular weights have been calculated from the Stokes radii, partial specific volume (assumed to be 0·725) and sedimentation coefficient.

Centrifugation of fraction VII on a 5 to 20% sucrose gradient containing 0·061 M-phosphate/0·01 M-EDTA revealed a sedimentation profile of 12P activity indistinguishable from that of a crude extract in BUM/EDTA (see Fig. 4), except that the pelleted fraction was either absent or considerably reduced. The sedimentation coefficient using catalase and alcohol dehydrogenase as calibration markers was 6·3 S, similar to the value obtained for crude extracts sedimented in BUM/EDTA. A slight leading edge was apparent on the 12P profile, as compared to the alcohol dehydrogenase sedimentation profile, suggesting that aggregation phenomena have not been entirely eliminated.

The elution profiles of 12P activity from G200 and Sepharose are presented in Figures 6 and 7, respectively. Most of the gene *12* product appears as a single peak on both gels but it is apparent that a higher molecular weight species is also present; moreover, both major peaks have a pronounced trailing edge, suggesting that the 12P reversibly dissociates or participates in a weak association with both gels. By the method of Ackers & Steere (1967), the 12P molecular weight has been estimated as 157,000 daltons on G200 and 108,000 daltons on Sepharose 4B. The large difference between the two estimates suggests that 12P associates with one or both gels (more strongly with Sepharose 4B), so that 157,000 daltons is probably a minimum estimate of the 12P molecular weight.

Fractions 23 to 29 and 46 to 53 from G200 and Sepharose 4B, respectively, were pooled and concentrated. When the protein content was estimated by the method of Lowry *et al.* (1951), the 12P from G200 and Sepharose was found to be 830- and 430-fold purified, respectively. The concentrated 12P has also been analyzed on SDS gels (Plate III). Only one major band is apparent in the G200 fraction (gel 4) two in the Sepharose fraction (gel 5), and three in fraction VII (gel 6). The high molecular weight band (gel 5) was faintly visible in the G200 gel analysis also, suggesting that the apparent difference between the Sepharose and G200 fractions might merely be due to the smaller amount of protein analyzed on gel 4. Autoradiographic analysis of gels 1 to 3, on which mixtures of G200 or Sepharose 12P and ^{14}C-labeled gene *27*⁻ extract were electrophoresed, revealed that the major stained band of the G200 fraction (gel 4), and the corresponding band of the Sepharose fraction, migrate with P12 of the

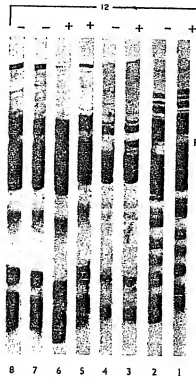

PLATE I. Electrophoresis of labeled extracts and particles. ^{14}C-labeled SDS and BUM extracts were prepared, as described in Materials and Methods, from cells infected with gene *27*⁻ and gene *12*⁻*27*⁻ phage.

Gels 1 and 2. Autoradiograms of SDS gels of gene *27*⁻ and gene *12*⁻*27*⁻ infected cells, respectively. Gels 3 and 4. Sweep experiment: $2{\cdot}5 \times 10^{12}$ acceptor particles (N69-N104 acceptor pellet) were complemented with 0·33 ml. of gene *27*⁻ or gene *12*⁻*27*⁻ ^{14}C-labeled BUM extracts (50 × concentrated). The complemented particles were then purified by differential centrifugation and CsCl zone sedimentation; the recovery of radioactivity was ~ 1% and the recovery of pfu ~ 30%. The particles were pelleted, resuspended in SDS sample buffer, dissociated at 100°C, and analyzed on SDS gels. Gel 3, gene *27*⁻ complemented particles; gel 4, genes *12*⁻*27*⁻ complemented particles.

Conditions: 2 hr at 30°C; BUM/chloramphenicol (90 μg/ml.).

Gels 5 to 8. Sweep-competition experiment: acceptor particles (N69-N104 acceptor pellet) at $7{\cdot}2 \times 10^{11}$/ml. were complemented with equal volumes of gene *23*⁻*27*⁻ or gene *12*⁻*23*⁻*27*⁻ extracts: the 12P activity of gene *23*⁻*27*⁻ was sufficient to saturate the gene *12*⁻ particles. The complemented particles were then diluted ~5-fold and portions containing $2{\cdot}5 \times 10^{11}$ particles were complemented a second time with 0·33-ml. portions of gene *27*⁻ or gene *12*⁻*27*⁻ ^{14}C-labeled BUM extracts (50 × concentrated). The particles were diluted 7-fold in RTE medium, purified, and analyzed as described for the sweep experiments, except that 0·35-ml. samples were applied to the SDS gels. During particle purification the recoveries of plaque-forming units ranged from 9 to 14%, while the recovery of radioactivity varied from 2 to 5%. Gel 5: complementation 1, gene *23*⁻*27*⁻, complementation 2, ^{14}C-labeled gene *27*⁻; gel 6: complementation 1, gene *12*⁻*23*⁻*27*⁻, complementation 2, ^{14}C-labeled *27*⁻; gel 7: complementation 1, gene *23*⁻*27*⁻, complementation 2, ^{14}C-labeled gene *12*⁻*27*⁻; gel 8: complementation 1, gene *12*⁻*23*⁻*27*⁻, complementation 2, ^{14}C-labeled gene *12*⁻*27*⁻.

Conditions: 2 hr at 30°C; BUM/chloramphenicol (50 to 100 μg/ml.).

[facing p. 468

PLATE II. Sweep experiment with ^{14}C-labeled gene *23*$^{-}$-*27*$^{-}$ and gene *12*$^{-}$-*23*$^{-}$-*27*$^{-}$ extracts (10 × concentrated). $3{\cdot}7 \times 10^{11}$ Acceptor particles (N69-N104 acceptor pellet) were complemented with 1·0-ml. volumes of labeled extract: the acceptor was in excess over the gene *12* product. Particles were then purified and analyzed as described for Plate I. The SDS sample volumes were 0·27 ml. for gels 1, 3 and 0·05 ml. for gels 2, 4. Gels 1 and 2, ^{14}C-labeled gene *23*$^{-}$-*27*$^{-}$ complemented particles: gels 3 and 4, ^{14}C-labeled gene *12*$^{-}$-*23*$^{-}$-*27*$^{-}$ complemented particles.
Conditions: 2 hr at 30°C: BUM

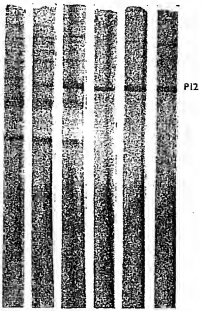

PLATE III. Sodium dodecyl sulfate gel electrophoresis of partially purified gene *12* product. G200 fractions 23 to 29 and Sepharose fractions 46 to 53 were pooled, precipitated with 75% (saturation) ammonium sulfate, resuspended in 0·1 volume of 0·0061 M-phosphate, and dialyzed *versus* 0·0061 M-phosphate; fraction VII was used without further concentration: the concentrations of the concentrated G200 and Sepharose 12P fractions were 44 and 88 μg/ml., respectively. A ^{14}C-labeled gene *27*$^{-}$ extract was used as a control (see text).

Gel 1, ^{14}C-labeled gene *27*$^{+}$; gel 2, ^{14}C-labeled gene *27*$^{-}$ —0·2 ml. G200 12P; gel 3, ^{14}C-labeled gene *27*$^{-}$ —0·2 ml. Sepharose 12P; gel 4, 0·2 ml. G200 12 P; gel 5, 0·2 ml. Sepharose 12P; gel 6, 0·05 ml. fraction VII 12P.

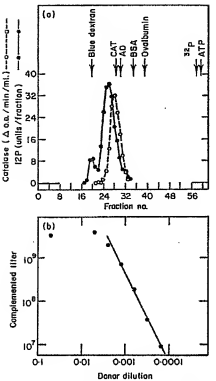

FIG. 6. (a) G200 gel filtration of partially purified 12P: 2·0 mL of fraction VII (Table 1, expt 1) was layered on a G200 column equilibrated with 0·061 M-phosphate/0·01 M-EDTA. 100-drop fractions (3·5 mL) were collected at a flow-rate of 10·4 mL/hr. The total recovery of 12P in fractions 17 to 34 was 72%, of which 9·2% was in fractions 17 to 22, 6·8% in fractions 30 to 34, and 56% in fractions 23 to 29. The elution volume (peak fraction) of various calibration markers have been indicated and an elution profile for catalase has been plotted (flow rate 10·5 mL/hr).

—●—●—, 12P; – – ○– – ○–, catalase. CAT, catalase; AD, alcohol dehydrogenase; BSA, bovine serum albumin.

(b) Complementation of G200 fraction 25 12P with purified acceptor (N69-N104). Two series of donor dilutions were complemented with CsCl purified gene *12*$^-$ particles and the average *in vitro* complementation has been reported in the Figure.

Conditions: 0·1 mL-0·1 mL; 2 hr at 30°C; BUM/BSA (50 μg/mL)/chloramphenicol (50 μg/mL)
Plating bacteria: CR63

^{14}C-labeled extract. P12 is therefore the major high molecular weight polypeptide of the active gene *12* product suggesting that 12P contains at least two P12 subunits. Intracistronic complementation between temperature-sensitive mutants of gene *12* has been observed (Edgar *et al.*, 1964) and interpreted to mean that the active form of the gene *12* product is multimeric. Since the analysis of the stained gels did not extend below a molecular weight of 20,000 the possibility that 12P contains additional low molecular weight components may not be eliminated.

(f) *Gene* 12 in vitro *complementation reaction is non-catalytic*

The following experiment asks whether 12P activity remains following *in vitro* complementation with an excess of gene *12*$^-$ particles. A series of 12P dilutions were

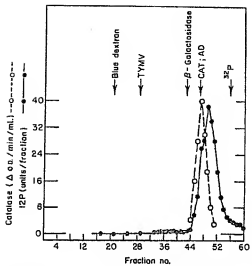

FIG. 7. Sepharose 4B gel filtration of partially purified 12P. The procedure is as described in the legend to Fig. 6(a), except that the column was eluted at 14·2 ml./hr. The recovery of 12P in fractions 33 to 60 was 74%, of which 2·4% was in fractions 33 to 44, 10·8% in 45 plus 54 to 60, and 61% in 46 to 53.
—●—●—, 12P; —○—○—, catalase. TYMV, turnip yellow mosaic virus; AD, alcohol dehydrogenase; CAT, catalase.

complemented with gene *12⁻ rdf* acceptors and, after an incubation period suitable for the *in vitro* reaction to go to completion, the reaction systems were tested for surviving 12P activity in a second complementation with N69-N104 acceptors. The results of the second incubation were assayed by plating on S26R1E, which is non-permissive for N69-N104 *rdf* phage.

These results, together with appropriate controls, are presented in Table 5. Comparison of columns 5 and 8 reveals that at the highest 12P donor concentration, incubation with N69-N104 *rdf* removed at least 37% of the 12P donor activity (assuming a second-order dilution curve at these 12P concentrations which, since the acceptor was almost saturated, probably underestimates the differences in 12P activity); at the next highest 12P concentration N69-N104 *rdf* removed the entire 12P complementing activity. A twofold drop in 12P concentration caused a drop in complemented titer 250-fold greater than expected (i.e. 1000-fold rather than 4-fold; cf. columns 5 and 8, Table 5). This fact suggests a non-catalytic reaction mechanism. This result is, of course, consistent with the sweep and sweep-competition experiments (Plate I).

(g) *Stoichiometry of 12P* in vitro *complementation*

Since the *in vitro* complementation reaction appears to be non-catalytic, the reaction can be analyzed quantitatively to determine the number of molecules of 12P required for activation of a gene *12⁻* particle and the number of 12P binding sites on a gene *12⁻* particle. To make this analysis the following assumptions were made: (a) binding sites are independent and attachment irreversible; (b) the 12P is well defined (e.g. not in equilibrium with various active and/or inactive states); (c) only one

TABLE 5

12P in vitro *complementation is non-catalytic*

1st incubation:	Gene *12⁻rif* acceptor × 12P donor					Gene *12⁻* acceptor × 12P donor	Buffer × 12P donor	
2nd incubation:	None	None	Buffer	Gene *12⁻* acceptor		None	Gene *12⁻* acceptor	
Plating bacterin:	CR63 (1)	S26R1E (2)	CR63 (3)	CR63 (4)	S26R1E (5)	CR63 (6)	CR63 (7)	S26R1E (8)
12P donor dilution†								
1/200	$9{\cdot}1 \times 10^8$	$9{\cdot}4 \times 10^4$	$9{\cdot}8 \times 10^8$	$1{\cdot}14 \times 10^9$	1×10^8	$7{\cdot}8 \times 10^8$	$7{\cdot}3 \times 10^8$	$2{\cdot}4 \times 10^8$
1/400	$7{\cdot}6 \times 10^8$	$5{\cdot}8 \times 10^4$	$6{\cdot}2 \times 10^8$	$8{\cdot}1 \times 10^8$	$9{\cdot}0 \times 10^4$	$6{\cdot}4 \times 10^8$	5×10^8	2×10^8
1/800	$1{\cdot}97 \times 10^8$		$2{\cdot}2 \times 10^8$	$2{\cdot}18 \times 10^8$	$8{\cdot}9 \times 10^4$	$1{\cdot}84 \times 10^8$	$1{\cdot}46 \times 10^8$	$7{\cdot}1 \times 10^7$
1/1600	$6{\cdot}8 \times 10^7$		$8{\cdot}2 \times 10^7$	$7{\cdot}9 \times 10^7$	$7{\cdot}4 \times 10^4$	$5{\cdot}2 \times 10^7$	$4{\cdot}1 \times 10^7$	$1{\cdot}26 \times 10^7$
1/3200	$4{\cdot}1 \times 10^7$		$3{\cdot}6 \times 10^7$	$4{\cdot}04 \times 10^7$	$5{\cdot}3 \times 10^4$	$3{\cdot}1 \times 10^7$	$1{\cdot}7 \times 10^7$	$5{\cdot}9 \times 10^6$
1/6400	$2{\cdot}2 \times 10^7$		$2{\cdot}4 \times 10^7$	$2{\cdot}66 \times 10^7$	$5{\cdot}9 \times 10^4$	$2{\cdot}05 \times 10^7$	$1{\cdot}06 \times 10^7$	$4{\cdot}6 \times 10^6$
1/12800	$1{\cdot}06 \times 10^7$		$1{\cdot}52 \times 10^7$	$1{\cdot}82 \times 10^7$	$6{\cdot}7 \times 10^4$	$1{\cdot}56 \times 10^6$	$7{\cdot}6 \times 10^6$	$2{\cdot}9 \times 10^6$
1/3200	$1{\cdot}91 \times 10^7$		$2{\cdot}3 \times 10^7$	$2{\cdot}4 \times 10^7$	6×10^4	$1{\cdot}67 \times 10^7$	$1{\cdot}03 \times 10^7$	$3{\cdot}8 \times 10^6$
1/3600	$1{\cdot}35 \times 10^7$		$1{\cdot}28 \times 10^7$	$1{\cdot}49 \times 10^7$	$4{\cdot}8 \times 10^4$	$1{\cdot}18 \times 10^7$	$0{\cdot}9 \times 10^6$	$2{\cdot}2 \times 10^6$
1/4400	8×10^6	4×10^3	8×10^6	$0{\cdot}1 \times 10^8$	$5{\cdot}5 \times 10^4$	$9{\cdot}6 \times 10^6$	$3{\cdot}0 \times 10^6$	$1{\cdot}24 \times 10^6$
buffer‡	$2{\cdot}4 \times 10^8$	$<10^2$	$2{\cdot}3 \times 10^8$	$3{\cdot}0 \times 10^8$	$5{\cdot}1 \times 10^4$	$1{\cdot}48 \times 10^8$	$1{\cdot}52 \times 10^8$	0×10^4

The 12P acceptors were N69-N104 and N69-N104 *rif* particle lysates; the donor was an EDTA treated and clarified gene *23⁻·27⁻* extract; the complementation buffer was BUM/BSA (50 μg/ml.)/chloramphenicol (50 μg/ml.).

In the first procedure (columns 1 to 5) N69-N104 *rif* was diluted 10-fold, complemented with an equal volume of gene *23⁻·27⁻* extract, and chilled; portions were diluted for plating (columns 1 and 2). Nine parts of the first complementation were then complemented with one part of twofold diluted N69-N104, chilled, and plated (columns 4 and 5), while another 9 parts were complemented with one part of a 1:1 mixture of buffer and M9S (column 3).

In the second procedure (columns 6 to 8) nine parts of a 1:1 mixture of gene *23⁻·27⁻* extract and buffer were complemented with one part of twofold diluted N69-N104 (column 6); the remainder of the 1:1 mixture of gene *23⁻·27⁻* extract and buffer was incubated for 2 hr at 30°C (1st complementation) before complementation of nine parts with one part of twofold diluted N69-N104 (second complementation; columns 7 and 8).

Columns 1 and 2 were corrected for direct comparison with columns 3 to 8 by multiplying the former by 0·9. Complemented titers are plaque-forming units/ml. in the second incubation mixture.

† Dilution used for first incubation.

‡ Indicates substitution of gene *23⁻·27⁻* extract by complementation buffer in the respective incubations.

molecule of 12P may attach at a binding site; (d) the equilibrium and kinetic reactions are a function of the 12P and gene *12*$^-$ particle concentrations only, i.e. there are no other species required for 12P *in vitro* complementation. The results of this study, described below, reveal that two molecules of 12P per acceptor are sufficient to activate, albeit at low efficiency, and that a gene *12*$^-$ particle contains three or more 12P binding sites.

(i) *The equilibrium reaction*

In order to study the equilibrium reaction (i.e. 2 hr at 30°C), *in vitro* complementation was measured at a fixed 12P concentration by varying the concentration of gene *12*$^-$ particles; this technique avoids the problem of possible dilution inactivation of the 12P since the entire assay is done with a single 12P dilution. The results are presented in Figures 8 and 9. In Figure 9 the data have been normalized for comparison with standard 12P dilution curves (cf. Fig. 2), yielding a typical curve of slope minus two. This behavior suggests that particles which have bound two 12P's have a finite plating efficiency whereas those which have bound only one have an insignificant plating efficiency which, for subsequent analysis, has been assumed to be zero.

In Figure 8 the complemented titer is plotted as a function of the gene *12*$^-$ particle concentration. At high gene *12*$^-$ particle concentrations the complemented titer

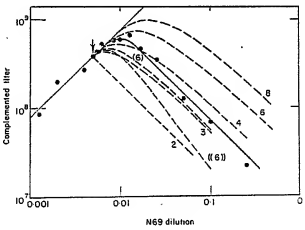

FIG. 8. Stoichiometry of *in vitro* complementation: the equilibrium reaction. N69 and gene *23*$^-$·*27*$^-$ extracts were diluted 3-fold with buffer (HUM/chloramphenicol (50 μg/ml.)); for subsequent discussion, these have been defined as undiluted extracts. The N69 extract was clarified, while the gene *23*$^-$·*27*$^-$ extract was first incubated with 0·025 M-EDTA for 15 min at 30°C and then clarified.

Various dilutions of N69 were prepared as indicated in the Fig. and 150-fold diluted gene *23*$^-$·*27*$^-$ extract was added to initiate the *in vitro* reaction. The data are expressed after subtracting the acceptor background; the results here and in Table 6 are the average of duplicate reaction mixtures. The solid line was drawn with slopes of +1 and −1 as an approximate fit to the data (●); the +1 line passes through a data point (not shown) for N69/10^4 *versus* gene *23*$^-$·*27*$^-$ extract/150. The dashed lines are for various models described in the text. ((6)) is calculated for a 6-site model with $\varepsilon_2 = 0{\cdot}4$, $\varepsilon_6 = 0{\cdot}4$; ((6)) is calculated for a 6-site model with $\varepsilon_2 = 0{\cdot}05$, $\varepsilon_6 = 0{\cdot}5$. The arrow marks the equivalence point determined from the data of Table 6.

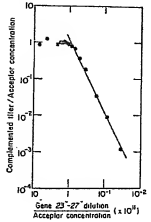

FIG. 9. Stoichiometry of *in vitro* complementation: the equilibrium reaction. The complementation in the Figure.

decreases almost linearly with increasing acceptor concentration; moreover, the results of a control in which T4⁺ was incubated with gene *12*⁻ particles show that the decrease in complemented titer is not explained by inactivation of phage by gene *12*⁻ particles (Mason, 1971). The data have therefore been compared with specific models by assigning the number of 12P binding sites, calculating the probability that an acceptor has received a given number of 12P's at discrete 12P to acceptor ratios, and summing the probabilities for each number of bound 12P's multiplied by assigned plating efficiencies e_i to give the fraction of acceptors which have been converted to plaque-forming units. In this formulation the probability for exactly r bound 12P's is (Feller, 1957):

$$P(r) = \binom{x}{r}\binom{a-x}{b-r} \div \binom{a}{b},$$

where a is the total number of 12P binding sites in the population of acceptors, b is the number of 12P's, and x is the number of binding sites per acceptor. In order to make a comparison between the data and the models it was necessary to determine the number of phage equivalents of 12P used for the experiments of Figures 8 and 9, and this determination is elaborated in Table 6.

Model calculations were made for $x = 2,3,4,6$ and 8, with $e_0 = e_1 = 0$; $e_2 = e_3 = e_4 = e_5 = e_6 = 1$. A model for $x = 6$, $e_0 = e_1 = 0$, $e_2 = 0{\cdot}2$, $e_3 = 0{\cdot}6$, $e_4 = e_5 = e_6 = 1$ has also been considered (Fig. 8). Since in the determination of the phage equivalents of 12P (Table 6) the amount of 12P absorbed by gene *12*⁻ particles may have been overestimated due to processes other than *in vitro* complementation acting upon free 12P (e.g. absorption to glass), the complementation data of Figure 8 may have to be shifted somewhat to the lower left to give the correct comparison with the models. The $x = 4,6$, and 8 ($e_2 = e_3 = \ldots = e_6 = 1$) models may therefore be discarded, but the $x = 3$ and $x = 6$ ($e_2 = 0{\cdot}2$, $e_3 = 0{\cdot}6$) models may not yet be eliminated, and it seems likely that models with $x = 4,5,6$, etc. could be adjusted to fit reasonably the data by

TABLE 6

Stoichiometry of in vitro *complementation: the equilibrium reaction*
Removal of 12P by complementation with gene 12⁻ particles

12⁻-Acceptor	12P-Donor	Complemented titer on CR63	Complemented titer on S26R1E
a. First complementation			
(1) N69-N104 *rdf*	*23⁻-27⁻*/1000	$2{\cdot}5\times10^{8}$	
(2) N69-N104 *rdf*	*23⁻-27⁻*/5000	$7{\cdot}8\times10^{6}$	
(3) N69-N104 *rdf*	Buffer	$2{\cdot}9\times10^{5}$	
(4) N69-N104 *rdf*	N69/400	5×10^{5}	
(5) N69/400	Buffer	$1{\cdot}7\times10^{5}$	
(6) N69/400	*23⁻-27⁻*/150	$2{\cdot}4\times10^{5}$	$1{\cdot}43\times10^{5}$
b. Second complementation			
(1) N69-N104 *rdf*	N69/400 × *23⁻-27⁻*/150 diluted 8-fold after 2 hr at 30°C.	$1{\cdot}92\times10^{7}$	$6{\cdot}2\times10^{6}$
(2) Buffer		$1{\cdot}13\times10^{7}$	$7{\cdot}4\times10^{6}$

The extracts used are described in the legend to Fig. 8.

An N69-N104 *rdf* lysate was diluted 10-fold for complementation with an equal vol. of 12P donor. Extracts were complemented for 2 hr at 30°C (first complementation) and then diluted as indicated for complementation with N69-N104 *rdf* (second complementation). The plating efficiency of complemented N69 on S26R1E was determined to be 62% of that on CR63 (lines a(6) and b(2)). Using this correction to compare the complementations of unadsorbed (lines a(1) and (2)) and pre-adsorbed 12P (line b(1)) with N69-N104 *rdf* indicates that approx. 52% of the 12P was removed by the first complementation with N69/400.

menipulation of the plating efficiencies c_i. The small plateau at the peak (Fig. 8), if real, eliminates the $x = 2$ model. The acceptors must therefore have more than two 12P binding sites, but determination of the exact number of binding sites by this technique is probably not feasible because the plating efficiencies c_i may be a function of the number and pattern of occupied sites.

(ii) *The kinetic reaction*

The kinetics of *in vitro* complementation were measured by following the time course of appearance of plaque-forming units when 12P is in appreciable excess over gene *12⁻* particles; in subsequent discussion the 12P concentration is assumed to have remained constant throughout the reaction. At indicated times the complementation of gene *12⁻* particles was terminated by adding portions of reaction mixture to a large excess of *12⁻rdf* particles; plating on S26R1E selected against any *12⁻rdf* particles that had been activated. Further details of the kinetic experiment are described in Figures 10, 11 and Table 7. Results shown in Figure 10 reveal that with 100-fold diluted donor extract the 12P concentration remained constant throughout the first half of the reaction. This 12P activity was at a 10- to 100-fold excess over acceptor (see Mason, 1971). N69-N104 *rdf* particles at the concentration used to terminate the kinetic reaction did not appreciably inactivate phage (complemented *12⁻* particles or T4, Table 7 and Mason, 1971); however, it was noted that the final complemented titer in the kinetic experiment (Fig. 10) was only 8 to 9×10^{6}, whereas the controls (Table 7) predicted a final titer greater than 10^{8}.

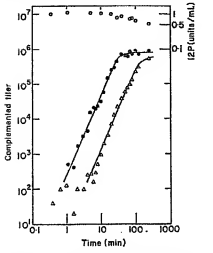

FIG. 10. Kinetics of *in vitro* complementation. The acceptors for *in vitro* complementation were N69-N104 and N69-N104 *rdf* acceptor pellets; the donor was a gene *23⁻-27⁻* extract which had been incubated with 0·025 M-EDTA for 16 min at 30°C, clarified for 10 min-5K-SS34 and then for 40 min-30K-30 rotor. The kinetic measurements were made in a cold room (4 to 7°C) in a water bath at 11·6°C. Pipets were chilled before use. The complementation reaction was initiated by mixing 2·5 ml. of donor with 2·5 ml. of acceptor. At the indicated times 0·2-ml. portions of reaction mixture were pipetted into 1·0 ml. of N69-N104 *rdf*/40 (at 11·6°C) and the "stopped" reaction mixes were then incubated 2 hr at 30°C. The kinetic data has been expressed after subtracting the $t = 0$ background. A measurable amount of *in vitro* complementation of genes *23⁻-27⁻* extract/100 with N69-N104 *rdf* occurred (as measured on CR63) and was used to define this donor's concentration *versus* time; the 16-sec sample was assigned a 12P activity of 1 unit/ml., giving the $t = 0$ sample a relative activity of 1·22 units/ml.

(●), Kinetics-(*23⁻-27⁻*/100 *versus* N69-N104/20,000); (○), 12P activity; (△) kinetics-(*23⁻-27⁻*/1000 *versus* N69-N104/20,000)

Conditions: BUM/BSA (50 μg/ml.)-chloramphenicol (50 μg/ml.)

In order to evalnate some simple models for *in vitro* assembly, their kinetics have been calculated and are plotted, together with the kinetic data from Figure 10, in Figure 11. The differential equations used, for instance, for a six-site model were (1) $d(\Delta P)/dt = 6 \times k \times (A) \ (P)$; (2) $d(\Delta P_2)/dt = 5 \times k \times (\Delta P) \times (P)$, . . . , (6) $d(\Delta P_6)/dt = k \times (\Delta P_5)$, where A is the gene *12⁻* particle concentration, P the concentration of unbound 12P, and k the intrinsic forward rate constant; we have assumed that all dissociation constants are zero and that P remains constant throughout the reaction. Plating efficiencies c_i have been assigned as indicated.

The one-site model ($x = 1$) is clearly inappropriate, as is the two-site model (Fig. 11). The two-site model with $k_{-1} \neq 0$ may also be eliminated since, for all values of $(\Delta P_2)/N_0$ (N_0 = final complemented titer), the rate of accumulation of plaque-forming units will be proportional to the number of acceptors with one bound 12P (ΔP); if k_{-1} is finite then ΔP will be less, for all values of $(\Delta P_2)/N_0$, than if $k_{-1} = 0$, and the rate of appearance of plaque-forming units (ΔP_2) will therefore be reduced.

A six-site model ((6)), with plating efficiencies c_i taken from the study of tail fiber attachment by Wood & Henninger (1969), has also been plotted in Figure 11, giving a reasonable fit to the data; increasing c_3 or decreasing c_3 would improve the fit. In

TABLE 7

Kinetics of in vitro *complementation: controls*

A. $t = 0$ controls

	Acceptor particles				Donor 1/100		Donor 1/1000	
	12P donor (ml.)	*12*$^-$ (ml.)	*12*$^-$ *rif* (ml.)	buffer (ml.)	Complemented titer on CR63	S26R1E	CR63	S26R1E
1.	0·1	0·1	1·0	—	$1{\cdot}32\times10^8$	$1{\cdot}72\times10^8$	—	$4{\cdot}8\times10^8$
2.	0·1	0·1	—	1·0	$4{\cdot}6\times10^8$	$1{\cdot}42\times10^8$	$3{\cdot}4\times10^6$	$7{\cdot}8\times10^6$
3.	0·1	—	1·0	0·1	$1{\cdot}16\times10^8$	10^2	$6{\cdot}4\times10^6$	$<10^2$
4.	—	0·1	1·0	0·1	—	5×10^2	—	$3{\cdot}8\times10^2$
5.	0·1	—	—	1·1	—	$<10^2$	—	$<10^2$
6.	—	0·1	—	1·1	—	$5{\cdot}8\times10^2$	—	$7{\cdot}8\times10^2$
7.	—	—	1·0	0·2	$4{\cdot}3\times10^8$	0	$4{\cdot}2\times10^6$	0

B. Lack of competition by N69-N104 *rif*

(N69-N104 × *23*$^-$*-27*$^-$/100) × N69-N104 *rif*	$1{\cdot}16\times10^8$
(N69-N104 × *23*$^-$*-27*$^-$/100) × buffer	$1{\cdot}06\times10^8$

The materials have been described in the legend to Fig. 10.

A. The results of control incubations (2 hr, 30°C) are presented. The reactants were N69-N104/20,000; N69-N104 *rif*/40, *23*$^-$*-27*$^-$/100, and *23*$^-$*-27*$^-$/1000. 12I^r donor is always the last reaction component added. Comparison of rows 1 and 2 shows that N69-N104 *rif*/40 is capable of stopping the reaction between N69-N104/20,000 and the gene *23*$^-$*-27*$^-$ donor at both donor dilutions.

B. N69-N104/20,000 was complemented with gene *23*$^-$*-27*$^-$/100 for 2 hr at 30°C, then mixed with 1·0 ml. N69-N104 *rif*/40 and incubated an additional 2 hr at 30°C. Plating bacteria were S26R1E.

Conditions: BUM/BSA (50 μg/ml.)-chloramphenicol (60 μg/ml.).

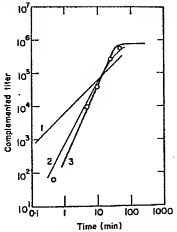

FIG. 11. Complementation kinetics: comparison with models. The heavy line (line 3) has been traced from Fig. 10 (23^--27^-/100). Lines 1 and 2 were calculated for 1 and 2 attachment sites, respectively. A six-site model ((6)) with $c_2 = 0{\cdot}05$, $c_3 = 0{\cdot}5$, $c_4 = c_5 = c_6 = 1$ is also shown (○). All calculations assume 8×10^5/ml. as a final complemented titer.

For $t = 13$ min, when the reaction was 10% complete, lines 1, 2 and 3 indicate titers of 8×10^4, $8{\cdot}8 \times 10^4$ and 8×10^4/ml., respectively.

Figure 8 these plating efficiencies were used to determine an equilibrium curve for *in vitro* complementation, and comparison with the equilibrium data suggests that the plating efficiency c_2 may in fact be greater than 0·05. Substituting $c_2 = 0{\cdot}2$, $c_3 = 0{\cdot}6$ into the six-site kinetic model gave a poor fit to the kinetic data, suggesting c_2 may be less than 0·2.

Because of the scatter in the data for the equilibrium and kinetic experiments we have not attempted to evaluate 3-, 4- or 5-site kinetic models to determine whether they can be adapted to describe both the equilibrium and kinetic experiments.

The kinetic data imply, in agreement with the equilibrium data, that gene 12^- particles must have at least three 12P binding sites.

(h) *11P does not sediment at low speed*

Simon *et al.* (1970) have published evidence that genes 11^- and 12^- particles are defective in the attachment of the short tail fibers to the bacterial surface. The binding of 12P to cellular debris may therefore have a functional significance. Thus the low-speed centrifugation properties of 11P have been examined; when a gene 23^--27^- extract was clarified all of the 11P *in vitro* activity remained in the supernatant while 70% of the 12P activity was found in the pellet fraction.

4. Discussion

Examination of gene 12^- particles complemented with labeled donor extracts by SDS gel electrophoresis on polyacrylamide gels has suggested that P12 is the only polypeptide of molecular weight greater than 10,000 to 20,000 daltons which is specifically bound by 12^- particles (Plates I and II); moreover, P12 appears to be the only polypeptide of greater than 10 to 20,000 daltons molecular weight which is missing from 12^- extracts (Plate I; Mason (1971)).

If 12P is the only macromolecule required to activate purified gene *12*⁻ particles then purified 12P should activate purified gene *12*⁻ particles. It has been shown that partially purified 12P complements CsCl purified acceptors (Fig. 6); in addition, this partially purified gene *12* product has been resolved as a single major band on SDS gels which migrates identically to P12 (Plate III).

It may be argued that the observation of complementation of purified 12P with purified acceptors mentioned above required a third component which was present as a contaminant of the purified preparations. If this hypothetical component were required in stoichiometric quantities then we might expect the amount of this component present in the purified preparations to limit the observable *in vitro* complementation. The specific activity of the partially purified 12P has therefore been calculated from the data in Figure 6(b). The equilibrium models for *in vitro* complementation [(6) and ((6)) of Fig. 8] and the estimated molecular weight of the 12P ($1{\cdot}67 \times 10^5$ daltons), together with the methodology of Ward *et al.* (1970) have been used in these calculations. According to model (6) fraction 25 (Fig. 6(a)) contained 2·25 μg of 12P/ml., while model ((6)) predicts 3·31 μg of 12P/ml. in fraction 25. The protein content of the 12P peak (fractions 23 to 29, Fig. 6(a)) was determined (Lowry *et al.*, 1951) and the protein content of individual fractions calculated by assuming that protein distributed in direct proportion to 12P activity. The protein content of fraction 25 was 4·75 μg/ml. Assuming that the colorimetric assay (Lowry *et al.*, 1951) gave a meaningful estimate of protein concentration, the 12P accounted for 50% or more of the protein in fraction 25.

The high specific activity of the purified 12P determined by complementation with purified gene *12*⁻ particles suggests, together with the purification data, that the *in vitro* reaction may only involve 12P and gene *12*⁻ particles as participants. It is also worth noting that a standard 12P dilution curve was obtained with the purified components (Fig. 6(b)).

In vitro complementation has also been utilized to study the stoichiometry of the interaction between the gene *9* product and the T4 base plate (Flatgaard, 1969); the requirement for 9P was found to be quantitatively similar to the 12P requirement.

Israel, Anderson & Levine (1967) have used *in vitro* assembly to study the morphogenesis of the tail of phage P22. The P22 tail consists of a short tube to which are attached six spikes and spikeless particles were obtained which could be complemented *in vitro* by available spike donors. Analysis of the data from experiments similar to those presented in Figures 1 and 8 lead them to conclude that three or more tail parts are required to activate the spikeless particle.

Edgar & Lielausis (1968) showed that 12P acts on the base plate or core-base plate of T4. The experiments of Simon *et al.* (1970) demonstrated that 12P is required for proper attachment of the short tail fibers to the cell surface and/or for coupling base plate attachment (to the cell surface) with injection of the phage DNA; however, because the short tail fibers of genes *11*⁻ and *12*⁻ particles were of normal dimensions (20 Å × 400 Å) these experiments did not reveal whether 11P or 12P were fiber components. Yanagida & Ahmad-Zadeh (1970) discovered that 12P specific antibody binds to the bottom of the T4 base plate, suggesting that the base-plate-associated 12P is exposed to antibody. Although the specific physiological role of the 12P is unknown we note that the possibility that 12P acts to fasten the short tail fibers to the cell surface is suggested by its apparent binding to cell debris.

If 12P interacts directly with the bacterial surface, host range mutations might be

found in gene *12*. Such mutants of T4 have been found in genes *7* and *8* (R. S. Edgar & S. Beckendorf, personal communication), both of which are necessary for base plate synthesis, suggesting that more than one species of base plate protein may be directly involved in the interaction between the base plate spikes and the cell surface. If host range mutants are not found for gene *12* it will be reasonable to conclude that either 12P does not interact with the cell surface during absorption/injection, that 12P binds to an invariant portion of the cell surface, or that its binding has a low specificity requirement.

This work was supported by research grant AI-09315 from the U.S. Public Health Service. One of us (W.S.M.) was a predoctoral trainee of the U.S. Public Health Service (GM 780) and held the James Franck Dissertation Fellowship in Biophysics. We thank Mrs A. Tomic for technical assistance and Mr G. Grofman for help with the photographs.

REFERENCES

Ackers, G. K. & Steere, R. L. (1967). In *Methods in Virology*, vol. 2, chap. 12. New York: Academic Press Inc.
Edgar, R. S., Denhardt, G. H. & Epstein, R. H. (1964). *Genetics*, **49**, 635.
Edgar, R. S. & Lielausis, I. (1968). *J. Mol. Biol.* **32**, 263.
Edgar, R. S. & Wood, W. B. (1966). *Proc. Nat. Acad. Sci., Wash.* **55**, 498.
Fairbanks, G., Jr., Levinthal, C. & Reader, R. H. (1965). *Biochem. Biophys. Res. Comm.* **20**, 393.
Feller, W. (1957). *An Introduction to Probability Theory and Its Applications*, vol. 1. New York: John Wiley and Sons Inc.
Flatgaard, J. E. (1969). Ph.D. Thesis, California Institute of Technology, Pasadena, California.
Hershey, A. D. & Chase, M. (1952). *J. Gen. Physiol.* **36**, 39.
Israel, J. V., Anderson, T. F. & Levine, M. (1967). *Proc. Nat. Acad. Sci., Wash.* **57**, 284.
King, J. (1968). *J. Mol. Biol.* **32**, 231.
Laemmli, U. K. (1970). *Nature*, **227**, 680.
Lowry, O., Rosebrough, N. J., Farr, A. L. & Randall, R. J. (1951). *J. Biol. Chem.* **193**, 265.
Martin, R. G. & Ames, B. N. (1961). *J. Biol. Chem.* **236**, 1372.
Mason, W. S. (1971). Ph.D. Thesis, University of Chicago.
Sekiguchi, M. & Cohen, S. S. (1964). *J. Mol. Biol.* **8**, 638.
Simon, L. D., Swan, J. G. & Flatgaard, J. E. (1970). *Virology*, **41**, 77.
Snustad, D. P. (1968). *Virology*, **35**, 550.
Steinberg, C. M. & Edgar, R. S. (1962). *Genetics*, **47**, 187.
Tanford, C. (1968). *Physical Chemistry of Macromolecules*. New York: John Wiley and Sons Inc.
Ward, S., Luftig, R. B., Wilson, J. H., Eddleman, H., Lyle, H. & Wood, W. B. (1970). *J. Mol. Biol.* **54**, 15.
Weber, K. & Osborn, M. (1969). *J. Biol. Chem.* **244**, 4406.
Winkler, U., Johns, H. E. & Kellenberger, E. (1962). *Virology*, **18**, 343.
Wood, W. B., Edgar, R. S., King, J., Lielausis, I. & Henninger, M. (1968). *Fed. Proc.* **27**, 1160.
Wood, W. B. & Henninger, M. (1969). *J. Mol. Biol.* **39**, 603.
Yanagida, M. & Ahmad-Zadeh, C. (1970). *J. Mol. Biol.* **51**, 411.

VIROLOGY 194, 117–127 (1993)

T4II, 50

GM

The Short Tail-Fiber of Bacteriophage T4: Molecular Structure and a Mechanism for Its Conformational Transition

A. M. MAKHOV,* B. L. TRUS,*‡ J. F. CONWAY,* M. N. SIMON,† T. G. ZURABISHVILI,§ V. V. MESYANZHINOV,§ AND A. C. STEVEN*,[1]

*Laboratory of Structural Biology, National Institute of Arthritis, Musculoskeletal, and Skin Diseases, and †Computer Systems Laboratory, Division of Computer Research and Technology, National Institutes of Health, Bethesda, Maryland 20892; ‡Department of Biology, Brookhaven National Laboratory, Upton, New York 10973; and §Ivanovsky Institute of Virology, Moscow 123098, Russia

Received October 12, 1992; accepted January 11, 1993

Electron microscopy, image processing, and computational sequence analysis were used to investigate the structure of the short tail-fiber of bacteriophage T4. This molecule, an oligomer of gp12, is an adhesin that binds the virion irreversibly to the bacterial surface. Short tail-fibers were isolated from mutant-infected cells in which gp12 is synthesized and assembled correctly, but not incorporated into virions. Visualized in negative stain, these filamentous molecules are ~38 nm in total length, with an arrowhead-shaped head (~10 nm long by 6 nm wide), a 24-nm shaft of uniform width (~3.8 nm), and a small, seemingly flexible, tail. The primary sequence contains a domain consisting of tandem quasi-repeats, each about 40 residues long, extending from ~residue 50 to residue 320. Molecular mass analyses by scanning transmission electron microscopy confirm that the molecule is a trimer. The masses of the head, shaft, and tail domains are consistent with (trimers of) the carboxy-terminus, the repeat region, and the amino-terminus, respectively. When short tail-fibers are visualized extending from baseplates, their heads are distal, i.e., detached, implying that it is the tail that remains in contact with the baseplate. Analysis of the molecules' curvature properties detects three hinge-sites: these suggest how the short tail-fiber may be initially accommodated in a compact conformation in the "hexagon" state of the baseplate, from which it converts to the extended conformation when the baseplate switches into its "star" state. © 1993 Academic Press, Inc

INTRODUCTION

The infection mechanism of bacteriophage T4 involves the interaction of two sets of filamentous viral proteins with receptors on the host cell surface (Goldberg, 1983). These proteins are, respectively, called the long and the short tail-fibers. The virion has a complement of six of each, symmetrically disposed around the baseplate of the phage [illegible] and [illegible] organelle. The long tail-fibers are responsible for the initial, reversible, attachment of the virion to the host cell. After at least three long tail-fibers have bound, the short tail-fibers bind irreversibly to their receptors. When the tail-sheath subsequently contracts, the short tail-fibers serve as inextensible stays that prevent retraction of the phage particle from the cell surface and thus ensure that the tail-tube penetrates the cell envelope (Kells and Haselkorn, 1974).

The short tail-fiber is composed of a single structural protein, the product of gene 12 (gp12) (Kells and Haselkorn, 1974). Based on its characteristics in gel filtration and density gradient ultracentrifugation, the isolated protein has been deduced to be a trimer (Mason and Haselkorn, 1972). Electron microscopy of negatively stained and shadowed specimens has depicted filamentous particles of 2.5–4.0 nm in width and 35 nm (Kells *et al.*, 1975) or 42–54 nm (Gorzopulos *et al.*, 1982) in length. Recently, the DNA sequence of gene 12 has been determined, describing an open reading frame for a 527-residue polypeptide chain, with a predicted molecular weight of 56,214 (Selivanov *et al.*, 1991).

The short tail-fiber is thought to assume two distinct conformations (Crowther *et al.*, 1977). Initially, it is incorporated as an integral component of the baseplate in its "hexagon" conformation. In this state, the short tail-fiber must assume a compact structure, because it does not appear to extend beyond the periphery of the baseplate which has an outer radius of ~16 nm. Subsequently, when the baseplate switches to its "star" conformation, one end of the short tail-fiber remains bound to the baseplate, from which the remainder of the molecule, now at full length, extends (Crowther *et al.*, 1977).

In the study reported here, we investigated the molecular structure of the short tail-fiber by applying image processing techniques (Steven *et al.*, 1988; Kocsis *et al.*, 1991) to electron micrographs of negatively stained specimens of purified protein, as well as

[1] To whom reprint requests should be addressed at Building 6, Room 114, N.I.H., Bethesda, MD 20892.

0042-6822/93 $5.00

to unstained molecules imaged by dark-field scanning transmission electron microscopy (Wall, 1979; Wall and Hainfeld, 1986). The latter data admit mass measurements for individual particles, and this approach was used to determine the stoichiometry of the short tail-fiber. Moreover, after image averaging, these data were used to quantify the mass of each distinct structural domain. These findings were combined with a systematic analysis of the primary sequence of gp12 to yield a relatively detailed molecular model.

MATERIALS AND METHODS

Purification of short tail-fibers

Ten liters of *Escherichia coli* B cells were grown at 37° with vigorous aeration to a concentration of 4 × 10^8 cells/ml. At this time, the bacteria were infected with double amber mutant T4 (6amN117.23amH11) in genes 6 (which codes for a baseplate component) and 23 (which codes for the major capsid protein) at a multiplicity of 5 and reinfected 8 min later at the same multiplicity. Ninety min after infection, the infected cells were harvested by centrifugation at 6000 *g* for 10 min at 4°. The pellet was resuspended in 100 ml of buffer (0.1 *M* Tris–HCl, 1 m*M* $MgSO_4$, pH 7.2), stirred for 20 min at 25°, and then homogenized by sonication (10 pulses, 30 sec each) with a Sonic 300 Dismembrator (Artek System Corp.). DNAase I (40 μg/ml) was added to the suspension, which was then incubated at 37° for 30 min before being centrifuged at 130,000 *g* for 30 min at 4°. The pellet was resuspended in 100 ml of 0.1 *M* Tris–HCl buffer, pH 7.2, and recentrifuged. This pellet was washed in 100 ml of 0.1 *M* Tris–HCl, pH 7.2, 20 m*M* EDTA, incubated for 30 min at 37°, and centrifuged again at 130,000 *g* for 30 min at 4°.

The last two supernatants were mixed, and ammonium sulfate was added to 43%. Proteins were precipitated overnight at 4° and collected by centrifugation at 8000 *g* for 40 min. The pellet was dissolved in 10 ml of 0.1 *M* sodium phosphate, pH 7.2 (Buffer A), and loaded on a DEAE-Sephacel column (1.6 × 10 cm) preequilibrated with Buffer A. The column was washed with 5 ml of Buffer A, and the proteins were eluted with 120 ml of a linear gradient of 0–1.0 *M* NaCl in buffer A. The short tail-fibers usually eluted at 0.18–0.20 *M* NaCl. The chromatography on DEAE-Sephacel was then repeated. The final yield was ~2.5 mg of short tail-fibers at approximately 80% purity, as judged by SDS–PAGE. The most conspicuous residual contaminants were the proximal and distal parts of the long tail-fibers, encoded by genes 34 and 37, respectively.

The purified protein was active according to an *in vitro* complementation test in which T4 12^- particles and purified short tail-fibers (50 μg/ml) were mixed: the plaque-forming titer rose from 6.5 × 10^7/ml to 1.5 × 10^{11}/ml over the first 30 min of the reaction.

Conventional transmission electron microscopy (CTEM)

Negative staining of purified protein adsorbed to a thin carbon film was carried out essentially according to Valentine and Green (1967). The stain used was uranyl acetate (2%). The specimens were observed with a Philips 400RT electron microscope.

Scanning transmission electron microscopy (STEM)

STEM microscopy was performed using the Brookhaven Biotechnology Resource instrument (Wall, 1979; Wall and Hainfeld, 1986). To prepare freeze-dried specimens, purified gp12 at ~300 μg/ml was diluted sixfold with buffer (10 m*M* Tris–HCl, 40 m*M* NaCl, pH 7.2) and then adsorbed to a thin (~3 nm) carbon film, according to the "wet film" technique (Wall *et al.*, 1985). Immediately beforehand, tobacco mosaic virus particles (TMV) had been applied to this film to serve as a mass standard (Molesson et al., 1981). The grid was washed 12 times with 20 m*M* ammonium acetate, pH 7.0, rapidly quenched in liquid N_2 slush, dried at a constant sublimation rate (controlled via specimen temperature) over 6 to 8 hr, and then transferred under vacuum into the microscope. Digital micrographs (512 × 512 pixels) were recorded at electron doses in the range of 100–500 electrons/nm², which cause no significant mass loss from specimens maintained at −160° (Wall, 1979). Images used for mass measurements were recorded at a magnification corresponding to an inter-pixel step of 1 nm.

Image processing

CTEM negatives were scanned using a Perkin–Elmer Model 1010MG scanning microdensitometer at a rate of 0.39 nm/pixel. STEM micrographs were recorded directly in digital form.

General image processing operations were performed using the PIC system of programs (Trus *et al.*, 1993), operating on a VAX 3500 computer (Digital Equipment Corporation, Maynard, MA) with a Model 9000 image processor (Gould Imaging & Graphics, Fremont, CA). Photographic output was obtained on an Imagecorder film recorder (Focus Graphics, Foster City, CA).

Particles were selected for analysis according to the following criteria, but otherwise without bias. They had to be (i) fully embedded in a continuous (i.e., non-granular) stain layer; (ii) not sharply kinked or broken (the straightening algorithm can only be expected to compensate reliably for smoothly varying curvature); and (iii) free-standing, i.e., not complexed with other particles, crossing them, or extending beyond the field of view. All such particles were straightened by means of

a two-dimensional cubic splines algorithm, which also calculated a curvature profile for each particle (Steven *et al.*, 1986; Kocsis *et al.*, 1991). The nodes used for straightening were determined using a low pass-filtered representation (covering the range 0.12 to 0.3 nm^{-1}) and then applied to the original (unfiltered) image. Curvature was given as the change in direction of the tangent to the particle centerline, from pixel to pixel (Fraser *et al.*, 1990). After straightening, the particles were brought into axial alignment by cross-correlation techniques. To calculate the requisite offset, a low pass-filtered version of each straightened image was used, as described above. Sets of aligned images were then normalized (constant mean and variance; Carrascosa and Steven, 1978); analyzed by multivariate statistics (van Heel and Frank, 1981), using the "principal components" formalism (Unser *et al.*, 1989); screened to eliminate outliers by the OMO algorithm (Unser *et al.*, 1986); and averaged. Resolution was assessed according to the SSNR criterion (Unser *et al.*, 1987). The statistical analyses were performed on images whose dimensions (150 by 24 pixels = 55.8 by 9.3 nm) were cropped relatively close to the edges of the molecules. For visual display, somewhat larger images (170 by 40 pixels) were used.

The average curvature profile was calculated after axial alignment (Fraser *et al.*, 1990; Kocsis *et al.*, 1991). The negatively stained data were used for this purpose on the grounds that their higher resolution (see Results) should allow more accurate definition of the particles' centerlines. In measuring dimensions from averaged images, the edges were defined as the points at which density fell to 25% of its maximum above background.

Analysis of amino acid sequence of gp12

The cDNA sequence of gene 12 predicts a 527-residue polypeptide chain, with a molecular weight of 56,214 (Selivanov *et al.*, 1990). The predicted amino acid sequence has been confirmed by determining the first eight residues of the purified protein, which also indicated that the f-Met residue is not present (V. V. Mesyanzhinov, unpublished).

Secondary structure predictions (Garnier *et al.*, 1978; Ptitsyn and Finkelstein, 1983), hydropathy profiles (Kyte and Doolittle, 1982), and flexibility profiles (Karplus and Schulz, 1985) were calculated on a VAX 3500, and matrix homology analysis and homology searches using the GENEBEE program (Brodsky *et al.*, 1991; Combee, Moscow, Russia) were calculated on an IBM PC-AT 386 computer. The reference data base was Swiss-Prot (release 21). Use was also made of the AASAP program kindly made available by Dr. D. A. D. Parry.

RESULTS

Structural analysis of purified short tail-fibers

A field of negatively stained molecules is shown in Fig. 1 and a gallery of representative specimens at higher magnification in Fig. 2. These filamentous particles are typically 3–5 nm in width and 35–40 nm in length and have a polar structure in that a globular "head" is reproducibly observed at one end, but not the other.

To put these observations on a more quantitative, statistically defined, basis, they were analyzed by correlation averaging (Steven *et al.*, 1988; Fraser *et al.*, 1990). First, since these molecules generally exhibit substantial, and variable, curvature, they were computationally straightened and then aligned to bring them into a standard frame of reference. In all, 287 randomly chosen particles were processed in this way. These images were then analyzed by multivariate statistics to identify any discrete subclasses that may be present and subjected to a screening procedure (OMO—Unser *et al.*, 1986) to eliminate particles that were anomalously different from the bulk of the data. The statistical analysis gave no indication that the data set contained more than one class of particles, consistent with the conclusion reached from visual appraisal of the images. The OMO analysis approved 193 (67%) of the straightened particles, which were then averaged (Figs. 3a–3c). The resolution of the resulting image (Fig. 3c) was 2.4 nm.

Filamentous particles generally flatten on the electron microscope grid and thus are viewed in a standard orientation (side-on). However, they may be expected to present more than one projection, i.e., to be viewed from different angular settings around their axis. The failure of our statistical analysis to pick out discrete classes suggests that the information content of the unprocessed images is insufficient to distinguish between such orientations. Accordingly, the averaged images (Figs. 3a–3c) represent the cylindrically averaged lateral projection of the short tail-fiber. It consists of several discrete domains: a globular head, a shaft that is uniform in width (~3.8 nm) and is 24 nm long, and a short, tapering "tail." The total molecular length is reproducibly 38 nm (cf. Figs. 3a and 3b). The dimensions of the various domains are given in Table 1. Midway along the shaft is a constriction that although slight is consistently observed in two independent averages (Figs. 3a, 3b, 4a) and which we therefore consider to be a genuine feature. Even at the present limited resolution, the head is clearly not spherical, but is somewhat elongated, with the shape of an arrowhead.

Most molecules exhibit some curvature and many are kinked, with the most frequent kink-site occurring approximately half way along the molecule (see Figs.

FIG. 1. Electron micrograph of purified T4 short tail-fibers, negatively stained with uranyl acetate. Bar = 30 nm.

1, 2). To analyze these properties in a more systematic way, the curvature profiles generated by the straightening procedure were averaged. The resulting profile (Fig. 4c) indicates that there are no completely rigid (i.e., curvature-free) segments of the molecule and that the head is more rigid than the tail, which contains three particularly susceptible sites (arrows). As expected, the major hinge-site lies near the midpoint of the shaft and coincides with the slight constriction observed in the averaged image (cf. Figs. 4a–4c); the other two are located at the junctions between head and shaft and between shaft and tail.

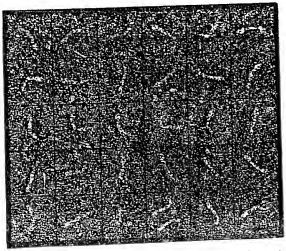

FIG. 2. Gallery of short tail-fibers, showing examples of recurring morphological types. Bar = 30 nm.

Determination of molecular mass and stoichiometry from STEM micrographs

To determine the mass and hence the stoichiometry of the short tail-fiber, we analyzed dark-field STEM micrographs of unstained specimens (Fig. 5a). The two-dimensional integral of the density associated with an

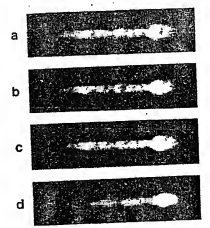

FIG. 3. Computer-averaged representations of T4 short tail-fibers: (a–c) are from negatively stained specimens; (a) and (b) are separate averages from two independent sets of images and convey reproducibility; (c) is the global average, from combining (a) and (b). (d) was obtained by averaging dark-field STEM micrographs of unstained, frozen-dried, molecules. According to our analysis (Discussion), the short tail-fiber is a trimer of gp12, with the three polypeptide chains arranged parallel and in-register, with the amino termini at the left-hand end (tail). Bar = 30 nm.

TABLE 1

DIMENSIONS AND MASSES OF VARIOUS DOMAINS OF THE T4 SHORT TAIL-FIBER

Molecular dimension (nm)	CTEM	STEM
Total length of short tail-fiber	37.7	32.2 (mass = 167 kDa)
Length of shaft	23.6	19.1 (mass = 86 kDa)
Length of head	10.4	12.0
Length of tail	3.7	2.1 (mass = 21.0 kDa)
Length of head-proximal part of shaft	11.0	10.0 (mass = 45.5 kDa)
Length of head-distal part of shaft	12.6	9.1 (mass = 40.5 kDa)
Width of shaft	3.8	4.3
Width of shaft at constriction	3.3	4.0
Width of head	5.9	5.8

Note. The dimensions listed were determined from the global average images (Figs. 3c and 3d, respectively), as described under Materials and Methods. The domainal masses were determined by integrating the density present in the corresponding regions of Fig. 3c and calibrated to a total molecular mass of 167 kDa (Results, Fig. 5b).

individual molecule provides a measurement of its mass. The resulting data are histogrammed in Fig. 5b. The distribution of measurements is symmetrical, suggesting a homogeneous population of molecules. The average mass is 167 kDa (SD = 21 kDa; SEM = 2 kDa; N = 167).

Since the gp12 monomer has a molecular weight of 56,114 (Selivanov *et al.*, 1990), the STEM-derived molecular mass translates into 2.97 subunits (±0.37 SD; ±0.03 SEM), i.e., a trimer, corroborating the conclusion of Mason and Haselkorn (1972). Since the molecule has a polar structure (Fig. 3), we infer that its three polypeptide chains are associated in parallel and in register. Theoretically, a configuration of "two up/one down" would also give a polar structure, but we reject this alternative both because it predicts heads at both ends—which is not observed—and because it corresponds to a nonequivalent bonding arrangement (Caspar and Klug, 1962).

Masses and dimensions of structural domains

The STEM micrographs were also analyzed by correlation averaging. The average of 145 OMO-approved images (out of an initial set of 153) is compared with the negatively stained representation in Figs 3c and 3d. Although the resolution of the STEM image is considerably lower (4.0 nm versus 2.4 nm), it matches the negatively stained rendition in almost every respect, except that the shaft is slightly shorter. Limited shrinkage has previously been observed on other freeze-dried specimens such as groups-of-nine hexons from adenovirus (Furcinitti *et al.*, 1989), and the relative reduction in shaft-length of the short tail-fiber after freeze-drying may represent a similar effect. The close agreement between the two different representations lends confidence that no substantial pieces of gp12 have been camouflaged, either by positive staining or disordering, in the negatively stained averaged image.

The mass of each morphologically distinct domain was determined by integrating the density contained in the corresponding area of the averaged unstained image (Fig. 3d). Thus the mass of the head was estimated to be 61 kDa (3 × 20 kDa); the shaft, 86 kDa (3 × 29 kDa); and the tail, 20 kDa (3 × 7 kDa). The slight constriction observed about half way along the shaft in the negatively stained representation is also discernible in the STEM image (Figs. 3d and 4b). The shaft segment adjacent to the head was estimated at 45 kDa (3 × 15 kDa) and the segment adjacent to the tail at 40.5 kDa (3 × 13.5 kDa). The dimensions and masses of the various domains are summarized in Table 1.

Orientation of the short tail-fiber in its extended conformation

When visualized extending from the T4 base-plate, the short tail-fiber clearly has a globule at its distal end

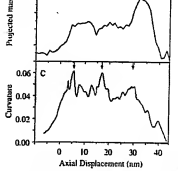

FIG. 4. Profiles of certain parameters plotted as a function of position along the T4 short tail-fiber: (a) stain-excluding density, calculated by integrating laterally across the averaged negatively stained representation of the molecule (Fig. 3c); (b) projected mass, calculated by lateral integration of the density across the averaged STEM image of unstained, freeze-dried molecules (Fig. 3d); (c) average curvature (flexibility) profile, obtained by combining the individual profiles calculated for each straightened, negatively stained particle (see Results). The maxima in this profile (arrows) denote putative hinge-sites.

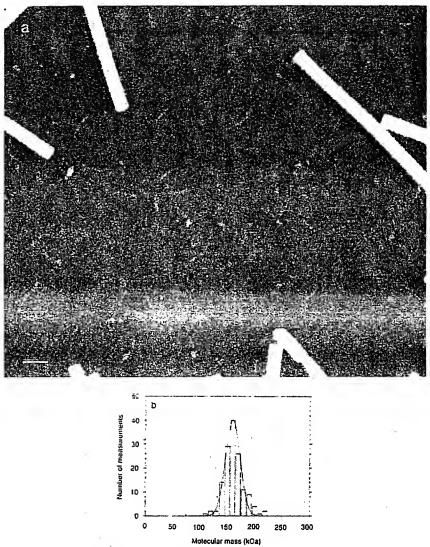

FIG. 5. (a) Dark-field STEM micrograph of purified short tail-fibers, imaged unstained, after freeze-drying. The thick rods are tobacco mosaic virus particles included for mass calibration. Bar = 30 nm. (b) Histogram of mass measurements of short tail-fibers calculated from STEM micrographs of unstained molecules (e.g., (a)). The distribution is symmetrical, as illustrated by the fitted Gaussian curve, implying a homogeneous population of molecules.

(Fig. 6). This feature is also discernible in previously published micrographs (Plate XXVII of Williams and Fisher, 1970; Fig. 10 of Crowther *et al.*, 1977), although we are not aware of its having been commented on before.

Analysis of primary sequence of Gp12

Detection of a domain with a repetitive substructure. We have analyzed the amino acid sequence of gp12 by a variety of computational procedures (see Materials and Methods). Our most striking finding is that a major segment of this polypeptide chain, starting around residue 48 and extending to approximately residue 290, has a repetitive structure composed of six tandem pseudo-repeats of about 40 residues in length. These are followed by two cycles of a somewhat different, shorter, repeat (Fig. 7) that extend the repetitive region of gp12 as far as residue 320 or thereabout. These repeats are readily detected in a homology matrix (Fig. 8).

The repeats are compared in Fig. 7. Their length is not precisely conserved, varying from ~39 to ~45 residues. The most notable departures from uniformity in length are an apparent insertion of about 12 residues (172–193) between the third and fourth repeat and a breakdown toward the end of the sixth unit. Within this array, the homology between the repeats, albeit not

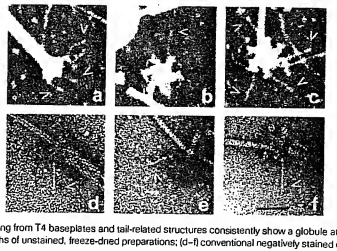

FIG. 6. Short tail-fibers extending from T4 baseplates and tail-related structures consistently show a globule at their distal ends (arrowheads). (a–c) STEM dark-field micrographs of unstained, freeze-dried preparations; (d–f) conventional negatively stained electron micrographs. Bar = 30 nm.

very conservative, is unmistakably present, particularly ... their amino-terminal sequences, and in such fea... was as a rather conservative proline residue. Secondary structure predictions anticipate that these motifs may be composed of alternating β-strands and β-turns (Fig. 7): possible foldings of these sequences have been modeled by Sobolev and Mesyanzhinov (manuscript in preparation).

Each of the major "40-residue" units is composed of two similar subdomains of approximately equal length. The subdivision of the "40-residue repeat" into two subdomains is not so evident on the basis of homology, but emerges consistently from secondary structure prediction (cf. Fig. 7), and from Fourier transform analysis of both the hydropathicity and flexibility profiles which show strong peaks at frequencies of ~(20 residues)$^{-1}$ in contrast to the much weaker spectral intensity at (40 residues)$^{-1}$ (data not shown). Thus, the two subdomains are distinguished ... the basis of a systematic trend in their sequence properties, rather than strict homology.

Both the hydropathicity and the flexibility profiles (Fig. 9) show a systematic change, starting around residue 522 at which point the sequence becomes systematically more hydrophilic and less flexible. This discontinuity distinguishes the carboxy-terminal third of gp12 from the rest of the molecule.

A limited homology between carboxy-terminal sequences of Gp12—The short tail-fiber and Gp37—The long tail-fiber of T4. A homology search was performed, comparing gp12 with the Swiss Prot data base, but no convincing homologies were found. We

	First Group	
	^^^^ ^^^^====== \^^^^======^^^^========== \^^^^==========	
50	SSTTKGLLFIPTEQEVIDGT-MNTK-AVTPAELATRLSYPNA	89
90	TSTVYGLTRYSTNDEAIAGV-NNES-SITPAKFTVALNWA-FETRVS	133
134	TNESNGVIKISSLPQALAGA-DDTT-AMTPLK-T---QG--LAIKLIAQIAP	177
178	SETTATSESQGVVQLAVVAQVRQGTLREGY-AISPYTPM----NSSS	219
220	TSEYKGVIKLQTQSEVNS---NNAEVAVTGATL----NGRGS	254
255	TTSHRGVVKLITTAGSQSGG-DASS-ALAWNADVI--	287
	Second Group	
	^^^^^====^^^^=======	
288	QQRGQQIIYGYLAIEDTFTI	307
308	ANGGANITGTVRM	320

FIG. 7. Tabulation of internal pseudo-repeats in the sequence of gp12. The repeats show considerable variation, but are anchored on relatively conservative sequences toward their amino termini. They also share a common tendency in anticipated secondary structure (Garnier *et al.*, 1978; Pitsyn and Finkelstein, 1983): the majority prediction of four β-turns (^^^^) and four β-strands (====) is shown. The secondary structure prediction also suggests that each primary repeat is composed of two subrepeats, each of two β-turns and two β-strands. The first putative ... strand of the second subrepeat indexes on the pentapeptide A-h-T-P-A, where h is a hydrophobic residue, and allowing some departures from ... motif. The connecting sequence between the third and fourth repeat (res. ~ 169–182) represents the most pronounced divergence from ... and, and this sequence is expected to be located at the "constriction" detected approximately half-way along the shaft of the short ... iber (Fig. 3). The two repeats between residues 288 and 320 are clearly more divergent in character, but resemble the proximal sub-repeats ... the first group in terms of predicted secondary structure.

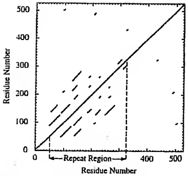

FIG. 8. Self-homology matrix revealing internal repeats in the amino acid sequence of gp12. The matrix was calculated using the GENEBEE program (Brodsky *et al.*, 1991). The repeat region is marked (horizontal axis).

Region 1		
	CCC^C===========CCCCC== ==	
gp12 386	PSNPGLPDMRGLFVRGSGRGSH-LT	409
	|| :||||| ::| | |:	
gp37 851	PS-GVIPDMRGQTIKGKPSGRAVLS	874
	^^ ^===========CCCC======	
Region 2		
	=========^ ^^^^^============	
gp12 500	TLNRPELIGN-ETRPWNISLNYIIKVKE	526 (C-terminus)
	|:: || |: ||::|||:::	
gp37 1001	TITVNST-GNTENTVKNIAFNYIVRLA	1026 (C-terminus)
	=====^^ ^^^================	

FIG. 10. Two regions of local homology between the sequences of gp12 (short tail-fiber) and gp37 (distal part of long tail fiber). The first region has an average homology of 48%, compared with an average of 28.7% (SD = 4.7) over 50 trials with randomized sequences, corresponding to a "probability" of random occurrence of $<10^{-4}$. The second homology is of marginal significance (33%, cf. 26.4 ± 4.5%), but the "probability" of *both* homologies arising as a random occurrence is at the 10^{-6} level.

did, however, detect some homology relating two segments of the respective sequences of gp12 and gp37 (Wood and Crowther, 1983) (Fig. 10). These homologies are neither very long nor very faithful, but, taken together, they appear to be statistically significant. This homology is intriguing because of the functional complementarity of these two proteins, both of which bind to receptors on the bacterial surface (Goldberg, 1983).

DISCUSSION

Our electron microscopic observations yield molecular dimensions that are largely consistent with those reported by Kells *et al.* (1975), but significantly shorter than the molecular lengths of Zorzopulos *et al.* (1982). The domainal organization of head, shaft, and tail revealed in our averaged micrographs (Fig. 3) differs considerably from earlier accounts (Kells *et al.*, 1975; Zorzopulos *et al.*, 1982); it does, however, fit cohesively with structural inferences based on the primary sequence of gp12. Both of these issues are discussed further below.

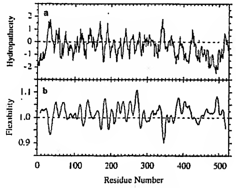

FIG. 9. (a) Hydropathicity (Kyte and Doolittle, 1982) and (b) flexibility (Karplus and Schulz, 1985) profiles of the gp12 sequence. Both show a change in character around residue 310 (i.e., about 60% of the way along the sequence). The carboxy-terminal domain is more hydrophilic and less flexible than the preceding sequence (apart from its extreme amino-terminus) and does not show the same oscillatory behavior that marks the "repeat region" in both profiles.

Orientation of Gp12 polypeptide chains within the molecule

Based on the proposition that the molecule is composed of three elongated monomers associated in parallel and in register, three arguments lead us to conclude that the head contains their carboxy-terminal domains, and the tail contains their amino termini.

First, repetitive sequences are generally associated with extended conformations, e.g., myosin (McLachlan and Karn, 1983), spectrin (Speicher and Marchesi, 1984), the adenovirus tail-fiber (Green *et al.*, 1983), etc. The repeat region of gp12 is flanked at its amino-terminus by a short domain (res. 1–47), and at its carboxy-terminal end by a much longer domain (res. 321–526). At opposite ends of the molecule's filamentous shaft are a small tail and a substantial head (Fig. 3). The masses of these three structural domains (Table 1) correlate closely with the divisions between the repetitive and nonrepetitive sequences, providing strong support for the proposed model.

Second, our curvature analysis of the electron micrograph data (Fig. 4c) indicate that the head is the most rigid part of the molecule, which correlates with the carboxy-terminal region having a systematically lower incidence of flexible residues (Fig. 9b).

Third, the hydropathicity profile (Fig. 9a) also shows that the carboxy-terminal third of the sequence is different from the rest of the sequence. This fraction correlates with the fraction of mass that resides in the head. We note that globular domains usually have a higher proportion of non-polar residues than filamen-

tous domains, whereas the reverse occurs in this case, i.e., the head has a higher average polarity than the shaft. We account for this "inversion" as follows: the repeat region sequence contains quite a high proportion of nonpolar residues, often configured in multiple "hydrophobic-hydrophilic" dipeptides that would generate one polar and one non-polar side of a β-sheet.

When the short tail-fiber extends from the baseplate, the head is distal (Fig. 6). It follows that amino termini (tail) remain in contact with the baseplate, while the carboxy-terminal domains bind to the bacterial cell surface. This view is contrary to the interpretation made by Yamamoto and Uchida (1975) of their observations concerning the properties (primarily, sensitivity to heat-induced tail contraction) and mapping of three heat-sensitive mutants in gene 12.

Repetitive substructure within the shaft

Previous studies have reported that the short tail-fiber has an axially beaded structure with a repeat of 4.5 nm (Kells *et al.*, 1975) or 3.1 nm (Zorzopulos *et al.*, 1982). Our data do not show such a pattern, in either the negatively stained (Figs. 3a–3c) or the unstained representation (Fig. 3d) of the molecule, which are quite consistent. However, the repetitive nature of the shaft domain sequence implies that it should have an extended, repetitive, structure. Taking its length to be 24 nm (Table 1) and that it consists of 7 "40-residue" repeats or 14 "20-residue" subrepeats, they should correspond to axial increments of ~3.4 or 1.7 nm, respectively. The former figure is fairly close to the spacing reported by Zorzopulos *et al.* (1982) although, in view of the difference in molecular length and the absence of a head on their molecules, it is not clear that both sets of observations apply to the same specimen. Moreover, the apparent presence of repeats in bright-field micrographs can be affected by defocus conditions. For this reason, it would be desirable to have further experimental information concerning axial repeats; possibly, paracrystals would be helpful for this purpose.

In particular, the structural properties of the shaft domain of the T4 short tail-fiber are reminiscent of those of the adenovirus fiber shaft, although the latter repeat, at about 15 residues (Green *et al.*, 1983), is shorter and more regular than the 20-residue subrepeat of gp12. The related axial repeat of ~1.3 nm detected by X-ray diffraction from crystals of the adenovirus fiber (Ruigrok *et al.*, 1990) is quite close to the 1.7 nm predicted here for the "20-residue" subrepeat of the T4 short tail-fiber. In this context, the triple-helical, inter-chain, β-sheet model of Stouten *et al.* (1992) for the adenovirus fiber shaft should be adaptable to the short tail-fiber, with the proviso that the latter molecule's β-strands are predicted to be somewhat longer (see Fig. 7) and in consequence, its shaft should have a correspondingly greater diameter.

Comparison with other viral adhesins: Common structural features

Essentially the same morphological motif, i.e., an elongated oligomeric molecule with a globular domain at its distal end, has also been observed in other viruses' counterparts of the T4 tail-fibers. These include both animal viruses and bacteriophages: the σ1 hemagglutinin of reovirus (Fraser *et al.*, 1990), the gp17 tail-fiber of phage T7 (Steven *et al.*, 1988), and the adenovirus fiber (Green *et al.*, 1983; Ruigrok *et al.*, 1990) all conform to this pattern. Interestingly, in all cases to date, the distal globule is thought to contain the carboxy termini. Some of these molecules contain α-helical coiled-coil segments (σ1, Bassel-Duby *et al.*, 1985; gp17, Steven *et al.*, 1988), but others do not; however, all contain segments that are predicted to be rich in alternating β-strands and β-turns. The latter segments include both filamentous domains and terminal globules. This trend implies that despite the absence of conspicuous homology among them, these domains may exhibit foldings that are variations on a common theme. Moreover, these structures may serve as stable platforms from which their specific, receptor-recognizing sequences are presented (Montag *et al.*, 1987).

It is also noteworthy that many of these filamentous molecules also tend to be either kinked (gp17, Steven *et al.*, 1988; adenovirus tail-fiber, Ruigrok *et al.*, 1990) or hinged (σ1, Fraser *et al.*, 1990; T4 long tail-fiber, Wood and Crowther, 1983) near their mid-points and in at least one other case (σ1—Furlong *et al.*, 1988) are thought to assume—like the short T4 tail-fiber—two distinct conformations (retracted and extended).

Conformational switching of the short tail-fiber in the hexagon → star transition of the T4 baseplate: A possible mechanism

The hinge region that we have detected midway along the shaft can account for the transition between the two conformations assumed by the short tail-fiber when associated with the T4 baseplate (Crowther *et al.*, 1977)—see Introduction. If this hinge is bent to an angle of 60° or more, the short tail-fiber can fit snugly into the "hexagon" baseplate and not protrude beyond its periphery (Fig. 11). When it converts to the "extended" state, the tail presumably remains in contact with the rest of the baseplate, while the head and shaft become detached and the short tail-fiber straightens out to its full length. In this state, the hinge at the tail-shaft junction can allow some freedom of movement to facilitate the attachment process. The short-tail-fiber

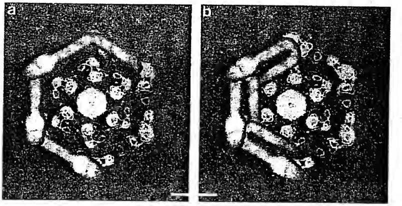

FIG. 11. (a) and (b) Models of possible folded conformations in which the short tail-fiber may be incorporated into the hexagon state of the T4 baseplate. Assuming that the short tail-fiber is assembled on to the underside of the baseplate (Eiserling, 1983; Khusainov *et al.*, 1993), these models represent the view from beneath. They were constructed by computationally folding (Kocsis *et al.*, 1991) the averaged image of the short tail-fiber (Fig. 3c) through 60° (a) or 180° (b) at the hinge-site near the center of the shaft and inserting the resulting images into a digitization of the baseplate as depicted by Crowther *et al.* (1977). Many aspects of this diagram were arbitrarily chosen (e.g., the handedness of the bent fibers, the points at which they make contact with the overlying baseplate, etc). These models are simply intended to illustrate two possible ways in which a molecule with the overall length (38 nm), domainal organization, and inferred hinge structure of the short tail-fiber may be accommodated in a baseplate that has an outer radius of 16 nm. We note that six equivalently packed short tail-fibers are present, although only three are [illegible] ease of illustration. Bar = 10 nm.

should, however, be inextensible and should remain firmly attached both to the baseplate and to the cell surface in order to fulfill its role as a molecular stay.

ACKNOWLEDGMENTS

We thank Dr. B. N. Sobolev for communicating his own observations and structural predictions for the gp12 repeat sequences, and Dr. E. Kocsis for help with image processing. This work was supported in part by grants from the Eastern European Initiative of the Fogarty International Center, and the Council of Protein Engineering of the Russian Academy of Sciences

REFERENCES

BASSEL-DUBY, R., JAYASURIYA, A., CHATTERJEE, D., SONENBERG, N., MAIZEL, J. V., and FIELDS, B. N. (1985). Sequence of reovirus hemagglutinin predicts a coiled-coil structure. *Nature (London)* 315, 421–423.

BRODSKY, L. I., DRACHEV, A. L., TATUZOV, P. L., and CHUMAKOV, K. M. (1991). Package of programs for analysis of the sequences of biopolymers—GENEBEE. *Biopolymers Cells* 7, 10–14. [publ. Naukova Dumka, Kiev, in Russian]

CARRASCOSA, J. L., and STEVEN, A. C. (1978). A Procedure for evaluation of significant structural differences between related arrays of protein molecules. *Micron* 9, 199–206.

CASPAR, D. L. D., and KLUG, A. (1962). Physical principles in the construction of regular viruses. *Cold Spring Harbor Symp. Quant. Biol.* 27, 1–24.

CROWTHER, R. A., LENK, E. V., KIKUCHI, Y., and KING, J. (1977). Molecular reorganization in the hexagon to star transition of the baseplate of bacteriophage T4. *J. Mol. Biol.* 116, 489–523.

EISERLING, F. A. (1983). Structure of the T4 virion. *In* "Bacteriophage T4" (C. K. Mathews, E. M. Kutter, G. Mosig, and P. B. Berget, Eds.), pp. 11–24. Am. Soc. Microbiol., Washington, DC.

FRASER, R. D. B., FURLONG, D. B., TRUS, B. L., NIBERT, M. L., FIELDS, B. N., and STEVEN, A. C. (1990). Molecular structure of the cell-attachment protein of reovirus: Correlation of computer-processed electron micrographs with sequence-based predictions. *J. Virol.* 64, 2990–3000.

FURLONG, D. B., NIBERT, M. L., and FIELDS, B. N. (1988). Sigma-1 protein of mammalian reoviruses extends from the surfaces of viral particles. *J. Virol.* 62, 246–256.

FURCINITTI, P. S., VAN OOSTRUM, J., and BURNETT, R. M. (1989). Adenovirus polypeptide IX revealed as capsid cement by difference images from electron microscopy and crystallography. *EMBO J.* 8, 3563–3570.

GARNIER, J., OSGUTHORP, J. D., and ROBSON, B. (1978). Analysis of the accuracy and implications of simple methods for providing the secondary structure of globular proteins. *J. Mol. Biol.* 120, 97–120.

GOLDBERG, E. (1983). T4 structure and initiation of infection: Recognition; attachment, and injection. *In* "Bacteriophage T4" (C. K. Mathews, E. M. Kutter, G. Mosig, and P. B. Berget, Eds.), pp. 32–39. Am. Soc. Microbiol., Washington, DC.

GREEN, N. M., WRIGLEY, N. G., RUSSELL, W. C., MARTIN, S. R., and MCLACHLAN, A. D. (1983). Evidence for a repeating cross-beta sheet structure in the adenovirus fibre. *EMBO J.* 2, 1357–1365.

KARPLUS, P. A., and SCHULZ, G. E. (1985). Prediction of chain flexibility in proteins. *Naturwissen* 72, 212–213.

KELLS, S. S., OHTSUKI, M., and HASELKORN, R. (1975). The structure of bacteriophage T4 gene 12 protein. *J. Mol. Biol.* 99, 349–351.

KELLS, S. S., and HASELKORN, R. (1974). Bacteriophage T4 short tail fibers are the product of gene 12. *J. Mol. Biol.* 83, 473–485.

KHUSAINOV, A. A., DEEV, A. A., and IVANITSKY, G. R. (1993). The role of baseplate in recognition and infection of host cells by T-even bacteriophages. *In* "Proceedings of Russian Academy of Sciences' Symposium on Protein–DNA Interactions (St. Petersburg)." Nova Science Publishers, New York (in press).

KOCSIS, E., TRUS, B. L., STEER, C. J., BISHER, M. E., and STEVEN, A. C. (1991). Image averaging of flexible fibrous macromolecules: the clathrin triskelion has an elastic proximal segment. *J. Struct. Biol.* 107, 6–14.

KYTE, J., and DOOLITTLE, R. F. (1982). A simple method for displaying the hydropathic character of a protein. *J. Mol. Biol.* 157, 105–132.

MASON, W. S., and HASELKORN, R. (1972). Product of T4 gene 12. *J. Mol. Biol.* 66, 445–469.

McLachlan, A. D., and Karn, J. (1983). Periodic features in the amino-acid sequence of nematode myosin rod. *J. Mol. Biol.* 164, 605–626.

Montag, D., Riede, I., Eschbach, M.-L., Degen, M., and Henning, U. (1987). Receptor-recognizing proteins of T-even type bacteriophages. Constant and hypervariable regions and an unusual case of evolution. *J. Mol. Biol.* 196, 165–174.

Mosesson, M. W., Hainfelo, J., Wall, J., and Haschemeyer, R. H. (1981). Identification and mass analysis of human fibrinogen molecules and their domains by scanning transmission electron microscopy. *J. Mol. Biol.* 153, 695–718.

Ptitsyn, O. B., and Finkelstein, A. V. (1983). Theory of protein secondary structure and algorithm of its prediction. *Biopolymers* 22, 15–25.

Ruigrok, R. W. H., Barge, A., Albiges, C., and Dayan, S. (1990). Structure of adenovirus fibre. II. Morphology of single fibers. *J. Mol. Biol.* 215, 589–596.

Selivanov, N. A., Prilipov, A. G., Efimov, V. P., Marusich, E. I., and Mesyanzhinov, V. V. (1990). Cascade of overlapping late genes in bacteriophage T4. *Biomed. Sci.* 1, 55–62.

Speicher, D. W., and Marchesi, V. T. (1984). Erythrocyte spectrin is comprised of many homologous triple helical segments. *Nature* 311, 177–180

Steven, A. C., Stall, R., Steinert, P. M., and Trus, B. L. (1986). The structure of intermediate filaments from electron microscopy [illegible] tentialities of computational straightening of curved filaments to admit Fourier analysis of helical organization. *In* "Electron Microscopy and Alzheimer's Disease," pp. 31–33 San Francisco Press, San Francisco

Steven, A. C., Trus, B. L., Maizel, J. V., Unser, M., Parry, D. A. D., Wall, J. S., Hainfeld, J. F., and Studier, F. (1988). Molecular [illegible] structure of a [illegible] receptor recognition protein. The gp17 tail-fiber of bacteriophage T7. *J. Mol. Biol.* 200, 351–365.

Stouten, P. F. W., Sander, C., Ruigrok, R. W. H., and Cusack, C. (1992). New triple-helical model for the shaft of the adenovirus fiber. *J. Mol. Biol.* 226, 1073–1084.

Trus, B. L., Unser, M., Pun, T., and Steven, A. C. (1993). Digital image processing of electron micrographs: The PIC system II. *Scan. Micr.*, in press.

Unser, M., Steven, A. C., and Trus, B. L. (1986). Odd Men Out: a quantitative objective procedure for identifying anomalous members of a set of noisy images of ostensibly identical specimens. *Ultramicroscopy* 19, 337–348.

Unser, M., Trus, B. L., and Steven, A. C. (1987). A new resolution criterion based on spectral signal-to-noise ratios. *Ultramicroscopy* 23, 39–52.

Unser, M., Trus, B. L., and Steven, A. C. (1989). Normalization procedures and factorial representations for classification of correlation-aligned images: A comparative study. *Ultramicroscopy* 30, 299–310.

Valentine, R. C., and Green, N. M. (1967). Electron microscopy of an antibody-hapten complex. *J. Mol. Biol.* 27, 615–617.

van Heel, M., and Frank, J. (1981). Use of multivariate statistics in analyzing the images of biological macromolecules. *Ultramicroscopy* 6, 187–194.

Wall, J. S. (1979). Biological scanning transmission electron microscopy. *In* "Introduction to Analytical Electron Microscopy" (J. J. Hren, J. I. Goldstein, and D. C. Joy, Eds.), pp. 333–342. Plenum, New York.

Wall, J. S., Hainfelo, J. F., and Cheung, K. (1985). Films that wet without glow discharge. *Proceedings: 43rd Annual Meeting of the EMSA* [illegible] San Francisco Press, San Francisco [illegible]

Wall, J. S., and Hainfeld, J. F. (1986). [illegible] ning transmission electron microscope. *Annu. Rev. Biophys. Biophys. Chem.* 15, 355–376.

Williams, R. C., and Fisher, H. W. (1970). "An Electron Micrographic Atlas of Viruses," pp. 105–107. Thomas, Springfield, IL.

Wood, W. B., and Crowther, R. A. (1983). Long tail fibers: Genes, proteins, assembly, and structure. *In* [illegible] Mathews, E. M. Kutter, G. Mosig, and P. B. Berget, Eds.), pp. 259–269. Am. Soc. Microbiol., Washington, DC.

Yamamoto, M., and Uchida, H. (1975). Organization and function of the tail of bacteriophage T4. I. Structural control of the tail contraction. *J. Mol. Biol.* 92, 207–223.

Zorzopulos, J., DeLong, S., Chapman, V., and Kozloff, L. M. (1982). Structural characteristics of the short-tail fibers of T4 bacteriophage. *J. Cell Biochem.* 18, 363–375.

JOURNAL OF BACTERIOLOGY, Jan. 2001, p. 358–366 Vol. 183, No. 1
0021-9193/01/$04.00+0 DOI: 10.1128/JB.183.1.358–366.2001

Phylogeny of the Major Head and Tail Genes of the Wide-Ranging T4-Type Bacteriophages†

FRANÇOISE TÉTART,[1] CARINE DESPLATS,[1] MZIA KUTATELADZE,[2] CAROLINE MONOD,[1] HANS-WOLFGANG ACKERMANN,[3] AND H. M. KRISCH[1]*

Laboratoire de Microbiologie et Génétique Moléculaire du CNRS, Toulouse, France[1]; George Eliava Institute of Bacteriophage, Microbiology and Virology, Georgian Academy of Sciences, Tbilisi, Georgia[2]; and Félix d'Hérelle Reference Center for Bacterial Viruses, Laval University, Quebec, Quebec, Canada[3]

Received 16 June 2000 /Accepted 4 October 2000

We examined a number of bacteriophages with T4-type morphology that propagate in different genera of enterobacteria, *Aeromonas*, *Burkholderia*, and *Vibrio*. Most of these phages had a prolate icosahedral head, a contractile tail, and a genome size that was similar to that of T4. A few of them had more elongated heads and larger genomes. All these phages are phylogenetically related, since they each had sequences homologous to the capsid gene (gene *23*), tail sheath gene (gene *18*), and tail tube gene (gene *19*) of T4. On the basis of the sequence comparison of their virion genes, the T4-type phages can be classified into three subgroups with increasing divergence from T4: the T-evens, pseudoT-evens, and schizoT-evens. In general, the phages that infect closely related host species have virion genes that are phylogenetically closer to each other than those of phages that infect distantly related hosts. However, some of the phages appear to be chimeras, indicating that, at least occasionally, some genetic shuffling has occurred between the different T4-type subgroups. The compilation of a number of gene *23* sequences reveals a pattern of conserved motifs separated by sequences that differ in the T4-type subgroups. Such variable patches in the gene *23* sequences may determine the size of the virion head and consequently the viral genome length. This sequence analysis provides molecular evidence that phages related to T4 are widespread in the biosphere and diverged from a common ancestor in acquiring the ability to infect different host bacteria and to occupy new ecological niches.

Bacteriophages, the viruses that infect bacteria, are ubiquitous in the environment (5, 10, 11, 39). New techniques have made it possible to directly and rapidly estimate the total abundance of phages in environmental samples (10, 24). The high phage titers found by such methods in the soil and in aquatic habitats, such as the sea ($>10^8$/ml), indicate that phages constitute a large fraction of the total biomass. Phages are probably the most abundant biological entities on the planet (15), but their diversity makes it extremely difficult to assess their impact on the biosphere (10) because, in general, each phage is infectious for only a minute fraction of the bacteria in its surroundings. However, the aggregated phage population must significantly influence microbial ecology and consequently affect the entire ecosystem.

Until recently, remarkably little was known about phage diversity because most research was focused on only a few laboratory isolates. The T phages (7) isolated on *Escherichia coli* B were long used as the paradigms for all virulent phages, but these phages do not satisfactorily represent even virulent coliphages, let alone phages in general. For example, of the original seven T phages, the three even-numbered viruses (T2, T4, and T6) are identical in morphology and are very closely related (16).

T4, the archetype of the T-even phages, has been the subject of intensive study and is one of the best-characterized phages. Although it was demonstrated a number of years ago that urea-treated T4 could propagate in the spheroplasts of a broad spectrum of bacterial species (38), only recently has it become clear that T4, as well as the other laboratory phages such as λ or Mu, has numerous relatives in nature that infect a wide variety of bacterial species (2, 12, 15, 32). A recent survey of the literature revealed more than 140 descriptions of phages with a morphology that resembled that of T4 (2). Many of these T4-like phages had been isolated on enterobacterial species closely related to *E. coli* (*Klebsiella*, *Shigella*, and *Yersinia*) and less frequently on *Citrobacter*, *Proteus*, *Salmonella*, and *Serratia*. Others propagate on more distantly related bacteria (*Acinetobacter*, *Aeromonas*, *Burkholderia*, and vibrios). A previous PCR analysis of many of the T4-like phages had identified a subgroup of these phages, named the pseudoT-evens, whose genomes are substantially diverged from those of T-even phages (23); for example, the sequences of RB49, the pseudoT-even phage that is the best characterized, are invariably less than 70% identical to the corresponding T4 genes (23).

In this communication we examine the phylogenetic relationships of T4-like phages isolated on diverse bacterial species.

MATERIALS AND METHODS

Phages and bacteria. All of the T4-type phages are from the Toulouse collection (70 isolates). Phages T2, T4, and T6 were obtained from R. H. Epstein of the University of Geneva in Switzerland. Except for coliphage KC69 (obtained from K. Carlson, University of Uppsala, Uppsala, Sweden), the sources of the T4-type phages (coliphages Tula, SV14, RB69, RB49, RB42, and RB43; *Enterobacter cloacae* phage 1; *Aeromonas salmonicida* phages 44RR2.8t (synonym, 44RR) and

* Corresponding author. Mailing address: Laboratoire de Microbiologie et Génétique Moléculaire, CNRS UMR 5100, 118 Route de Narbonne, 31062 Toulouse Cedex, France. Phone: (33) 5 61 33 58 81. Fax: (33) 5 61 33 58 86. E-mail: krisch@ibcg.biotoul.fr.

† This paper is dedicated to the memory of Ulf Henning of Tübingen, Germany.

65; *Aeromonas hydrophila* phage Aeh1; *Burkholderia cepacia* phage 42; *Vibrio natriegens* phage nt-1; and *Vibrio parahaemolyticus* phages KVP20 and KVP40) are found in reference 2. For phages that grow on *E. coli* B^E, standard techniques were used for their propagation and the preparation of their DNA (23). The T4-type phages of non-*E. coli* hosts were grown as suggested in the information sheets provided with the phages by the Félix d'Hérelle Reference Center for Bacterial Viruses (Quebec, Quebec, Canada).

Electron microscopy. Cycles of differential centrifugation were used to purify some of the phages for electron microscopy (23). The non-*E. coli* phages Aeh1, KVP20, KVP40, nt-1, 42, 44RR, and 65 to be examined by electron microscopy were sedimented at 25,000 × *g* for 60 min in a JA-18.1 rotor using a Beckman J2–21 centrifuge. This was followed by two washes in 0.1 M ammonium acetate (pH 7.0). Particles were deposited on copper grids with carbon-coated Formvar films and were stained with 2% potassium phosphotungstate (pH 7.2) or 2% uranyl acetate (pH 4.0). Magnification was controlled with catalase crystals (19).

PCR and oligonucleotide primers. The consensus primers used to amplify the central portion of gene *23* of the various T4-type phages were Mzia1 (5′-TGT TATTGGTATGGTTCGTCGTGCTAT-3′) and CAP8 (5′-TGAAGTTACCTTC ACCACGACCGG-3′). These primers flank the sequences shown in the compilation (see Fig. 3), and they correspond respectively to the nucleotide sequences encoding T4 gene *23* amino acid (aa) residues 95 to 103 and 368 to 375 (26). The conditions used for the amplification reaction with these primers involved 28 cycles consisting of a 30-s denaturation at 96°C, a 2-min annealing at 62°C, and a 3-min extension at 72°C. With this protocol, an approximately 850-bp PCR product was produced from the DNA of phages T4, T6, Tula, KC69, SV14, RB69, RB49, RB42, RB43, 42, 44RR, 1, nt-1, 65, and Aeh1.

The primers initially used to amplify the gene *18* analogue of the T4-type phages were FT18-N2 (5′-GGTAAATTCCAATGGGGTCCAGCTT-3′) and FT18-C1 (5′-TATCAGCAGCCAACGGAACCCAA-3′) or FT18-C3 (5′-ATGT TAAACAGACGACGAACGTTAAT-3′). These oligonucleotides are based on the sequence motifs conserved in T4 and RB49 gene *18*. They respectively correspond to the T4 gene *18* sequences encoding aa residues 31 to 38, 467 to 473, and 551 to 558 (4). For the gene *18* amplification, the reactions involved 10 cycles consisting of a 10-s denaturation at 94°C, a 30-s annealing at 54°C, and a 10-s extension at 68°C, followed by an additional 15 cycles with a 10-s denaturation at 94°C, a 30-s annealing at 54°C, and a 15-s extension at 68°C. Hot Tub polymerase from Amersham International plc (Little Chalfont, United Kingdom) was used.

PFGE of phage genomes. For pulsed-field gel electrophoresis (PFGE) of phage genomes, blocks of 1% agarose containing 10^5 to 10^6 PFU were incubated overnight at 55°C in a lysis buffer containing 0.5 M EDTA, 10 mM Tris-HCl (pH 8), 1% sodium dodecyl sulfate, and proteinase K (0.5 mg/ml). These blocks were then dialyzed three times for 1 h against 10 ml of TE (Tris-EDTA). One-third of the block was analyzed by electrophoresis for 14 h in 1% agarose (0.5× TBE [1× TBE is 2 mM EDTA plus 90 mM Tris-borate]) at 275 V with a pulse time of 8 s on the Pulsaphor Plus system (Pharmacia & Upjohn AB, Uppsala, Sweden). The gel was then stained with ethidium bromide for 30 min, destained for 15 min, and photographed.

PCR sequencing. The PCR products were purified (6) and sequenced with an Amersham Life Science Thermo Sequenase kit. The gene *18*, *19*, and *23* nucleotide sequences of the various T4-type phages were determined by a primer walking procedure (27).

Nucleotide sequence accession numbers. The nucleotide sequences of the central portion of gene *23* of T4-type phages have been deposited in the GenBank database under accession no. AF221994 to AF222003. The sequences of the entire gene *18* of T4-type phages RB49, 42, and nt-1 have been deposited in the GenBank database under accession no. Z78090, AF222058, and AF222059, respectively. The nucleic acid sequences of gene *19* of phages 42, RB49, and nt-1 have been deposited in the GenBank database under accession no. AF223001 to AF223003, respectively.

RESULTS

T-even and pseudoT-even subgroups of T4-type phages. The term "T4-type" refers to all of the 140 known phages with a virion morphology that generally resembles phage T4 (1, 2). Most of these phages have been isolated on various enterobacterial hosts, primarily *E . coli*, *Shigella*, and *Klebsiella*. The T4-type morphology is characterized by a moderately elongated icosahedral head (111 by 78 nm) connected by a collar to a contractile tail. The contractile tail (113 by 16 nm) is terminated by a base plate that carries six long, kinked tail fibers. These tail fibers are held in a folded configuration by "whisker fibers" extending from the collar (40). All of the phages initially in the Toulouse collection had T4-type morphology, and it was assumed, on this basis, that they all belonged to the T-even phages (T2, T4, and T6). Among the T-even phages the nucleotide sequences of homologous genes typically differ from each other by less than 5% (18, 22, 23, 29, 35). However, it was demonstrated (23) that some of the phages with T4-type morphology had genome sequences that were evolutionarily distant from the T-evens (namely, the coliphages RB42, RB43, and RB49 as well as the *Aeromonas* phage 44RR). In these phages, which we called the pseudoT-evens, only a small portion (about 10%) of the DNA hybridizes to the T4 genome under stringent conditions. In RB49 the nucleotide sequence encoding the major virion capsid protein was among those that diverged the least, about 30%, from the corresponding T4 sequence (23). Sequences of the RB49 genome containing the early and DNA replication genes had diverged even more from T4 (23; C. Desplats and H. M. Krisch, unpublished data). In addition, random genomic sequencing indicated that about a third of the RB49 DNA has no homology at all to T4.

Several of the T4-type phages (Tula, RB69, and SV14) that we previously analyzed seem to occupy an "intermediate" position between T-even and pseudoT-even phages (23). For example, phage RB69 appears to be a chimera composed of segments derived from both T-even and pseudoT-even genomes. Its gene *43* sequence differs from T4 at a level that would be expected for a pseudoT-even phage (42); yet, as will be shown, its gene *23* sequence is typical of that of a T-even phage. A similar genomic chimerism was indicated by DNA hybridization studies and sequence analysis of a few of the genes of Tula and SV14 (23; N. Vanzo and H. M. Krisch, unpublished data). Thus, there is good evidence that genetic exchanges occur between the T-even and pseudoT-even groups of phages, at least occasionally.

A more distant subgroup of T4-type phages, the schizoT-evens. We performed electron microscopy on a number of additional T4-type phages that were isolated on hosts other than *E. coli* (1, 2). Although some of them (e.g., *B. cepacia* phage 42) were indistinguishable from T4 (Fig. 1), others had slightly longer heads about 137 nm in length (phage Aeh1 of *A. hydrophila*, phage 65 of *A. salmonicida*, and phage nt-1 of *V. natriegens*). The recently described T4-like phages KVP20 and KVP40 of *V. parahaemolyticus* (20) have a morphology identical to that of *V. natriegens* phage nt-1 (data not shown). To distinguish phages with aberrant head morphology from the T4-type phages with the standard T4 morphology (the T-evens and pseudoT-evens), we propose to name them the schizoT-evens.

Genome size of T4-type phages. Since T4 packages its genome by a head-filling mechanism (30), any change in head size should simultaneously alter the size of the viral genome. The genome of T4 has been completely sequenced and is 169 kb in length (GenBank accession no. AF158101). Electron micrographs of other T-even genomes (T2 and T6) indicated a size close to that of T4 (16). We compared the sizes of the genomes of some of the pseudo- and schizoT-even phages to that of T4 by PFGE. As shown in Fig. 2, although the pseudoT-even phages had genomes with sizes comparable to that of T4,

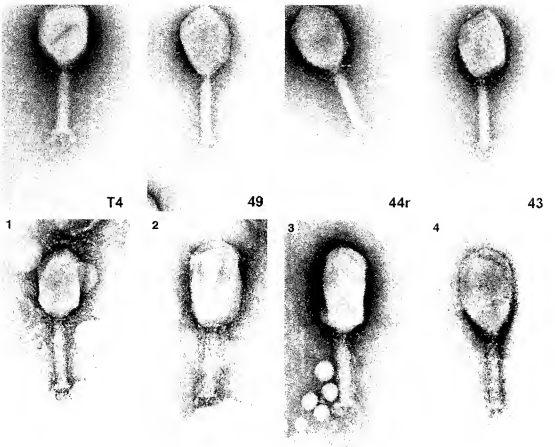

FIG. 1. Micrographs in the top row represent T4 and three previously characterized pseudoT-even phages (RB49, 44RR, and RB43) stained with phosphotungstate (23). Below are four additional T4-type phages that were isolated on nonenterobacterial hosts. (1) *B. cepacia* pseudoT-even phage 42; (2) *A. hydrophila* schizoT-even phage Aeh1; (3) *V. natriegens* schizoT-even phage nt-1; and (4) *A. salmonicida* schizoT-even phage 65. Magnification, about 150,000.

the schizoT-even phages, with their more elongated heads, had significantly larger genomes. The genome of phage Aeh1 from *Aeromonas* was estimated to be approximately 230 kb. Matsuzaki et al. (20) have recently reported that phage KVP40, which is closely related to nt-1, has a genome size of approximately 250 kb. The additional DNA sequence present in the schizoT-even phages is thus sufficient to encode more than 50 supplementary genes.

Sequence of the major capsid gene (23) in diverse T4-type phages. We had previously designed a pair of degenerate primers based on two regions in the gene *23* sequence of the phages T4, T6, SV14, and RB49 that are conserved (23). With these primers we could generate a gene *23*-specific PCR product with many of the T4-type phages, including members of T-even, pseudoT-even, and schizoT-even subgroups. The gene *23* sequences of some of the more distantly related T4-type phages were directly sequenced, including *V. natriegens* phage nt-1, *B. cepacia* phage 42, and *E. cloacae* phage 1. The inclusion of these gene *23* sequences in the alignment allowed us to further refine the consensus gene *23* primers and to amplify gene *23* from additional phages. The sequences of gene *23* from *A. hydrophila* phage Aeh1 and *A. salmonicida* phage 65 were determined from such PCR products. Both of these phages and nt-1 have elongated heads identical in length. Figure 3 shows the alignment of these sequences. Although this comparison reveals significant aa sequence differences between the phages, some blocks of aa sequence are universally conserved. The 70-amino-acid sequence between residues 230 and 300 of the T4 capsid gene is the most notable of these (Fig. 3). Many of the T4 mutants with aberrant head formation map within this conserved segment of gene *23*. An important role of this sequence in head morphogenesis would explain the unusually strong constraints on its divergence. Interestingly, a sequence closely related to these 70 aa is also found in T4 gene *24*, the head vertex protein. Gene *24* is believed to have arisen from an ancient duplication of gene *23*. The interactions between gp23 and gp24 (9, 21) are now thought to have only a minor role in the determination of virion shape and size (14). Some of the phylogenetically variable patches in gp23, however, could slightly modify the interactions between the gene *23* subunits in the virion, and this could result in differences in virion head size and shape. Other patches of variable sequence in gene *23* could be the sites that bind the various head accessory proteins on the surface of the capsid (41).

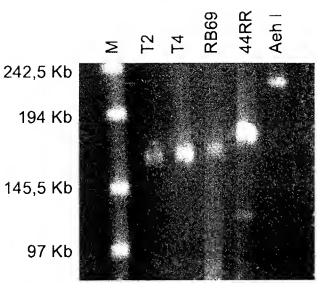

FIG. 2. PFGE of the genomes of phages T2, T4, RB69, 44RR, and Aeh1. There are differences in nucleotide modifications and glucosylation of the DNA in these phages (23); thus, besides their size, the migration of the genomes may be slightly influenced (5 to 10%) by such factors. The DNA minor band present in the 44RR lysate probably corresponds to a small fraction of heads that have an isometric morphology, a similar band was also detected in T4 lysates, where electron microscopy revealed some petite (isometric) variants. To the left is a lane containing size markers consisting of ligated concatemers of the phage λ genome.

Our alignment of 18 T4-type gene *23* sequences suggests that this phage gene has a modular or mosaic design. In a modular gene, recombination occurring in the flanking conserved motifs could replace a variable sequence by a different version. Further evidence for the modularity of gene *23* is illustrated by the sequence comparison in Fig. 4. For more than 90% of the gene *23* aa sequence, phage SV14 diverges from the T4 sequence by 5 to 10% (23), but in a 50-aa segment towards the center of the gene (Fig. 4A), it diverges by 50%. A similar, but less pronounced, increase in the divergence of the same sequence is also found (Fig. 4B) in phage AR1 (GenBank accession no. AAD01755). This is what would be expected if these phages had acquired this small segment of gene *23* by a genetic swap with a distantly related phage. Such events, even if extremely rare, could have major evolutionary consequences. For example, some nonconserved sequences in the gene *23* sequence must provide binding sites for the various head accessory proteins (41) that interact with exposed motifs of gp23 on the capsid surface. Altering the accessory capsid proteins would change the physical and antigenic properties of the virion head.

Sequences of major tail genes *18* and *19*. The contractile tail of the T-even phages has a complex structure that is perhaps the most reliable diagnostic feature of the T4-type phages. In T4, gene *18* encodes the tail sheath protein. The assembly of 144 molecules of gp18 into the sheath (24 stacked annuli each

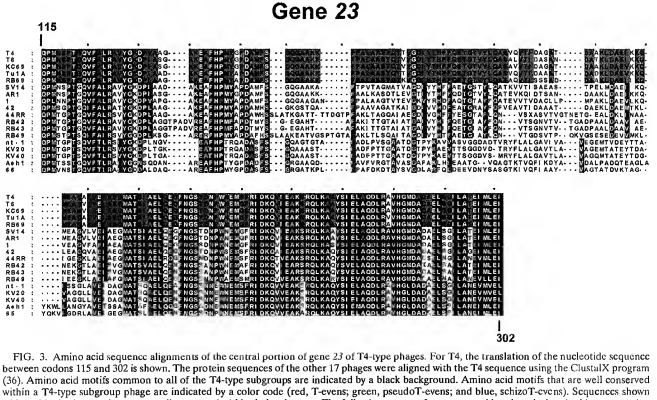

FIG. 3. Amino acid sequence alignments of the central portion of gene *23* of T4-type phages. For T4, the translation of the nucleotide sequence between codons 115 and 302 is shown. The protein sequences of the other 17 phages were aligned with the T4 sequence using the ClustalX program (36). Amino acid motifs common to all of the T4-type subgroups are indicated by a black background. Amino acid motifs that are well conserved within a T4-type subgroup phage are indicated by a color code (red, T-evens; green, pseudoT-evens; and blue, schizoT-evens). Sequences shown with a white background were not well conserved within their subgroup. The following groups of aa were considered equivalent in this presentation (D = N, E = Q, K = R, F = Y = W, and L = I = V = M). A dash indicates a space was inserted in the sequence to preserve the alignment. An ambiguity in the nucleotide sequence is indicated by an X for the corresponding codon. The coordinates of the T4 gene *23* aa sequence are shown at the extremities of the comparison in bold characters.

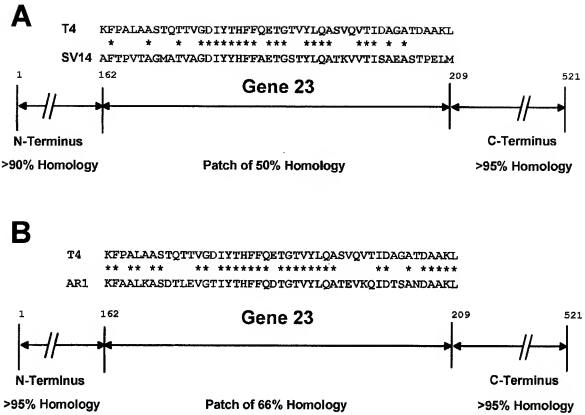

FIG. 4. (A) Comparison between the sequences of gene *23* in phages T4 and SV14. The level of homology is shown below the diagram for the N- and C-terminal segments as well as for a small patch of sequence near the center of the gene. The comparison of this divergent patch in each phage sequence is shown above the diagram. Asterisks between the alignments of the two sequences indicate identical residues in both genes. In the patch between aa 162 and aa 209, the SV14 DNA sequence differs by 47% from the T4 sequence, while in the remainder of the gene the divergence is 12%. (B) Comparison between sequences of gene *23* in phages T4 and AR1. The presentation is the same as in panel A, except that the sequence comparison is between T4 and AR1. In the patch between aa 162 and aa 209, the AR1 DNA sequence differs by 27% from the T4 sequence, while in the remainder of the gene the divergence is less than 2%.

composed of six subunits) depends on the underlying tail tube structure, containing a similar number of gp19 subunits (8, 17), but additional gene products such as gp3 appear to be involved in length determination (37). Relatively little is known about the structure of gp18 protein and how its conformational changes result in tail contraction, except that it hydrolyzes ATP to ADP during contraction and that it has two nucleotide binding motifs (3, 31). It is still not clear, however, that this ATP hydrolysis is directly involved in the conformational changes involved in tail sheath contraction.

The complete sequence of gene *18* of the pseudoT-even phage RB49 was determined by taking advantage of two small randomly determined sequences of this phage genome that, based on the gene order of the T4 genome, should flank gene *18* (23). PCR primers based on these sequences were used to amplify a fragment that was directly sequenced and shown to contain a gene *18* analogue. The RB49 gp18 aa sequence was 63% identical to the gp18 sequence of T4, but the differences were unevenly distributed. The 75 aa at the N terminus were 68% conserved. The next 325 aa of the gp18 protein diverged more (58% identity), but the last 250 aa (67% identity) of this 690-aa protein contained some blocks of sequence that were nearly identical to T4 (Fig. 5). These conserved sequences at the beginning and the end of gene *18* provided us with PCR primers that could amplify related sequences from many of the T4-type phages, including both pseudo- and schizoT-evens. We sequenced gene *18* fragments from the pseudo T-even phage 42 of *B. cepacia* and the schizoT-even phage nt-1 of *V. natriegens* by primer walking (27). The alignment of these sequences is shown in Fig. 5. The overall impression from comparing the gene *18* sequence is quite similar to that obtained from the gene *23* sequence comparison. The sequence of the schizoT-even phage nt-1 has clearly diverged more from T4 than have the pseudoT-evens. Gene *18* appears to be a patchwork composed of variable sequences interspersed between small conserved motifs and several large blocks of near identity. It seems likely that among the large conserved domains are those that mediate the structural changes in gp18 that contract the tail. In this regard, it should be noted that the nucleotide binding motif at residue 530 is located in a highly conserved domain. Some of the non-conserved sequences could provide binding sites for accessory structures that can interact with the contractile tail.

Using similar methods, we also analyzed the sequence of

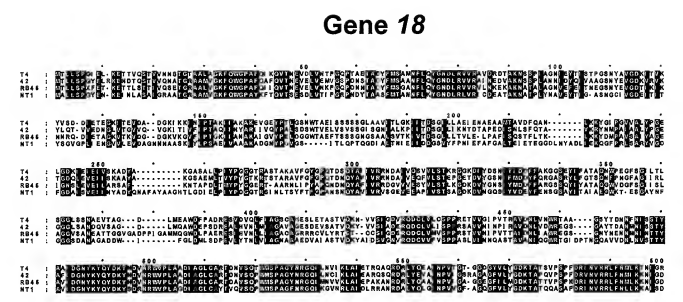

FIG. 5. Amino acid sequence comparison of the entire gene *18* of four T4-type phages (T4, RB49, 42, and nt-1). The homologous sequences of these phages were aligned with the T4 sequence as in Fig. 3. The conventions used in this presentation are the same as in Fig. 3, except that a black background indicates aa residues shared by all four of the phages while those that are present in only three phages are indicated by a gray background. The sequences shown with a white background were not conserved. The coordinates of the T4 gene *18* sequence are shown in the top line of the comparison.

gene *19* (31), which codes for the tail tube through which the phage DNA is injected into the cell. The strong constraints on the dimensions of this hollow tube might be expected to impose limits on gene *19* sequence divergence. Indeed, the alignment of gene *19* sequences from six T4-type phages shows a more uniform distribution of sequence conservation, but the overall level is similar to that in genes *18* and *23* (Fig. 6).

Phylogeny of the major virion genes of the T4-type phages. The phylogenetic trees (25) obtained for all of the viral structural genes are similar, and thus, only the data for gene *23* is shown in Fig. 7. The aa sequences of gene *23* differ by less than 10% within the T-even group, and in contrast, the eight pseudoT-evens differed from the T4 gene *23* sequence by 10 to 45%. Finally, five schizoT-evens differ in the gene *23* sequence from T4 by over 45%. Within each group the members were more closely related to each other than to any members of another group. This phylogenetic analysis classifies the T4-type phages as follows: T-evens (T4, T6, KC69 Tu1a, and RB69), pseudoT-evens (AR1, SV14, RB49, RB42, RB43, 42, 44RR, and 1) and schizoT-evens (nt-1, KVP20, KVP40, 65, and Ach1).

Only the virion structural genes appear to be sufficiently

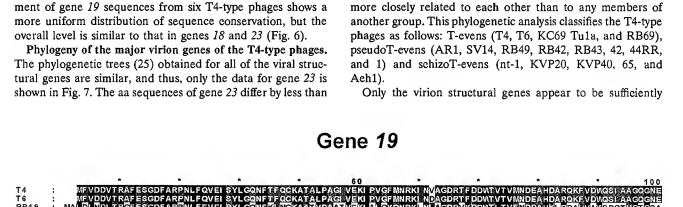

FIG. 6. Amino acid sequence alignments of gene *19* of T4-type phages. The protein sequences of the other five phages were aligned with the T4 sequence as in Fig. 3. The conventions used in this presentation are the same as in Fig. 3.

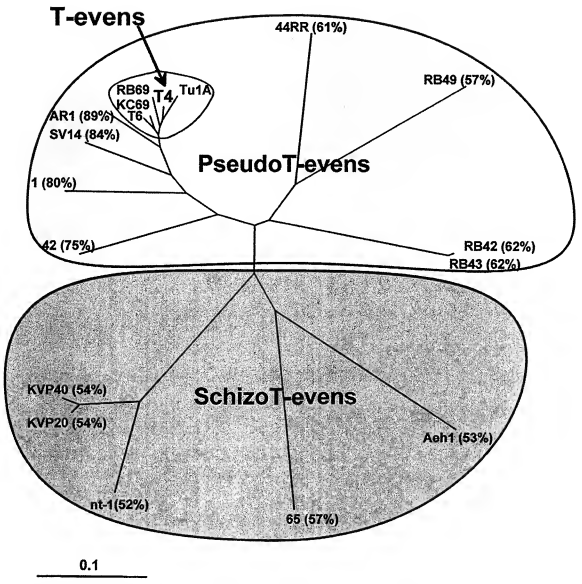

FIG. 7. Phylogenetic tree constructed by the TreeV32 program (25) using the sequence of gene *23* from 18 T4-type pheges. The percentages of aa identities between the T4 gene *23* sequence and that of the other T4-type phages are shown beside each branch of the tree. The various subgroups are indicated by the shaded areas (white, T-evens; light gray, pseudoT-evens; and dark gray, schizoT-evens). In addition to the gene *23* sequence data, this classification reflects the sequences of other genes (genes *18* and *19*, etc.) and DNA hybridizations results (23).

conserved to construct a phylogeny by this method. Attempts to analyze nonstructural genes (e.g., the DNA polymerase gene *43*) were unsuccessful. The divergence of such genes in the various T4-type phages is too great to obtain PCR amplification with primers based on the T4 sequence (23). More laborious methods could be used to isolate and eventually sequence the gene *43* analogues of two of the pseudoT-even phages (RB49 and 44RR) (Desplats and Krisch, unpublished). However, primers based on the most conserved sequences in gene *43* of phages T4, RB49, and 44RR did not permit PCR amplification of gene *43* from any additional T4-type phages. Nevertheless, the gene *43* sequences of these pseudoT-evens (Desplats and Krisch, unpublished) are compatible with the phylogeny established for these phages on the basis of their virion structural genes. We have now sequenced more than 60% of the genome of the pseudoT-even phage RB49; this sequence analysis (Desplats and Krisch, unpublished) confirms the phylogenetic relationship of this phage to T4 predicted exclusively on the basis of the sequences of the major head and tail genes. Nevertheless, the RB49 genome does have one small sequence that it must have recently acquired from a genetic exchange with a T-even phage. Such events seem to be rare and do not alter a picture of a generally distant phylogenetic relationship between RB49 and T4. More limited

genomic sequencing of 44RR also confirms the position of this phage in the phylogenetic tree of the T4-type phages (Desplats and Krisch, unpublished).

DISCUSSION

Monod et al. (23) showed that primers based on the sequence of conserved segments of the capsid gene could be used to PCR amplify analogous DNA segments from distantly related T4-type phages. By sequencing such "PCR homologues," we have been able to compare diverse phages of the T4 type. All of the phage genomes analyzed had sequences homologous to the major structural genes of T4 (genes *18*, *19*, and *23*). Three subgroups of the T4-type phages can be distinguished: the T-evens, the pseudoT-evens, and the schizoT-evens. The vast majority of the known T4-type phages were isolated on enterobacteria, and most of them belong to the T-even subgroup. In contrast, the T4-type phages isolated on *Aeromonas*, *Burkholderia*, and *Vibrio* belong to either the pseudoT-even or schizoT-even subgroup and their genomes have diverged considerably.

The existence of the schizoT-even phage group demonstrates that the morphology of the virion head can vary within a family of phages. The similarity in morphology of the schizoT-evens to some of the aberrant phage produced by T4 "giant" point mutants (*9*) suggests that evolutionary transformations of head morphology may be accomplished without enormous difficulty. We expect that T4-type phages with smaller isometric heads or with a different length of the contractile tail can be isolated. It will be interesting to identify and analyze the sequences of the genes responsible for such morphological variations. The limits of the morphological variation of the T4-type phages have certainly not yet been circumscribed.

Our extensive analysis of a number of gene *23* sequences suggests a modular construction of its protein. Sequence comparisons of gene *18* (tail sheath protein) suggest that this gene has a similar modular organization. Gene mosaicism is most clearly evident in the T-even phage tail fibers (13, 28), where it facilitates swapping of the adhesin domains between phages (34). This may enable the phages to infect new hosts and thus would be an important evolutionary advantage. The patchwork structure of the tail fiber genes has been viewed as a consequence of the extreme pressures on their adhesin sequences to diversify (34). However, our sequence analysis of genes *23* and *18* in the T4-type phages now suggests that many more structural genes could have a similar, if less obvious, mosaic design.

As the fine structure of the T4-type virion becomes better understood, it will be interesting to determine the exact function of the various conserved motifs in the virion proteins. Many presumably have a role in determining the intrinsic structural features of the protein, but others could be engaged in protein-protein interactions between the different virion subunits (34). Another intriguing possibility is that some of these conserved sequences actually have a nonstructural role in promoting homologous recombination. As we have previously suggested, in a mosaic gene small conserved motifs could mediate the genetic swapping of the variable patches that they flank (33, 34). This could create increased diversity in specific domains of an otherwise conserved structural protein.

With the techniques reported here it is now easy to rapidly identify and characterize the T4-type phages in a feral phage population. For example, we have recently identified and characterized various T4-type phages isolated from pulmonary fluids of hospital patients with respiratory infections caused by *Pseudomonas aeruginosa* (M. Kutateladze, R. Adamia, F. Tétart, and H. M. Krisch, unpublished observations).

ACKNOWLEDGMENTS

We thank Rezo Adamia, Karin Carlson, Dick Epstein, Eric Miller, Jim Karam, and Lucien Caro for their diverse contributions. Our colleagues Marc Dreyfus, Jean-Pierre Claverys, and A. J. Carpousis tried to improve the manuscript. Germaine Burgener Krisch suggested the names of the T4-type phage subgroups, Yvette de Preval synthesized the oligonucleotides, and David Villa prepared the figures.

This research was financed by the CNRS and by grants from the Association pour la Recherche sur le Cancer (ARC), the Midi-Pyrénées Regional Council, the European Union INTAS-Georgia Initiative, and the NATO Collaborative Research Program.

REFERENCES

1. **Ackermann, H. W.** 1998. Tailed bacteriophages: the order Caudovirales. Adv. Virus Res. **51**:135–201.
2. **Ackermann, H.-W., and H. M. Krisch.** 1997. A catalogue of T4-type bacteriophages. Arch. Virol. **142**:2329–2345.
3. **Arisaka, F., L. Ishimoto, G. Kassavetis, T. Kumazaki, and S. Ishii.** 1988. Nucleotide sequence of the tail tube structural gene of bacteriophage T4. J. Virol. **62**:882–886.
4. **Arisaka, F., T. Nakako, H. Takahashi, and S. Ishii.** 1988. Nucleotide sequence of the tail sheath gene of bacteriophage T4 and amino acid sequence of its product. J. Virol. **62**:1186–1193.
5. **Bergh, O., K. Y. Borsheim, G. Bratbak, and M. Heldal.** 1989. High abundance of viruses found in aquatic environments. Nature **340**:467–468.
6. **Bouet, J. Y., J. Woszczyk, F. Repoila, V. François, J.-M. Louarn, and H. M. Krisch.** 1994. Direct PCR sequencing of the ndd gene of bacteriophage T4: identification of a product involved in bacterial nucleoid disruption. Gene **141**:9–16.
7. **Demerec, M., and U. Fano.** 1945. Bacteriophage-resistant mutants of *Escherichia coli*. Genetics **30**:119–136.
8. **DeRosier, D. J., and A. Klug.** 1972. Structure of the tubular variants of the head of bacteriophage T4 (polyheads). I. Arrangement of subunits in some classes of polyheads. J. Mol. Biol. **65**:469–488.
9. **Doermann, A. H., A. Pao, and P. Jackson.** 1987. Genetic control of capsid length in bacteriophage T4: clustering of *pig* mutations in gene 23. J. Virol. **61**:2823–2827.
10. **Fuhrman, J. A.** 1999. Marine viruses and their biogeochemical and ecological effects. Nature **399**:541–548.
11. **Fuhrman, J. A. and C. A. Suttle.** 1993. Viruses in marine planktonic sytems. Oceanography **6**:51–63.
12. **Fuller, N. J., W. H. Wilson, I. R. Joint, and N. H. Mann.** 1998. Occurrence of a sequence in marine cyanophages similar to that of T4 g20 and its application to PCR-based detection and quantification techniques. Appl. Environ. Microbiol. **64**:2051–2060.
13. **Haggård-Ljungquist, E., C. Halling, and R. Calendar.** 1992. DNA sequence of the tail fiber genes of bacteriophage P2: evidence for horizontal transfer of tail fiber genes among unrelated bacteriophages. J. Bacteriol. **174**:1462–1477.
14. **Haynes, J. A., and Elserling F. A.** 1996. Modulation of bacteriophage T4 capsid size. Virology **221**:67–77.
15. **Hendrix, R. W., M. C. Smith, R. N. Burns, M. E. Ford, and G. Hatfull.** 1999. Evolutionary relationships among diverse bacteriophages and prophages: all the world's a phage. Proc. Natl. Acad. Sci. USA **96**:2192–2197.
16. **Kim, J. S., and N. Davidson.** 1974. Electron microscope heteroduplex studies of sequence relations of T2, T4 and T6 bacteriophage DNAs. Virology **57**:93–111.
17. **King, J. and Mykolajewycz, N.** 1973. Bacteriophage T4 tail assembly: proteins of the sheath, core and baseplate. J. Mol. Biol. **75**:339–358.
18. **Looyza, D., A. J. Carpousis, and H. M. Krisch.** 1991. Gene 32 transcription and mRNA processing in T4-related bacteriophages. Mol. Microbiol. **5**:715–725.
19. **Luftig, R. B.** 1967. An accurate measurement of the catalase crystal period and its use as an internal marker for electron microscopy. J. Ultrastruct. Res. **20**:91–102.
20. **Matsuzaki, S., T. Inoue, M. Kuroda, S. Kimura, and S. Tanaka.** 1998. Cloning and sequencing of major capsid protein (mcp) gene of a vibriophage, KVP20, possibly related to T-even coliphages. Gene **222**:25–30.

21. **McNicol L. A., and L. E. Simon.** 1977. A mutation which bypasses the requirement for p24 in bacteriophage T4 capsid morphogenesis. J. Mol. Biol. 116:261–283.
22. **McPheeters, D. S., G. Gosch, and L. Gold.** 1988. Nucleotide sequences of the bacteriophage T2 and T6 gene 32 mRNAs. Nucleic Acids Res. 16:9341.
23. **Monod, C., F. Repoila, M. Kutateladze, F. Tétart, and H. M. Krisch.** 1997. The genome of the pseudoT-even bacteriophages, a diverse group that resembles the T-even phages. J. Mol. Biol. 267:237–249.
24. **Noble, R. T., and J. A. Fuhrman.** 1998. Use of SYBR Green I for rapid epifluorescence counts of marine viruses and bacteria. Aquat. Microb. Ecol. 14:113–118.
25. **Page, R. D. M.** 1996. TREEVIEW: an application to display phylogenetic trees on personal computers. Comput. Appl. Biosci. 12:357–358.
26. **Parker, M. L., A. C. Christensen, A. Boosman, J. Stockard, E. T. Young, and A. H. Doermann.** 1984. Nucleotide sequence of bacteriophage T4 gene 23 and the amino acid sequence of its product. J. Mol. Biol. 180:399–416.
27. **Repoila, F., F. Tétart, J.-Y. Bouet, and H. M. Krisch.** 1994. Genomic polymorphism in the T-even bacteriophages. EMBO J. 13:4181–4192.
28. **Sandmeier, H.** 1994. Acquisition and rearrangement of sequence motifs in the evolution of bacteriophage tail fibers. Mol. Microbiol. 12:343–350.
29. **Selick, H. E., G. D. Stormo, R. L. Dyson, and B. M. Alberts.** 1993. Analysis of five presumptive protein-coding sequences clustered between the primosome genes, 41 and 61, of bacteriophages T4, T2, and T6. J. Virol. 67:2305–2316.
30. **Streisinger, G., J. Emrich, and M. M. Stahl.** 1967. Chromosome structure in phage T4. III. Terminal redundancy and length determination. Proc. Natl. Acad. Sci. USA. 57:292–295.
31. **Takeda, S., F. Arisaka, S. Ishii, and Y. Kyogoku.** 1990. Structural studies of the contractile tail sheath protein of bacteriophage T4. 1. Conformational change of the tail sheath upon contraction as probed by differential chemical modification. Biochemistry 29:5050–5056.
32. **Takeda, S., T. Sasaki, A. Ritani, M. M. Howe, and F. Arisaka.** 1998. Discovery of the tail tube gene of bacteriophage Mu and sequence analysis of the sheath and tube genes. Biochim. Biophys. Acta 1399:88–92.
33. **Tétart, F., F. Repoila, C. Monod, and H. M. Krisch.** 1996. Bacteriophage T4 host range is expanded by duplications of a small domain of the tail fiber adhesin. J. Mol. Biol. 258:726–731.
34. **Tétart, F., C. Desplats, and H. M. Krisch.** 1998. Genome plasticity in the distal tail fiber locus of the T-even bacteriophage: recombination between conserved motifs swaps adhesin specificity. J. Mol. Biol. 282:543–556.
35. **Thcimer, C. A., Y. Wang, D. W. Hoffman, H. M. Krisch, and D. P. Giedroc.** 1998. Non-nearest neighbor effects on the thermodynamics of unfolding of a model mRNA pseudoknot. J. Mol. Biol. 279:545–564.
36. **Thompson, J. D., D. G. Higgins, and T. J. Gibson.** 1994. CLUSTAL W: improving the sensitivity of progressive multiple sequence alignment through sequence weighting, position-specific gap penalties and weight matrix choice. Nucleic Acids Res. 22:4673–4680.
37. **Vianelli, A., G. R. Wang, M. Gingery, R. L. Duda, F. A. Eiserling, and E. B. Goldberg.** 2000. Bacteriophage T4 self-assembly: localization of gp3 and its role in determining tail length. J. Bacteriol. 182:680–688.
38. **Wais, A. C., and E. B. Goldberg.** 1969. Growth and transformation of phage T4 in E. coli B/4, Salmonella, Aerobacter, Proteus, and Serratia. Virology 39:153–161.
39. **Wommack, K. E., R. T. Hill, M. Kessel, E. Russek-Cohen, and R. R. Colwell.** 1992. Distribution of viruses in the Chesapeake Bay. Appl. Environ. Microbiol. 58:2965–2970.
40. **Wood, W. B., and M. P. Conley.** 1979. Attachment of tail fibers in bacteriophage T4 assembly: role of phage whiskers. J. Mol. Biol. 12:715–729.
41. **Yanagida, M., Y. Suzuki, and T. Toda.** 1984. Molecular organization of the head of bacteriophage T-even: underlying design principles. Adv. Biophys. 17:97–146.
42. **Yeh, L. S., T. Hsu, and J. D. Karam.** 1998. Divergence of a DNA replication gene cluster in the T4-related bacteriophage RB69. J. Bacteriol. 180:2058–2063.

INFECTION AND IMMUNITY, Jan. 1970, p. 88-97
Vol. 1, No. 1

Printed in U.S.A.

Bacteriophage Attachment to the Somatic Antigen of *Salmonella*: Effect of O-Specific Structures in Leaky R Mutants and S, T1 Hybrids

ALF A. LINDBERG, MATTI SARVAS, AND P. HELENA MÄKELÄ

Department of Bacteriology, Statens Bakteriologiska Laboratorium, Stockholm, Sweden, Department of Bacteriology and Serology, University of Helsinki, and State Serum Institute, Helsinki, Finland

Received for publication 9 July 1969

The phage adsorption ability and serological specificity of different *Salmonella* strains having either complete or leaky mutations in their lipopolysaccharide (LPS) synthesis were compared, together with their genotype and sugar composition, to provide a set of standards relating these parameters to LPS structure. Strains that had T1-specific side chains in their LPS, both with or without O side chains, were examined to learn more about the organization of these two side chains in the LPS and a possible competition between them. It was found that (i) adsorption of O-specific antibodies was a very sensitive test for the presence of even very small amounts of O-specific structures, (ii) that phage P22 adsorption was dependent on the presence of a nearly complete O side chain complement, and both long and numerous O side chains were required, and (iii) that the adsorption of the phages FO (Felix O-1), 6SR, and Br2, which attach to structures in the LPS core, was a sensitive indicator of any defect in O-antigen synthesis, and well developed O side chains blocked their attachment efficiently. Semirough (SR) strains with only one O-specific repeating unit per side chain adsorbed FO efficiently, whereas the access of the 6SR and Br2 phages to their receptors was blocked. Strains with T1 side chains adsorbed the FO and 6SR phages efficiently, whereas the adsorption of the Br2 phage was blocked to a large extent. The phage adsorption of four S,T1 strains (with both O and T1 side chains) showed that, as the amount of O side chain material increased, there was a reduction of the adsorption of phages in the following order: 6SR, Br2, and FO. P22 attachment appeared with the increase of O side chains. The LPS composition of these strains revealed a 10-fold reduction of the O-specific structures compared to the smooth parent strain, whereas the amount of T1-specific material was the same as in T1 strains. The short O side chains of a SR,T1 strain were, however, not reduced in number, suggesting that the apparent competition between O and T1 side chains may not be a competition for available sites in the LPS.

Two major factors in the lipopolysaccharide (LPS) structure seem to play a role in phage attachment. First, the LPS must have the structures that serve as phage receptors. It is apparent from the available knowledge that different phages attach to different receptor structures even in the same LPS molecule (11, 12; R. G. Wilkinson, Ph.D. Thesis, Univ. of London, London, England, 1966). Secondly, the receptor must be accessible to the phages. A receptor site in the innermost, core part of the LPS may be blocked by other cell wall components, for example, rough (R) mutants are sensitive to many phages to which smooth (S) forms are not. A quantitative determination of the attachment of phages to their host can be obtained by measuring the adsorption rate constant (ARC).

The phage adsorption, serological specificity, and LPS composition were compared among *Salmonella* strains having different amounts of O side chain material. The reduction of the normal amount of O-specific material in these strains was due to different causes (P. H. Mäkelä and B. A. D. Stocker, Annu. Rev. Genet., *in press*). Some of the strains had blocks in the synthesis of the LPS core (Fig. 1) owing to a *rfa* mutation; the block was however incomplete or "leaky," which resulted in the synthesis of an enzyme catalyzing

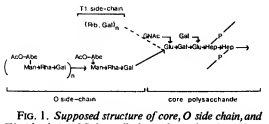

FIG. 1. *Supposed structure of core, O side chain, and T1 side chain of Salmonella lipopolysaccharide. Abbreviations: Hep, heptose; Glu, glucose; Gal, galactose; GNAc, N-acetyl glucosamine; Rha, rhamnose; Man, mannose; Abe, abequose; AcO, O-acetyl; Rib, ribose.*

the step concerned with a much reduced efficiency. In consequence of this, the LPS would have most of its side chains incompletely stopped at the site of the block, but have some, those where the deficient enzyme had acted, completed to full length. Other strains had comparable mutations in *rfb* genes, concerned with the synthesis of the repeating units which constitute the building blocks of the O side chains. Still others had defects in the polymerization of the repeating units (*rfc* mutants), resulting in LPS in which each side chain had one O-specific repeating unit only.

All these strains may be used to learn more about the factors influencing serological specificity and phage attachment, and they provide a system for relating these parameters to LPS structure. The results obtained were applied to an examination of strains with T1 side chains (*see* references 8, 20; Mäkelä and Stocker, Annu. Rev. Genet., *in press*) together with (i) normal O side chains (S, T1 forms), (ii) the short O side chains of SR, T1 forms, or (iii) without O side chains [T1 forms (18)].

MATERIALS AND METHODS

The individual bacterial strains used are described in connection with the results. The SH strains come from the collection of P. H. Mäkelä and M. Sarvas, and the SL strains from the collection of B. A. D. Stocker, Department of Microbiology, Stanford University, Stanford, Calif. Most of the strains are derivatives of *Salmonella typhimurium* line LT2; the T1 parent strain is *S. paratyphi* B, T1 form from F. Kauffman (8); and some strains were derived from *S. abony*. The relevant smooth O-antigen of all these strains is 4, 12, since the bacteria react with specially prepared "anti-4" and "anti-12" sera; some of the strains may also react with "anti-1" or "anti-5" sera, or both, but the presence or absence of these "minor" factors does not affect smoothness, that is, amount or arrangement of O-specific repeating units in the LPS.

The serological behavior of the bacteria was studied by slide agglutination in 4% saline and in predetermined dilutions (made up in 0.2% saline) of anti-R, anti- 4,12, and anti-T1 sera, prepared by immunizing rabbits with bacterial suspensions held 2.5 hr at 100 C (9). The anti-R serum prepared against a *r/a* mutant was known to agglutinate a large number of R (*r/a* or *rfb*) and SR (*rfc*) mutants but not the S [4,12] or T1 forms of *S. typhimurium*. The anti-4,12 serum had some anti-R activity in agglutination, but S [4,12] strains agglutinated in large clumps, whereas the R strains gave a fine granular agglutination. The anti-T1 serum was specific for T1 at the dilution (1:100) used here; at lower dilutions it also had anti-R activity.

The ability of the bacteria to adsorb specific (anti-4, 12 or anti-T1) antibodies from the rabbit sera was tested by adding approximately 10^{10} or 10^{9} bacteria (collected from nutrient agar plates and held at 100 C for 30 min) to 1 ml of the appropriate serum diluted to contain about 200 times the minimum agglutinating dose. The mixture was shaken well, and kept at 37 C for 2 hr or at 4 C overnight. The tubes were then centrifuged, and the supernatant fluid was titrated in tube agglutination against suspensions of either S [4, 12] or T1 bacteria (9). When the smaller amount of bacteria was able to remove all the agglutinins, the result was given as ++++; when it left some, although the larger amount removed all agglutinating antibodies, the result was scored as +-+; and when the larger number of bacteria removed part but not all of the agglutinins, the response was +. Techniques for testing the nutritional characteristics of the bacteria and obtaining genetic crosses have been described before (18).

For studies on the chemical composition of the LPS, the bacteria were grown and the LPS was extracted as has been described earlier (5). The quantitative analyses of the monosaccharide constituents were made by gas-liquid chromatography of glycitol acetates produced from acid hydrolysates of the LPS preparations (7). The sugars were not isolated in the present study but had been identified previously (19). The relative peak areas were determined, and the molecular ratios for the constituent sugars were calculated from these. The quantities of the individual sugars, determined as mole per cent of detected sugars, were used for the estimation of the number of O-specific repeating units and T1-specific structures in the side chains. The calculations presume a LPS structure, according to Fig. 1, with two heptose units in each core stub and each core stub capped by an O-specific or T1-specific side chain. The number of repeating units in each O side chain was estimated from the ratio of mole per cent mannose + mole per cent rhamnose to mole per cent heptose and for the T1 side chain from the ratio of mole per cent ribose × 2 to mole per cent heptose (presuming a ribosyl-galactosyl repeating unit). The values given in Tables 1 and 2 are rounded to the next whole number.

A sample of the batch culture for the LPS analyses was stored in a nutrient agar stab culture and several colonies were examined within 1 to 3 weeks for agglutinability, phage sensitivity, and often for the nutritional requirements of the strains. A similar test was performed on the batch of bacteria grown for phage adsorption tests.

The bacteriophages used consisted of the S-specific *S. typhimurium* phages P22c2, and 9NA (4), the general *Salmonella* phage FO (Felix O-1), and the

R-specific phages 6SR, Br60, Ffm, and Br2. The phages were obtained through the courtesy of B. A. D. Stocker, Stanford University, Calif. They were propagated on the appropriate host strains, and their lytic spectrum was checked on selected S and R strains. Some of their properties were described by Wilkinson and Stocker (25). The phage sensitivity of the bacterial strains was tested by spotting drops of phage containing approximately 10^8 plaque-forming units per ml on surface-inoculated nutrient agar plates. Sometimes the test was repeated by applying the phage and bacteria in soft agar layer (1). Phage adsorption was followed by determining the ARC as described previously (13).

RESULTS

Table 1 shows the behavior of various smooth (S), semirough (SR = *rfc*) and rough (R) variants of *S. typhimurium* LT2. The strains were selected to include leaky mutants, i.e., ones whose defects were more or less incomplete. As a result, the LPS of these strains contained varying amounts of O-specific sugars.

The first two strains (SL683, SH1430) had no defects and showed the typical behavior of S strains. They were agglutinated in anti-4,12 and not in anti-R sera, nor in saline, they adsorbed anti-4,12 antibodies efficiently, and their LPS had O-specific components corresponding to an average of 7 to 10 repeating units per core stub. They were sensitive to the S-specific P22 and 9NA phages and to the FO phage but not to R-specific phages. They adsorbed P22 with a high ARC (313 and 346), but no attachment of the FO and R phages was measurable. In fact, they did adsorb FO as they score as FO-sensitive but the ARC was too low to be detected here (13).

The three following strains showed slight deviations from the S pattern. SL 749 was sensitive to phage P221, which does not attack S bacteria—the strain has been suspected of being a very leaky *rfc* mutant (B. A. D. Stocker, *personal communication*). It had the normal amount of O-specific sugars and behaved like a S strain except for a slight adsorption of FO (ARC 31 compared with the < 5 found with the S strains). Its P22 ARC was 218, which is rather lower than that for the S strains, although the difference might not be significant. The next strain, SH 1002, had a reduced amount of O-specific sugars (equivalent of 2 repeating units per core stub), and it adsorbed P22 at a somewhat lower rate (ARC 129) than the S strains. This lower adsorption might be due to the fact that the strain is lysogenic for P22. It has been shown previously that lysogenicity for P22 reduces the ability of a strain to adsorb this phage (27). But the strain also adsorbed FO and the R-specific phage Br2, although with low rates.

Finally, SL 902 is a leaky temperature-sensitive phosphoglucose isomeraseless (*pgi*) mutant (3), unable to synthesize glucose for LPS synthesis. When grown on complex media, it gets enough glucose from the medium to build up a nearly normal LPS; however, under these conditions it still gives only minute plaques with the phage P22. That the reduced plaque size is connected with the *pgi* mutation was made likely by the following experiment: SL 902 as recipient was crossed with smooth donor bacteria, and recombinants that had received the donor *metA*+ allele (concerned with methionine biosynthesis) were selected. Because *pgi* is known to be closely linked with *metA* (3), most of these recombinants had now the *pgi*+ allele of the donor and gave normal size plaques with P22. All the reactions of SL 902 (grown in complex media with 1% glucose) given in Table 1 are smooth, except that it adsorbed P22 at a somewhat lower rate (ARC 138) and that FO adsorption (ARC 14) had become demonstrable.

The next three strains in Table 1 are SR, defective in repeating unit polymerase and therefore having O chains with only one repeating unit. They were very similar. The agglutination pattern was typical SR, with a barely observable granular agglutination in 4% saline. They adsorbed anti-4,12 antibodies much less efficiently than do S strains. They were sensitive to the phage FO only and adsorbed this phage with an ARC of 111 to 280. SH 1493 adsorbed the R phage Br2 also. The phage adsorption pattern of SL 901 was different from the other two. It adsorbed both P22 and R-specific phages to some extent, but its immediate derivative, SH 1493, did not show these reactions. The most likely explanation may be that the P22 adsorption was due to *rfc*+ revertants or contaminants in the batch, although the control sample tested appeared homogeneous. The adsorption of 6SR and Br2 by SL 901 cannot be explained at present. In the phage sensitivity test, SL 901 showed the typical SR behavior.

The third group of bacterial strains have mutations mapping as *rfb*. All these mutants have the normal LPS core and were sensitive to the R-specific and FO phages whose receptors appear to be in the core. All the strains in this group adsorbed FO and R-specific phages with high rate constants. An exception is strain SH 1003, in which the defect appears to be very leaky: this strain was still sensitive to 9NA (P22 could not be tested because the strain is P22 lysogenic), and not sensitive to 6SR. It adsorbed P22 at a low rate (ARC 9), 6SR not at all, and Br2 at a lower rate than the other *rfb* mutants. The typical *rfb* mutants tested agglutinated in saline, anti-R, and also in anti-4,12 serum. The agglutination in the

TABLE 1. *Comparison of various S, SR, and R strains of Salmonella typhimurium LT2*

Strain		Phage sensitivity[a]						ARC (× 10^{-11} ml/min)				LPS composition[b]	Agglutination in				Absorption of anti-4,12	Further description of and reference to the strain
		P22	9NA	FO	6SR	Br2	Br60	P22	FO	6SR	Br2		4% NaCl	anti-R	anti-4, 12			
S	SL 683	+	+	+	−	−	−	346	<5	<5	<5	10	−	−	+++	+++		
	SH 1430	+	+	+	−	−	−	313	<5	<5	<5	7	−	−	+++			
	SL 749	+	+	+	−	−	−	218	31	<5	<5	5	−	−	+++	+++		P221 sensitive, very leaky *rfc*[c,d]
S(?)	SH 1002	−	+	+	−	−	−	129	20	<5	24	2	−	−	+++	+++		P22 lysogenic. Adsorption batch = many R mutants
	SL 902[e]	+[f]	+	+	−	−	−	138	14	<5	<5	6	−	−	+++	+++		Phosphoglucose isomeraseless on complex medium (3)
SR	SL 901	−/−	−/−	+	−	−	−	8[g]	280	17	106	1	+	++	++	+		*rfc*, not transduced by P22 (4)
rfc	SH 1493	−	−	+	−	−	−	<5	192	<5	13	1	+	++	++			Derivative of SL 901
	SL 1506	−	−	+	−	−	−	<5	111	<5	<5	1	+	++	++	+		*rfc* (?), transduced by P22 (4)
R	SH 1003	−	+	+	−	+	+	9	252	<5	69	2	−	−	+++	+++		P22 lysogenic sister clone of the smooth SH 1002
Leaky	SL 1112	−/+	−/+	+	+	+	+	<5	411	30	378	0.5	−	++	+++	++		Similar to "rouB, culturally S" (4, 25)
	SL 1153	−/−	−/−	+	+	+	+	<5	268	26	384	−[e]	++	++	++	++		—[d]
rfb Nonleaky	TV 119	−	−	+	+	+	+	25[h]	442	63	460	0.1[h]	++	++	++			(23)
	SH 1432	−	−	+	+	+	+	<5	336	96	575	−[e]	++	++	++			Derivative of TV 119 (23)
	SH 180	−/−	−/−	+	+	+	+					−[e]	++	++	++	−		*rfb* deletion *his*-658 (16) (obtained from H. Nikaido)
R	SL 733	−	−/−	−/−	+	+	+	12	<5	<5	100	0.5	−	++	+++	+++		(26)
rfa Leaky	SL 1111	−/+	−/+	−/−	−	+	+	<5	<5	<5	<5	2	−	+	+++	+++		Semirough class D-ii (4)

[a] Determined by the standard method of applying drops of phage (10^8 plaque-forming units per ml) on surface-inoculated nutrient agar plates, and sometimes also by applying the phage and bacteria in soft agar layer. Symbols: +, when lysis was obtained by standard method; −, when negative by standard method and not tested by agar layer; −/+, when negative by standard method and positive by agar layer; and −/−, when negative by both methods.

[b] O-specific repeating units (moles of rhamnose + mannose) per 2 moles of heptose (=1 core stub).

[c] Indicates that the LPS contained less than 1 mole per cent of O-specific sugars in the analyses.

[d] B. A. D. Stocker, *personal communication*.

[e] ARC to SL 902 as well as its LPS composition was determined after cultivation in complex medium with 1% glucose.

[f] Minute plaques.

[g] Possibly due to *rfc*[+] back mutations because the derivative on the next line is completely SR.

[h] Possibly due to *rfb*[+] back mutation because the derivative on the next line is completely R.

last serum was probably due to anti-R antibodies. Many of the mutants have some O-specific structures, as demonstrated by their capacity to adsorb anti-4,12 antibodies and in many cases by the presence of O-specific sugars in the LPS (7). SH 180, which is the strain *his*-658 described by Nikaido et al. (16), has a long chromosomal deletion covering both parts of the histidine operon and the *rfb* cluster. It should, therefore, be totally devoid of *rfb* activity and serve as a definite nonleaky mutant in this group. No O specificity could be detected either from its absorption behavior towards anti-4,12 sera or in the analysis for O-specific sugars in the LPS.

Two of the *rfb* mutants (SL 1112, SH 1003) had distinctly leaky mutations. SL 1112 is one of the "rouB, culturally S" class, isolated by Wilkinson (Ph.D. Thesis, University of London, 1966) and described also by Gemski and Stocker (4); it did not agglutinate in saline but was agglutinated in anti-R and anti-4,12 sera, giving large, nearly S-like clumps in the latter. Its LPS had an average of 0.5 repeating units per core stub. The phage sensitivity was typical of *rfb* mutants; however, when the phages were applied in soft agar layer, P22 and 9NA gave small and very turbid plaques, indicating that they were adsorbed poorly or perhaps to only a fraction of the bacteria. The ARC for phage P22 was found to be 0.9 when the number of phage-infected bacteria were counted instead of the number of phages in the supernatant fluid. The strain SH 1003 was much more leaky than SL 1112. It was serologically nearly indistinguishable from S strains (it was agglutinated to a slightly higher titer by anti-4,12 sera than was its parent SH 1002), it had an average of 2 repeating units per core stub just like its smooth sister clone, SH 1002, but it was sensitive to both S- and R-specific phages as described above. Why SH 1003 and SH 1002 have the same content of O-specific sugars, but differ in phage sensitivity and adsorption can only be guessed at. The cause of this apparent anomaly may be a difference in the LPS structure in the two strains: SH 1003, for example, might have a reduced number of O side chains of "normal" length, whereas SH 1002 had a normal or elevated number of shortened side chains.

The four nonleaky *rfb* mutants did not show any P22 or 9NA plaques even in soft agar layer. The phage adsorption measurements did not show a deviation from the *rfb* pattern; neither did measurement of phage-infected bacteria reveal any attachment. (It is probable that the slight P22 adsorption by TV119 was due to few smooth back mutants in the batch.)

The fourth group of strains in Table 1 consists of two core (*rfa*) mutants, both of which have leaky defects. They had a strong O-specificity in the serum adsorption test and O-specific sugars in their LPS. SL 733, which is strain St/22 of Yamamoto and Anderson (26), is resistant to P22 but sensitive to a P22 variant P22h (14, 28) as well as to R phages. In this assay it showed some adsorption of P22, which could be related to the P22h sensitivity and indicate the presence of some phage receptors or could also be due to revertants in the batch. SL 1111, a strain isolated by Wilkinson (Ph.D. Thesis, Univ. of London, London, England, 1966) and inferred to be a leaky *rfa* mutant because of its phage sensitivity pattern, gave very turbid small plaques with P22 and 9NA in soft agar layer but showed no FO sensitivity by any method. No P22 phage adsorption was detected, although the LPS content of O-specific sugars was as high as the equivalent of 2 repeating units per core stub. However, it is possible that the LPS preparation of this strain was contaminated with traces of the O-specific hapten (2), and, thus, the true content of O-specific sugars in the LPS was less than that recorded.

To summarize the results of Table 1, the different S, *rfc*, *rfb*, and *rfa* strains have their characteristic patterns, when the behavior in all the test systems is taken into account. R mutants which are only slightly leaky or not detectably leaky (as SL1153 in Table 1), as judged by LPS content of O-specific sugars, showed O-specificity towards antiserum. A higher degree of leakiness is required before adsorption of O-specific phages can be recognized. On the other hand, even slightly impaired synthesis of the O-antigenic side chains increased the ability of the strain to adsorb the phages that attach to the core.

The results of similar tests on various strains with and without T1 side chains are compiled in Table 2. The parental T1 strain is the original *Salmonella paratyphi* B T1 (8). It lacks O specificity, due to a *rfb* mutation (20); the presence of T1 specific groups in LPS is determined by gene(s) at a separate *rft* locus (18). It is possible to produce strains with both T1 and O specificities through a conjugational cross by introducing the *rft*+ allele from the donor derivative of the T1 parent into S or SR recipient strains (18). The resulting hybrids with both O and T1 side chains are described as S, T1 or SR, T1, respectively. When the *rft*+ allele was introduced into any *rfb* mutant, the hybrid had only T1 specificity.

The hybrid strains obtained when the T1 donor parent was crossed with S, or with SR, or with R-recipient bacteria are compared in Table 2. From each cross, a pair of recombinants was selected one with and the other without the *rft*+ allele, but otherwise as similar as possible. Sometimes the recipient parent was tested as well.

TABLE 2. *Comparison of strains with and without T1 antigen*

Species or line	Strain	Genetic make-up			Phage sensitivity[a]						ARC[a] ($\times 10^{-11}$ ml/min)				LPS composition[a]		Agglutination in			Absorption of anti-		Estimation of the amount of mutants or reversions in batch for[d]	
		rfc	*rfb*	*rfl*	P22	9NA	FO	6SR	Br2	Br60	P22	FO	6SR	Br2	S[b]	T1[c]	4% NaCl	Anti-4, 12	Anti-T1	4, 12	T1	Phage adsorption	LPS isolation
Salmonella paratyphi B T1	SH 1308	+	−	+	−	−	+	+	+	+	<5	457	29	34	−	10	−	−	+++	−	+++	None	None
T1	SH 1120	+	−	+	−	−	+	+	+	+	<5	283	5	36	−	7	−	−	+++	−	+++	All R	All R
S. paratyphi B R	SH 1310				−	−	+	+	+	+	<5	176	86	442			++		−				
rfb	SH 1311	+	−	−	−	−	+	+	+	+	<5	188	72	360			++		−				
	SH 1312				−	−	+	+	+	+	<5	422	53	512			++		−				
	SH 1313	+	−	−	−	−	+	+	+	+	<5	267	28	298			++		−				
	SH 1314				−	−	+	+	+	+	<5	258	55	527			++		−				
LT 2 S	SH 1430	+	+	−	+	+	+	−	−	−	313	<5	<5	<5	7	−	−	+++	−	+++	−		
S, T1	SH 1429	+	+	+	+	+	+	−	−	−	<5	42	<5	<5	1	15	−	+	+++	−	+++	None	None
LT 2 S	SL 683	+	+	−	+	+	+	−	−	−	346	<5	<5	<5	10	−	−	+++	−	+++	−		
S, T1	SH 1413	+	+	+	+	+	+	−	−	−	53	63	<5	<5	6	2	−	+++	+++	+	+++	None	Many T1⁻ mutants
S. abony S	SH 1515	+	+	−	−	+	+	−	−	−	55	<5	<5	<5	7	−	−	+++	−	++	−	None	None
S, T1	SH 1517	+	+	+	−	−	+	−	−	−	<5	34	<5	<5	1	10	−	+	+++	−	+++	None	None
LT 2 SR	SL 901	−	+	−	−	−	+	−	−	−	8	280	17	106	1	−	−	++	−			None	None
SR	SH 1493	−	+	−	−	−	+	−	−	−	<5	192	<5	13	1	−	−	++	−	+	−	None	None
SR, T1	SH 1490	−	+	+	−	−	+	−	−	−	52	308	32	100	1	5	−	+	+++	−	++	6% SR colonies	8% SR colonies
S, T1	SH 1483	+	+	+	+	+	+	−	−	−	16	123	<5	<5	1	10	−	+++	+++	−	+++	34% S colonies	24% S colonies
LT 2 R	SL 1112	+	−	−	−	−	+	+	+	+	<5	411	30	378	0.5	−	+	++	−			None	None
T1	SH 1436	+	−	+	−	−	+	+	+	+	<5	287	46	239	−	4	−	−	+++	−	+++	50% R colonies	10% R colonies
LT 2 R	TV 119	+	−	−	−	−	+	+	+	+	25	442	63	460	0.1	−	++	++	−			None	None
R	SH 1432	+	−	−	−	−	+	+	+	+	<5	336	36	575	−	−	++	++	−	−	−	None	None
T1	SH 1433	+	−	+	−	−	+	+	+	+	<5	407	20	352	−	4	−	−	+++	−	+++	50% R colonies	5% R colonies

[a] Assays as in Table 1.
[b] O-specific repeating units per 2 moles of heptose as in Table 1.
[c] T1-specific "units" (moles of ribose × 2) per 2 moles of heptose.
[d] Controls were tested after 1 to 3 weeks in stab culture; the percentage of mutants or revertants is probably an overestimate of the situation in the batch.

The *Salmonella paratyphi* B T1 donor (SH 1308) gave, to a large extent, the typical *rfb* behavior familiar from the *rfb Salmonella typhimurium* mutants in Table 1; however, the ARC of Br2 was low. There was no O specificity detectable either in the LPS composition or in serum adsorption. The amounts of the T1 sugars ribose and galactose were equivalent to 10 monosaccharides of each per core stub. Several T1$^-$ (and therefore R) derivatives of SH 1308 were tested for comparison, i.e., strains SH 1310 to SH 1314 in Table 2. Their phage adsorption was typical of *rfb* mutants, even for Br2.

T1 strains are known to be genetically unstable; in our experience, fresh cultures segregate T1$^-$ mutants so that overnight cultures contain about 1% and older culture many more T1$^-$ forms. Therefore, we planned to test the purity of the batches grown for LPS isolation or phage adsorption very carefully. However, the 1- to 3-week period between the batch culture and its testing turned out to be too long, so that in many cases the proportion of T1$^-$ colonies found was very high, higher than was possible as judged from the chemical analysis of the LPS.

There are three sets of *rft*$^+$ and *rft*$^-$ pairs in smooth strains (Table 2). Two of them are *Salmonella typhimurium* LT2 and, therefore, directly comparable with the strains in Table 1. One is *S. abony* (also with the O-antigenic formula 4, 12), which adsorbed P22 at a lower rate than did the LT2 strains. In all three sets, when the *rft*$^+$ allele was introduced, the ability of the smooth strain to adsorb phage P22 was much reduced. Some receptors were still available to the phage since the *rft*$^+$ strains were sensitive to P22 in spot assay. At the same time, the rate of adsorption of FO was much increased, although still remaining lower than in *rfb*, T1 strains. In each case, the amount of O-specific sugars per core stub was decreased. The number of T1-specific structures within the *rft*$^+$ organisms listed in Table 2 are very variable, perhaps in keeping with the instability of the T1$^+$ state. Yet, the S, T1 strains did not seem to have any less T1-specific sugars than did the T1 (*rfb*) strains, either in *S. paratyphi* B or in LT2 (*see* Table 2).

The next series of strains represents a combination of SR (*rfc*) with T1. Here the *rfc*$^-$, *rft*$^-$ parent is the strain SL 901, which was discussed in connection with Table 1 and which showed some adsorption of both P22 and R-specific phages, whereas the presumably similar (i.e., *rfc*$^-$, *rft*$^-$) recombinant SH 1493 did not adsorb P22. The *rfc*$^-$, *rft*$^+$ recombinant SH 1490, like SL 901, adsorbed both P22 and R-specific phages. The LPS composition and the control from both the adsorption and the LPS batches behaved as expected of this genotype, and the phage sensitivity was typical of *rfc*. It is not known why the *rfc*$^-$ strains SL 901 and SH 1490 showed this adsorption pattern, especially how they could adsorb P22 although they were not sensitive to infection by it even when tested in the soft agar layer. The combination of *rft*$^+$ with *rfc* requires a more thorough analysis. It seems safe to conclude, however, that the presence in the LPS of the equivalent of 5 "units" (for this purpose defined as ribosyl-galactose) of T1-specific material per core stub did not decrease the amount of O-specific sugars (1 unit per core stub) in this SR strain. Neither did the fact that in the *rfc* strain the core stubs were—as is inferred—nearly fully capped by the O chains (14) decrease the amount of T1-specific sugars. The last recombinant in this set, SH 1483, had its *rfc* gene replaced by its smooth allele, resulting in the genotype *rfc*$^+$, *rft*$^+$, serologically S, T1. The content of O- and T1-specific sugars in the LPS was similar to other S, T1 strains and so was the behavior towards phage.

Data in Table 2 represent *rfb* mutants with or without T1 (therefore either T1 or R). The phage adsorption pattern was typical of *rfb* mutants in each case. No decrease in ARC for Br2 was observable in the T1 strains in this case; we do not know why these strains differed from the *S. paratyphi* B strains in this respect, but a possible explanation could be the frequency of T1$^-$ revertants.

DISCUSSION

The main results of this work have been compiled in Fig. 2, which shows the relationship between the LPS structure and the behavior of the bacteria towards anti-O serum and the different phages. This figure is necessarily very schematic involving too many unknowns. We do not know the spatial arrangement of the LPS layer on the bacterial surface or the exact structures of the phage receptors.

In the electron micrographs of Shands (21, 22), the O antigen was visualized by ferritin-conjugated anti-O antibody: in *S. typhimurium* the antibody stain was visible as a layer extending about 50 nm outside the bacterial cell wall or sticking out the same length from aggregated LPS. On the other hand, the average O side chain of *S. typhimurium* was estimated to contain 8 to 11 repeating units (5, 6) which would correspond to about 10 nm in length. However, it is possible that this value could represent an average of very unequal lengths. In Fig. 2, we have drawn the O antigen as a layer of 50 nm to conform to the electron micrograph picture.

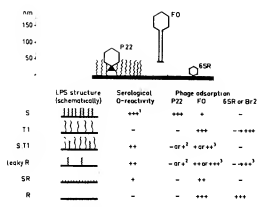

FIG. 2. *Diagram relating the LPS structure with observed serological specificity and phage adsorption ability. O side chain (jagged lines) attached to the core, as in S; T1 side chain (wavy lines) attached to the core, as in T1; single O repeating unit (short, straight lines) attached to the core, as in SR. Note 1, −, +, ++, and +++ represent arbitrary gradations of the ability of the bacteria to absorb specific antibody or to attach phages. Note 2, adsorption efficiency increasing with increasing amounts of O-specific material. Note 3, adsorption efficiency increasing with increasing exposure of core structures.*

The shapes and sizes of the phages are better known: P22 has a head of 60 nm and a short tail of 17.5 nm with short tail fibers (24); FO has a very long tail of about 150 nm with long tail fibers (11), whereas 6SR is a small phage with a diameter of about 30 nm and no distinct tail (10). Br2 is not included in the picture, but preliminary electron microscope studies indicated that it is rather similar to 6SR (*unpublished data*).

The receptor structures for all these phages are found in the bacterial LPS (12). The FO bacteriophage requires the complete core with its terminal *N*-acetylglucosamine for attachment (11, 12, 13, 25). This glucosamine probably forms a branch from the main chain of the core, to which the O and T1 side chains are attached (15; *see* also Fig. 1). The phages 6SR and Br2 can attach to a core structure which may not be complete (12, 25; Wilkinson, Ph.D. Thesis, Univ. of London, London, England, 1966). P22 is strict in its requirement for O side chains with the antigen 12 (28). SR forms which contain only one repeating unit are resistant to P22 (4, 14), which might indicate that the critical site for attachment is the junction between successive repeating units, or that the site is larger than one repeating unit. Most leaky R mutants adsorb P22 poorly or not at all, and the adsorption is directly correlated with the amount of O-specific material (equal to the number of O side chains) present (Fig. 2). Many of those mutants which adsorb P22 to some extent can be transduced with it (4). Some leaky R mutants allow the formation of plaques by P22, although the plaques are small and very turbid (e.g., SL 1112, Table 1). It appears that for rapid adsorption phage P22 requires a nearly complete S LPS with long side chains sufficiently close to each other. The above information suggests that attachment involves multiple sites on many side chains.

Serological O reactivity. The comparison of the different S and leaky R strains showed that smooth O reactivity could be detected even when the LPS synthesis was impaired to a large extent. Apparently only a few O-specific groups per cell were enough to fix antibodies from the sera and cause both specific agglutination and antibody absorption. For example, SL 1153 (Table 1) absorbs anti-O quite well, although no O-specific sugars were detected chemically. In fact most R mutants which have been tested show O reactivity in the absorption assay. The specificity of this absorption appears to be proven by the fact that the *rfb* deletion mutant SH 180 showed no absorption. However, the antibody absorption assay could not easily detect differences in the quantity of O-specific structures.

The SR strains with about 10% of the normal amount of O-specific sugars absorbed antibody less efficiently than leaky R mutants with smaller amounts of the sugars. This difference suggests that the O repeating units in these two types of mutants were arranged differently. Since the SR mutants have only one repeating unit per side chain (17), the leaky R mutants may have longer but fewer O side chains.

FO and R-specific phages. Sensitivity to R-specific phages or increased attachment of phage FO, or both, proved to be sensitive indicators for a defect in LPS synthesis (Fig. 2). Well developed O side chains of the S form apparently prevent the access of the phages to their receptor sites on the core, probably through steric hindrance. The long-tailed phage FO was not affected as much as were the others; although the ARC for FO in S forms, as measured here, was too low to be detected most S forms are usually sensitive to FO. A good exception is a *S. montevideo* (O antigens 6 and 7) strain, which had a low sensitivity to FO, giving very turbid plaques. Because all *rfb* mutants of this strain were fully sensitive to the phage, with clear plaques, it was believed that the poor sensitivity of the S form in this case was due to a more efficient covering of the core by the O side chains than occurred in most *Salmonella* strains. The reduction in the length of O side chains seen in SR forms increased the absorption of FO to nearly full

efficiency. The SR forms probably have their core stubs "capped" by an O-specific unit more completely than do S forms: there was no serological R reactivity, which would mean a reaction of the core structures, detectable either by complement fixation (14) or hemagglutination inhibition in the SR lipopolysaccharide, whereas R reactivity was often found in LPS from S strains (O. Lüderitz, *personal communication*).

The amount of O-specific sugars in the SR lipopolysaccharide corresponded to one repeating unit per two heptoses (one core stub). The analytical procedures can measure the sugar components to within an accuracy of ± 3%; within this limit, all core stubs are probably capped by repeating units, since no O side chains contained more than 1 repeating unit. We would expect the SR strains to be resistant to FO if the attachment of an O unit blocked the receptor site for FO, but they were in fact sensitive and showed high ARC values.

The adsorption of the R-specific phages 6SR and Br2 increased more slowly than that of FO with decreasing amounts of O-specific material. Whereas mutants with a very leaky defect, allowing the production of substantial amounts of O side chains (e.g., SH 1003, Table 1), adsorbed FO efficiently, the adsorption of 6SR and Br2 was poor or nondetectable. These phages also seem to be inhibited by the short O side chains of the SR forms.

The FO and 6SR phages attach to T1 bacteria as they do to the *rfb* strains. Br2 seems to be inhibited by T1 to some extent: its ARC to the T1 form of *S. paratyphi* B is 10% of that to the isogenic R forms (Table 2), although no difference is seen in the T1 and R strains of *S. typhimurium*. The S,T1 strains adsorb all these phages less than the T1 or R strains and even less than the very leaky R mutant SH 1003, which contains as much O-specific sugars in its LPS as S,T1. These results imply that the T1 side chains alone are not sufficient to cause steric hindrance of the core receptor sites (except perhaps to Br2), but, together with O side chains, there was significant hindrance. The lack of steric hindrance of the T1 chains may be related to the following facts. The amount of monosaccharides present in T1 chains is about 50% of that present in O chains. There is also a qualitative difference in the monosaccharide constituents; the O side chain contains the less hydrophilic deoxy- and dideoxyhexoses, rhamnose and abequose. There could be a difference in the arrangement of the side chains in the LPS: T1 side chains might be considerably longer and consequently fewer than are O side chains. This situation is suggested by the fact that, although the O and T1 side chains probably are attached to the same terminal glucose of the core (15; M. Berst, *personal communication*), the SR, T1 strains, which like SR forms have their core stubs nearly completely capped by O units, still have the same amount of T1 material as T1 forms and the same amount of O units as the SR strains.

T1 and O side chains in the same organism. The quantitative data on the sugar composition of the LPS from the four S,T1 strains (Table 2) provide the first proof of a competition between T1 and O side chains, a competition that has been suggested on the basis of the serological behavior of these hybrid strains (18). In three of the four S,T1 strains, the amount of O-specific sugars was reduced from 7 to 10 repeating units per core stub (as observed in the S forms in this study) to about 1 repeating unit per core stub, whereas the amount of ribose was the same as in T1 forms. An apparent exception is SH 1413 with more O-specific than T1-specific units. Because the batch used for LPS extraction in this strain contained many T1$^-$ mutants (which were S), it is probable that they account for the high amount of O-specific sugars. The few O units are probably arranged as few long O side chains, since their phage adsorption properties are different from SR or SR, T1 forms that have numerous but short side chains.

At which stage does the competition take place? The first guess would be that it is a competition for available attachment sites in the core. We believe that the behavior of the SR, T1 form makes this possibility unlikely. This strain (SH 1490, Table 2) has as much O-specific material as do SR forms and, therefore, probably has its core stubs nearly completely capped by the O units (*see above*), yet has as much T1 material as do T1 forms. We hope that the studies on the biosynthesis of the T1 antigen now in progress help to clarify this question.

ACKNOWLEDGMENTS

The technical assistance of Mary Anderzon, Gunnel Ljunggren, Aila Jauhiainen, and Marianne Hovi is gratefully acknowledged.

This investigation was supported by Swedish Medical Research Council grant B68-40x-656-03, by the Finnish Medical Research Council, and Public Health Service grant GM-12046 from the National Institute of General Medical Sciences.

LITERATURE CITED

1. Adams, M. H. 1959. Bacteriophages. Interscience Publishers, Inc., New York.
2. Beckmann, L, T. V. Subbaiah, and B. A. D. Stocker. 1964. Rough mutants of *Salmonella typhimurium*. 2. Serological and chemical investigations. Nature (London) 201:1299–1301.
3. Fraenkel, D., M. J. Osborn, B. L. Horecker, and S. M. Smith. 1963. Metabolism and cell wall structure of a mutant of *Salmonella typhimurium*. Biochem. Biophys. Res. Comm. 11:423–428.

4. Gemski, P., Jr., and B. A. D. Stocker. 1967. Transduction by bacteriophage P22 in nonsmooth mutants of *Salmonella typhimurium*. J. Bacteriol. 93:1588–1597.
5. Hellerqvist, C-G., B. Lindberg, S. Svensson, T. Holme, and A. A. Lindberg. 1968. Structural studies on the O-specific side chains of the cell wall lipopolysaccharide from *Salmonella typhimurium* 395MS, Carbohyd. Res. 8:43–55.
6. Hellerqvist, C-G., B. Lindberg, S. Svensson, T. Holme, and A. A. Lindberg. 1969. Structural studies on the O-specific side chains of the cell wall lipopolysaccharide from *Salmonella typhimurium* LT2. Carbohyd. Res. 9:237–241.
7. Holme, T., A. A. Lindberg, P. J. Garegg, and T. Onn. 1968. Chemical composition of cell-wall polysaccharide of rough mutants of *Salmonella typhimurium*. J. Gen. Microbiol. 52:45–54.
8. Kauffmann, F. 1956. A new antigen of *Salmonella paratyphi* B and *Salmonella typhimurium*. Acta Pathol. Microbiol. Scand. 39:299–304.
9. Kauffmann, F. 1966. The bacteriology of *Enterobacteriaceae*. Munksgaard, Copenhagen.
10. Kay, D., and D. E. Bradley. 1962. The structure of bacteriophage φR. J. Gen. Microbiol. 27:195–200.
11. Lindberg, A. A. 1967. Studies of a receptor for Felix 0-1 phage in *Salmonella minnesota*. J. Gen. Microbiol. 48:225–233.
12. Lindberg, A. A., and T. Holme. 1969. Studies on *Salmonella* lipopolysaccharides using the phage inactivation technique, p. 141–154. *In* La structure et les effets biologiques des produits bactériens provenant de germes gram-negatifs, 24–26 Octobre 1967. Colloques Internationaux du Centre National de la Recherche Scientifique (Paris).
13. Lindberg, A. A., and T. Holme. 1969. Influence of O side chains on the attachment of Felix 0-1 phage to Salmonella bacteria. J. Bacteriol. 99:513–519.
14. Naide, Y., H. Nikaido, P. H. Mäkelä, R. G. Wilkinson, and B. A. D. Stocker. 1965. Semirough strains of *Salmonella* Proc. Nat. Acad. Sci. U.S.A. 53:147–153.
15. Nikaido, H. 1969. Structure of cell wall lipopolysaccharide from *Salmonella typhimurium* I. Linkage between O side-chain and R core. J. Biol. Chem. 244:2835–2845.
16. Nikaido, H., M. Levinthal, K. Nikaido, and K. Nakane. 1967. Extended deletions in the histidine rough B region of the *Salmonella* chromosome. Proc. Nat. Acad. Sci. U.S.A. 37:1825–1832.
17. Nikaido, H., Y. Naide, and P. H. Mäkelä. 1966. Biosynthesis of O-antigenic polysaccharides in *Salmonella*. Ann. N.Y. Acad. Sci. 133:299–314.
18. Sarvas, M. 1967. Inheritance of *Salmonella* T1 antigen. Ann. Med. Exp. Fenn. 45:447–471.
19. Sarvas, M., O. Lüderitz, and O. Westphal. 1967. Immunochemical studies on T1,S hybrids of *Salmonella paratyphi* B. Ann. Med. Exp. Fenn. 45:117–126.
20. Sarvas, M. and P. H. Mäkelä. 1965. The production, by recombination, of *Salmonella* forms with both T1 and O specificities. Acta Pathol. Microbiol. Scand. 65:654–656.
21. Shands, J. W., Jr. 1965. Localization of somatic antigen on gram-negative bacteria by electron microscopy. J. Bacteriol. 90:266–270.
22. Shands, J. W., Jr., J. A. Graham, and K. Nath. 1967. The morphologic structure of isolated bacterial lipopolysaccharide. J. Mol. Biol. 25:15–21.
23. Subbaiah, T. V., and B. A. D. Stocker. 1964. Rough mutants of *Salmonella typhimurium*. 1. Genetics. Nature (London) 201:1298–1299.
24. Vieu, J. F., O. Croissant, and C. Dauguet. 1965. Structure des bacteriophages responsables des phénomènes de conversion chez les *Salmonella*. Ann. Inst. Pasteur 109:160–166.
25. Wilkinson, R. G., and B. A. D. Stocker. 1968. Genetics and cultural properties of mutants of *Salmonella typhimurium* lacking glucosyl or galactosyl lipopolysaccharide transferases. Nature (London) 217:955–957.
26. Yamamoto, N., and T. F. Anderson. 1961. Genomic masking and recombination between serologically unrelated phages P22 and P221. Virology 14:430–439.
27. Zinder, N. D. 1958. Lysogenization and superinfection immunity in *Salmonella*. Virology 5:291–326.
28. Zinder, N. D., and J. Lederberg. 1952. Genetic exchange in *Salmonella*. J. Bacteriol. 64:679–699.